

**Ubiquitin C-terminal hydrolase-L1 (UCH-L1) stabilizes NOXA  
and impacts on cancer chemosusceptibility**

Inaugural-Dissertation

zur

Erlangung des Doktorgrades

der Mathematisch-Naturwissenschaftlichen Fakultät

der Universität zu Köln

vorgelegt von

**Kerstin Brinkmann**

aus Kirchheimbolanden

Berichterstatter:

**Prof. Dr. Thomas Langer**

**Prof. Dr. Thorsten Hoppe**

Tag der mündlichen Prüfung: 14.05.2012

## Content

Abstract .....	I
Zusammenfassung .....	II
Abbreviations .....	IV
1 Introduction .....	1
1.1 Hallmarks of cancer .....	1
1.2 Apoptosis .....	2
1.3 The Bcl2 protein family .....	9
1.4 p53-mediated apoptosis in response to DNA damage .....	12
1.5 The Ubiquitin-Proteasome System .....	14
1.6 Aim of the work .....	17
2 Material and methods .....	19
2.1 Chemicals .....	19
2.2 DNA constructs .....	19
2.3 Cell culture and transfection .....	21
2.4 Cytotoxic treatments and cell viability .....	22
2.5 qPCR .....	23
2.6 Sample preparation and immunoblotting (IB) .....	23
2.7 Immunoprecipitations (IP) .....	26
2.8 In vitro deubiquitylation and binding assays .....	27
2.9 Fluorescence microscopy .....	27
2.10 Flow cytometry (FACS) .....	28
2.11 Tissue immunohistochemistry (IHC) .....	28
3 Results .....	30
3.1 Proteasome inhibition induces mitochondrial apoptosis in a cohort of tumour entities .....	30
3.2 NOXA accumulates at the post-transcriptional level after proteasome inhibition .....	34

3.3	NOXA protein is less stable in bortezomib-sensitive tumour cells .....	36
3.4	NOXA is increasingly ubiquitylated in bortezomib-sensitive tumour cells .....	37
3.5	The deubiquitylating enzyme (DUB) UCH-L1 is absent in bortezomib-sensitive tumour cells.....	39
3.6	The DUB UCH-L1, binds, deubiquitylates and stabilizes NOXA <i>in vitro</i> .....	41
3.7	UCH-L1-expression correlates with increased NOXA-expression in tumour tissue sections of melanoma and CRC patients .....	45
3.8	UCH-L1 depletion is associated with chemoresistance in tumour cells .....	47
4	Discussion.....	50
4.1	NOXA accumulation as a key event in proteasome inhibition-induced apoptosis .....	50
4.2	Post-transcriptional regulation of NOXA by the UPS .....	53
4.3	Increased NOXA degradation as a result of lacking UCH-L1 expression, the specific DUB of NOXA.....	53
4.4	UCH-L1 as a modulator of apoptosis .....	55
4.5	UCH-L1 as an important component of the DNA damage response by stabilization of NOXA.....	56
4.6	Conclusion.....	57
5	References.....	59
6	Appendix .....	67
6.1	Microarray .....	67
6.1	Patient data .....	69
6.2	Vector maps .....	72
6.3	Danksagung .....	73
6.4	Erklärung .....	74
6.5	Lebenslauf.....	75

## Abstract

Resistance to apoptosis is a hallmark of tumour cells. It constitutes an important clinical problem since chemotherapy and irradiation act primarily by inducing apoptosis. Compounds inhibiting proteasomal activity are able to selectively induce tumour cell apoptosis and a growing body of evidence suggests the up-regulation of NOXA (a BH3-only protein) upon proteasome inhibition to be one of the essential events. However, the underlying molecular mechanisms giving rise to the selective NOXA up-regulation in tumour cells is poorly understood.

The current work shows that in cells susceptible to proteasome inhibition NOXA protein was significantly less stable and continuously degraded by the Ubiquitin-Proteasome System (UPS). Amongst others, the degradation of substrates by the UPS is regulated by E3-ubiquitin ligases and deubiquitylating enzymes (DUBs). In the current work UCH-L1 was identified as a responsible DUB of NOXA, which was epigenetically silenced in tumour cells susceptible to proteasome inhibition. UCH-L1 binds and stabilizes NOXA by removing the Lys<sup>48</sup>-linked polyubiquitin chains that normally mark NOXA for proteasomal degradation. In line with these observations, increased UCH-L1 expression correlated with increased NOXA protein expression in human melanoma and colorectal cancer patient samples. As one of the genes responsive to genotoxic stress, NOXA has been considered as the BH3-only protein to be involved in the fine-tuning of apoptosis. Correspondingly, the current work demonstrates that UCH-L1 expression is important for DNA-damage induced apoptosis. Down-regulation of UCH-L1 results in decreased susceptibility to DNA damage-induced apoptosis accompanied by a decreased NOXA accumulation.

Taken together, the current work identified UCH-L1 as an important component of the DNA damage response that impacts on the susceptibility of cancer cells toward chemotherapy by stabilizing NOXA.

## Zusammenfassung

Tumore zeichnen sich unter anderem durch eine Apoptoseresistenz aus, die ein gravierendes Problem in der Krebsbehandlung darstellt, da sowohl Chemotherapie als auch Bestrahlung primär über die Induktion der Apoptose wirken.

Inhibitoren des humanen 26S Proteasoms sind beschrieben, selektiv in Tumorzellen Apoptose zu induzieren. Essentiell für die Induktion der Apoptose nach Behandlung mit Proteasominhibitoren ist die Akkumulation des pro-apoptotischen "BH3-only"-Proteins NOXA, wobei der Mechanismus nicht vollständig aufgeklärt ist.

Die vorliegende Arbeit zeigt, dass die Fähigkeit von Proteasominhibitoren, Apoptose zu induzieren unter Tumorzellen von verschiedenen Individuen stark variiert. Außerdem wurde gezeigt, dass die Stabilität des essentiellen "BH3-only"-Proteins NOXA ebenfalls unter Tumorzellen von verschiedenen Individuen stark variiert. In Tumorzellen die nach Proteasominhibition Apoptose induzieren ist die Stabilität von NOXA stark verringert. Es wurde demonstriert, dass die verringerte Stabilität von NOXA die Folge einer verstärkten Ubiquitinierung und somit Degradation durch das Ubiquitin-Proteasome System (UPS) ist. Die Degradation von Proteinen durch das UPS wird unter anderem durch E3-Ubiquitin-Ligasen und deubiquitinierende Enzyme (DUB) reguliert. In der vorliegenden Arbeit wurde Ubiquitin-C-terminal hydrolase-L1 (UCH-L1) als spezifische DUB von NOXA identifiziert. In Tumorzellen, die eine verringerte Stabilität von NOXA aufweisen wurde UCH-L1 nicht exprimiert. Als direkter Interaktionspartner von NOXA war UCH-L1 in der Lage, NOXA zu deubiquitinieren und somit zu stabilisieren. In Übereinstimmung mit biochemischen und zellbiologischen Ergebnissen zeigten Expressionsanalysen von NOXA und UCH-L1 in Geweben von 81 Melanom- und 26 Colonicarcinompatienten ebenfalls eine Korrelation der Expression. Gewebe in den denen UCH-L1 exprimiert war, wiesen eine erhöhte Expression von NOXA auf.

NOXA ist ursprünglich als ein Protein beschrieben, das für die zelluläre Antwort zu genotoxischem Stress wichtig ist, indem es an der Feinabstimmung der mitochondrialen Membranpermeabilisierung (MOMP) beteiligt ist. Die vorliegende Arbeit zeigt, dass auch UCH-L1 für den Ablauf von Apoptose nach DNS-Schädigung

wichtig ist, indem es die Stabilität von NOXA kontrolliert.. Herunterregulation der UCH-L1 Expression in UCH-L1-exprimierenden Tumorzellen verringerte deren Fähigkeit nach Schädigung der DNS Apoptose zu induzieren. Dies war die Folge einer verringerten Fähigkeit NOXA zu akkumulieren.

Zusammenfassend wurde in dieser Arbeit UCH-L1 als spezifische DUB von NOXA identifiziert. Durch die Fähigkeit NOXA zu stabilisieren spielt UCH-L1 in der zellulären Antwort auf DNS-Schädigung eine entscheidende Rolle und beeinflusst die Sensitivität von Tumorzellen gegenüber Chemotherapie.

## Abbreviations

Only abbreviations are listed that have not been described in the text

$\alpha$	anti
$^{\circ}\text{C}$	Degree Celsius
$\mu\text{g}$	Microgramm
$\mu\text{l}$	Microliter
$\mu\text{M}$	Micromolar
aa	amino acids
ATP	adenosine triphosphate
bp	basepairs
BSA	bovine serum albumin
C-terminal	carboxyterminal
Da, kDa	Dalton, Kilodalton
DMSO	Dimethylsulfoxid
DNA	Deoxyribonucleic acid
ds	double stranded
DTT	Dithiothreitol
<i>E.coli</i>	Escherichia coli
DTT	Dithiothreitol
EDTA	ethylene diamine tetraacetic acid
<i>et al.</i>	<i>et alteri</i> /-a /-um (and others)
FCS	fetal calf serum
Fig.	figure
GFP	green fluorescent protein
FITC	fluorescein-5-isothiocyanat
HEPES	4-(2-hydroxyethyl)-1-piperazineethanesulfonic acid
His, H	Histidine
HRP	horse radish peroxidase
IgG	Immunglobuline G
K	Lysine



## Abbreviations

kb	kilo base
kDa	kilo dalton
N	Asparagin
NaCl	Sodium chloride
nm	Nanometer
N-terminal	aminoterminal
MEFs	mouse embryonic fibroblasts
MW	molecular weight
ORF	open reading frame
ON	over night
PBS	phosphate buffered saline
PCR	polymerase chain reaction
pH	<i>potentium hydrogenii (lat.)</i>
pmol	Picomol
RT	room temperature
SDS	sodiumdodecylsulfat
SDS-PAGE	SDS polyacrylamid gel electrophoresis
Tab.	table
Tris/HCl	tris[hydroxymethyl]aminoethane
V	Volt

# 1 Introduction

## 1.1 Hallmarks of cancer

The formation of malignant tumours is characterized by defects in cell proliferation and homeostasis eventually resulting in overgrowth and thereby loss of function of healthy tissue.

It is thought that the transformation of a healthy cell into a malignant cell is a multistep process with alterations in major signalling pathways. The vast majority of cancer cell genotypes is a manifestation of eight essential alterations in cell physiology that collectively dictate malignant growth: self-sufficiency in growth signals, insensitivity to growth-inhibitory (antigrowth) signals, evasion of programmed cell death (apoptosis), limitless replicative potential, sustained angiogenesis, tissue invasion and metastasis, reprogramming of energy metabolism and evading immune destruction (Hanahan and Weinberg, 2000, 2011). Underlying those alterations are dynamic disorders within the genome. Previous analyses of malignant tissues have identified several genes, which are involved in malignant formation, either by a gain-of-function, referred to as oncogenes, or by a loss-of-function, referred to as tumour suppressors (Weinberg, 1996).

Furthermore, tumours are more than just a vast array of uncontrolled proliferating cancer cells. Rather they are a complex construction composed of multiple distinct - also non-malignant - cell types, which facilitate the acquisition of the hallmarks of cancer by forming the tumour microenvironment. How developing tumours acquire the hallmarks of cancer is a diverse process leading to hundreds of distinct types of cancer and numerous subtypes of tumours within specific organs. Nevertheless, the recognition of these common hallmarks enabled the introduction of mechanism-based targeted therapies, such as the reactivation of the apoptotic machinery (Hanahan and Weinberg, 2011).

## 1.2 Apoptosis

Apoptosis describes programmed cell death or cell suicide (Kerr et al., 1972). It is crucial for sculpting the embryo, maintaining tissue homeostasis, shaping the immune repertoire, terminating immune responses and restricting the progress of infections. The average adult human body generates approximately 60 billion cells per day, and as a consequence an equal number of cells must die by apoptosis to maintain tissue homeostasis. Disturbed regulation of this vital physiological process can result in numerous diseases including autoimmunity, degenerative disorders as well as cancer. Resistance to apoptosis can also permit tumour cells to escape from immune surveillance. (Strasser et al., 1991; Watanabe-Fukunaga et al., 1992), (Barr and Tomei, 1994; Thomson, 1995) (McDonnell and Korsmeyer, 1991; Strasser et al., 1990). Moreover, because chemotherapy and irradiation act primarily by inducing apoptosis, defects in the apoptotic pathway contribute to the resistance of cancer cells to conventional therapy, which constitutes an important clinical problem (Kerr et al., 1994).

The process of a programmed cell death was first described by Carl Vogt in 1842 (Vogt, 1842). The German scientist studied the development of tadpoles, and described the programmed cell death as a crucial step in the embryonic development of tadpoles. The drawings by Walther Flemming in 1885 provided the first morphological description of the programmed cell death. Those drawings clearly show cell shrinkage, nuclear fragmentation and apoptotic body formation, which are by now accepted hallmarks of apoptosis. However, a more detailed description was lacking until 1972 when Kerr, Wyllie and Curie were able to distinguish the programmed cell death and the traumatic or necrotic cell death (Necrosis) by electron microscopic analysis (Kerr et al., 1972). They introduced the word "apoptosis" (ἀπόπτωση) which in Greek describes the "dropping off" or "falling off" of petals from flowers, or leaves from trees. 30 years later, in 2002 Bob Horvitz received the Nobel Prize in Physiology and Medicine for his pioneering work unravelling the fundamental aspects of the biology of apoptosis, using the nematode *Caenorhabditis elegans* (*C. elegans*) as a model system (Horvitz, 2003a, b).

Morphological apoptosis is characterized by defined cellular changes. These changes include blebbing, cell shrinkage, nuclear fragmentation, chromatin condensation, chromosomal DNA fragmentation (Wyllie et al., 1980) and the

exposure of phosphatidyl-serines on the plasma membrane (Fadok and Henson, 1998). Apoptosis produces cell fragments called apoptotic bodies that are engulfed and quickly removed by phagocytic cells before the contents of the cell can spill and cause damage. In contrast, necrotic cell death is characterized by cell swelling, chromatin digestion, and disruption of the plasma membrane and organelle membranes (Enari et al., 1998; Fadok and Henson, 1998; Kerr et al., 1972; Wyllie et al., 1980). Leaky necrotic cells release intracellular contents, thereby causing inflammation (Fig. 1.1). While apoptosis often provides beneficial effects to the organism, necrosis is almost always detrimental and can be fatal. Necrosis is caused by factors external to the cell or tissue, such as infections, toxins, or trauma. In contrast, apoptosis is a naturally occurring cause of cellular death and tightly regulated by intracellular signalling pathways in response to cellular stress (Ellis and Horvitz, 1986; Vaux et al., 1988).

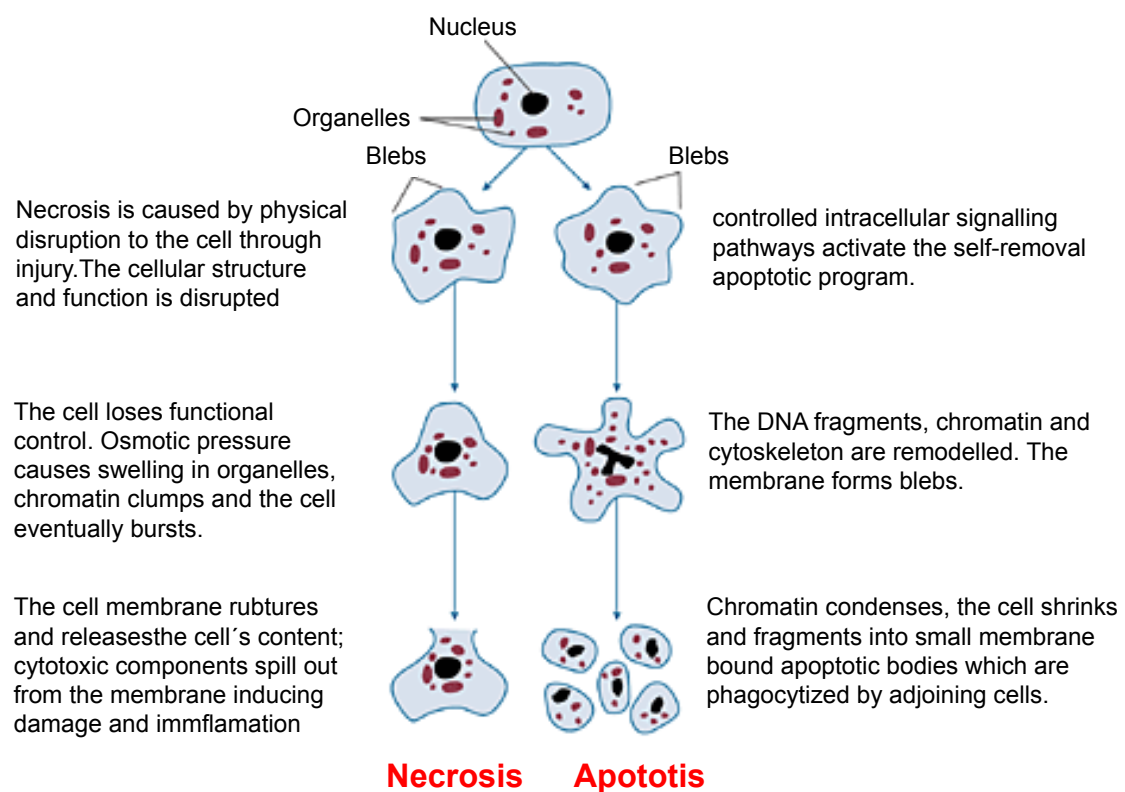


**Figure 1.1 | Morphology of apoptosis and necrosis.** Apoptosis is characterized by nuclear and DNA fragmentation, cell shrinkage and the formation of apoptotic bodies. Phagocytic cells engulf apoptotic bodies without activating the inflammatory response (right). Necrotic cell death is characterized by cell swelling, chromatin digestion and disruption of the plasma membrane resulting in the release of intracellular material and the activation of the inflammatory response (left) (Goodlett and Horn, 2001).

## 1.2.1 Apoptotic signalling

In principle, there are two alternative pathways that initiate apoptosis: one is mediated by death receptors on the cell surface — referred to as the "*extrinsic pathway*"; the other is mediated by mitochondria — referred to as the "*intrinsic or mitochondrial pathway*". The initiation of extrinsic and mitochondrial apoptotic pathways occur by engagement of extracellular "*death receptors*" and intracellular stress (e.g. inadequate cytokine support, diverse types of cellular damage), respectively (Strasser et al., 2000).

Both pathways involve the activation of cysteine aspartidyl-specific proteases (caspases) - the main executioners of the apoptotic process (Kumar and Lavin, 1996; Nicholson and Thornberry, 1997).

### 1.2.1.1 Caspases

Caspases cleave cellular substrates and thus initiate the biochemical and morphological changes that are characteristic of apoptosis. For instance, caspases process the inhibitor of the caspase-activated-DNase (CAD) resulting in active CAD that is responsible for DNA fragmentation (Sakahira et al., 1998). Moreover caspases induce the processing of the nuclear protein lamin and the poly (ADP-ribose) polymerase (PARP), which plays an important role in DNA damage repair, and its processing serves as a marker of ongoing apoptosis (Masson et al., 1995). Furthermore, regulators of the cytoskeleton and adhesion proteins are processed by caspases resulting in cell shrinkage and disruption of the extracellular matrix (Sanghavi et al., 1998).

Caspases are a highly conserved family of cysteine proteases that cleave their substrates specifically after certain aspartate residues (Alnemri et al., 1996). Based on their intracellular function, caspases can be divided into three subgroups: cytokine activators (caspase 1, 4, 5, 11, 12, 13, 14), the initiator caspases (caspase 2, 8, 9, 10) and the effector caspases (caspase 3, 6, 7), while only initiator- and effector caspases play a role during apoptotic signalling (Denault and Salvesen, 2002). Caspases are constitutively expressed in most cell types and reside as zymogenes in the cytosol (Nicholson, 1999). Structurally caspases consist of an amino-terminal (N-terminal) pro-domain, a large and a small subunit (Denault and Salvesen, 2002). Upon activation, the large and the small subunit are separated by proteolytic

cleavage, and in a second step the pro-domain is removed. Active caspases form tetramers consisting of two small and two large subunits, which form two active sites (Widlak et al., 2003). The large subunit comprises the catalytic cysteine residue (Walker et al., 1994; Wilson et al., 1994) (Fig. 1.2). Some caspases also possess interaction domains such as the caspase associated recruitment domain (CARD) or the death effector domain (DED) (Ashkenazi and Dixit, 1998).

The activation of the caspase cascade is a point of no return. Once initiator caspases are activated, they activate the effector caspases by proteolytic cleavage resulting in degradation of the apoptotic substrates (Nicholson and Thornberry, 1997).

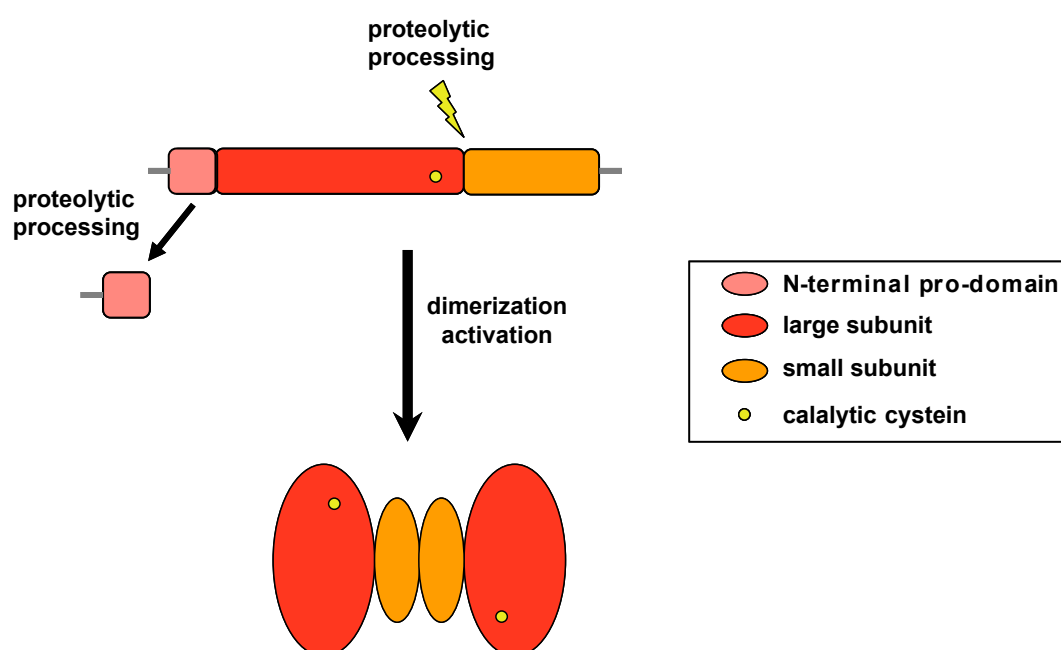


**Figure 1.2 | Activation of caspases.** Caspases consist of a pro-domain, a large and a small subunit. Upon activation the large and small subunit are separated by proteolytic cleavage and the pro-domain is removed (Denault and Salvesen, 2002). Active caspases form dimers comprising two large and two small subunits that form two active sides with the catalytic cysteine residing in the large subunit (Widlak et al., 2003).

### 1.2.1.2 The extrinsic apoptotic signalling pathway

The extrinsic apoptotic-signalling pathway plays an important role during the development of T- and B-cells and is essential for the immune response.

Extrinsic apoptotic signalling is initiated through ligand binding (e.g.  $\text{TNF}\alpha$ , CD95) to the extracellular domain of a death receptor of the TNF superfamily such as TNFR1 or CD95/FAS receptor (Ashkenazi, 2002). Characteristic for death receptors are a

cytosolic death domain (DD) and a death effector domain (DED) that upon activation initiate receptor-oligomerization and interaction with adaptor proteins (e.g. TRADD (TNF associated death domain) or FADD (Fas-associated-death-domain)), respectively. The resulting death inducing signalling complex (DISC) in turn leads to the recruitment of several pro-caspase 8 - or in some cases also pro-caspase 10 - molecules through their DED. The proximity of the zymogens provokes their dimerization and subsequent autocatalysis (Boatright et al., 2003).

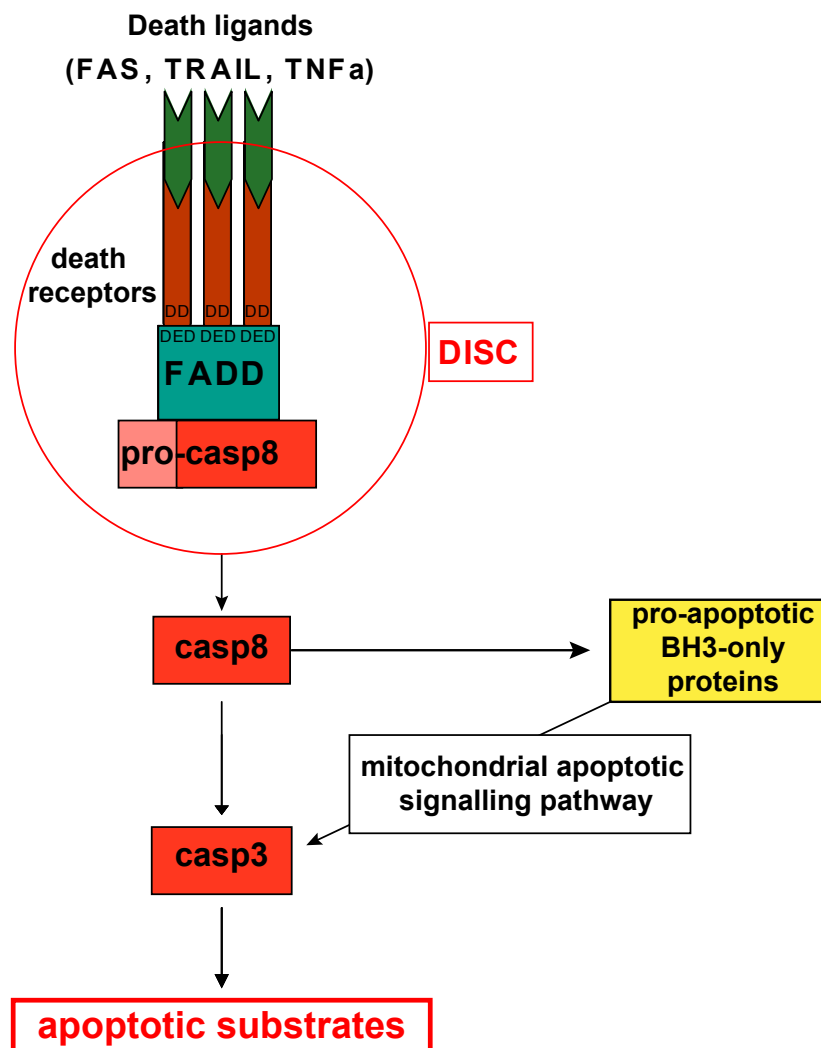


**Figure 1.3 | The extrinsic apoptotic signalling pathway.** Upon binding of a death ligand (e.g. FAS, TRAIL, TNFα) the death inducing signalling complex (DISC) is formed, resulting in active caspase 8 (casp8). Caspase 8 directly activates caspase 3 (casp3) or indirectly by engaging the mitochondrial apoptotic signalling pathway via members of the pro-apoptotic BH3-only family. Active caspase 3 cleaves the apoptotic substrates and apoptotic cell death occurs.

Alternatively, the extrinsic apoptotic pathway can be triggered by cytolytic T-cells or natural killer (NK) cells with the release of perforine and granzyme B. Perforine-release results in extracellular membrane permeabilization of the target cell and allows granzyme B to enter the cell (Lord et al., 2003).

Active caspase 8 or intracellular granzyme B proteolytically activate effector caspases such as caspase 3 irrevocably resulting in apoptotic cell death. Besides the direct activation of caspase 3, caspase 8 and granzyme B induce the mitochondrial apoptotic signalling pathway through engagement of pro-apoptotic BH3-only proteins (Fig. 1.3) (Luo et al., 1998; Wei et al., 2000).

### **1.2.1.3 Intrinsic/mitochondrial apoptotic signalling pathway**

The intrinsic apoptotic signalling pathway is also often referred to as the mitochondrial apoptotic signalling pathway since the release of pro-apoptotic molecules from the mitochondrial inter-membrane space is the central event. The release of mitochondrial pro-apoptotic molecules is regulated by pro- and anti-apoptotic members of the Bcl2 protein family (Kluck et al., 1997; Vander Heiden et al., 1997; Yang et al., 1997). Upon intracellular stress, pro-apoptotic Bcl2 proteins (BH3 only proteins, see 3.2) are activated which in turn leads to the activation of the pro-apoptotic multi-domain proteins BAX and BAK. Upon activation, BAX and BAK undergo conformational changes and form homodimers (Hsu et al., 1997) that are thought to form pores in the mitochondrial outer membrane. This event is also referred to as mitochondrial outer membrane permeabilization (MOMP).

Another model states that induction of MOMP might occur by direct interaction of BAX and BAK with channels in the outer mitochondrial membrane such as VDAC (voltage dependent anion channel) or PTPC (permeabilization transition pore complex), rather than forming pores by themselves. Although a lot of research has been conducted in this field, the precise mechanism of MOMP is still not understood (Tait and Green, 2010). However, there is agreement about the fact that Bcl2-mediated MOMP subsequently results in the release of pro-apoptotic molecules such as cytochrome c and SMAC (second mitochondrial activator) (Newmeyer and Ferguson-Miller, 2003). Cytosolic cytochrome c binds in an ATP or dATP-dependent manner to APAF1 resulting in the recruitment of pro-caspase 9 molecules. The generated multiprotein complex, referred to as apoptosome, triggers the activation of



the initiator caspase 9. The initiator caspase directly activates the executioner caspase 3 and mediates subsequent continuation of apoptosis (Green, 2000).

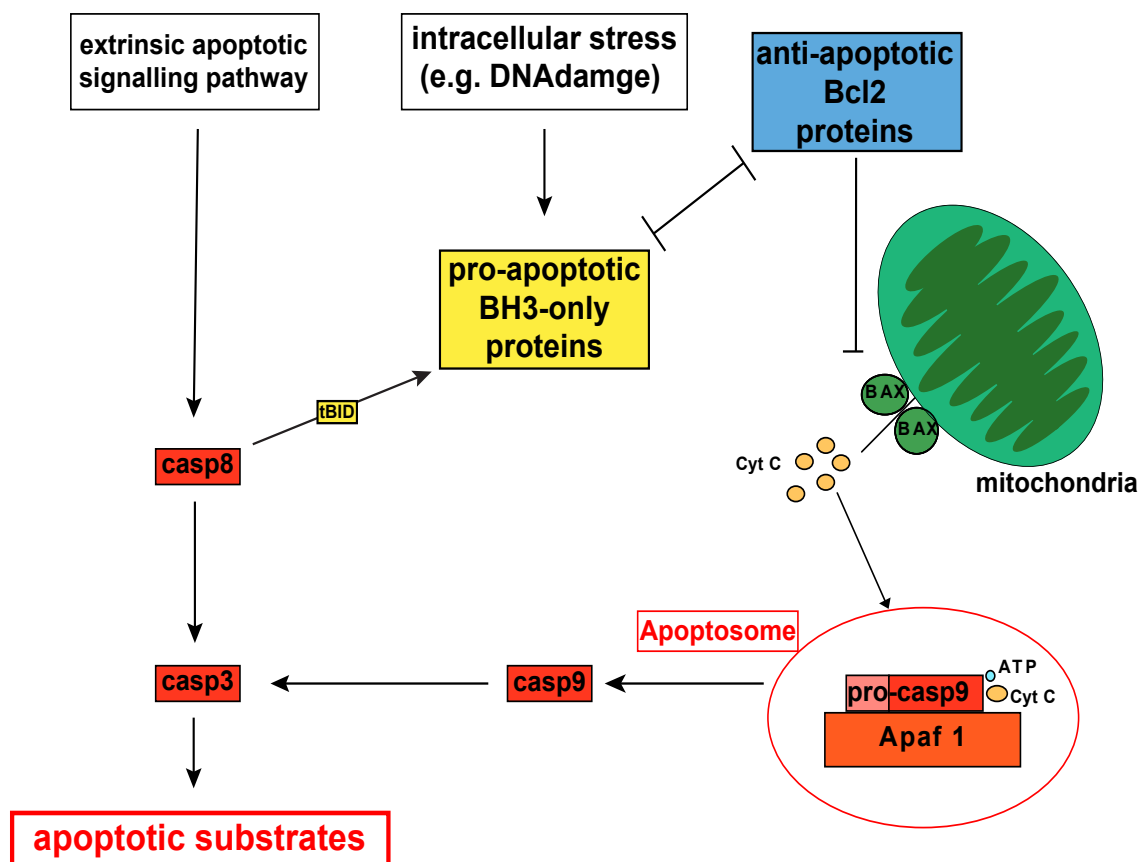


**Figure 1.4 | The mitochondrial apoptotic signalling pathway.** The mitochondrial apoptotic signalling pathway is induced upon intracellular stress. This leads to the activation of pro-apoptotic BH3-only proteins and BAX/BAK-dependent MOMP with the release of cytochrome C (Cyt C) from the mitochondrial intermembrane space. Cyt C forms a complex, the apoptosome, with ATP, APAF1 and pro-caspase 9 (pro-casp9), resulting in the activation of caspase 9 (casp9). Caspase 9 activates caspase 3 (casp3) and apoptosis proceeds. The mitochondrial apoptotic signalling pathway can also be engaged by the extrinsic pathway. Active caspase 8 (casp8) cleaves and thereby activates the BH3-only protein BID, ultimately resulting in MOMP.

As mentioned above the mitochondrial apoptotic signalling pathway is also induced upon activation of the extrinsic pathway. Active caspase 8 or granzyme B can directly cleave BID thereby forming the active tBID (truncated BID), which in turn activates BAX and BAK resulting in MOMP (Fig. 1.4) (Luo et al., 1998; Wei et al., 2000). Depending on the cell type, this interference of both signalling pathways either resembles an amplification loop or is essential for the progression of apoptosis. Cells which can undergo apoptosis independently of MOMP are referred to as type I cells

(e.g. hepatocytes, pancreatic cells) and cells which depend on MOMP to effectively induce apoptosis are referred to as type II cells (e.g. lymphocytes) (Yin et al., 1999).

### 1.3 The Bcl2 protein family

The Bcl2 protein family regulates stress-induced apoptosis by an evolutionary highly conserved mechanism found in species as distantly related as humans and nematodes. The family consists of anti-apoptotic (e.g. BCL2, BCL<sub>xl</sub>, BCL<sub>w</sub>, A1) and two groups of pro-apoptotic members: the multidomain or BAX/BAK like proteins (e.g. BAK, BAX) and the BH3-only proteins (e.g. BIM, BID, PUMA, BAD, NOXA). Members of the Bcl2 protein family share at least one conserved Bcl2 homology domain (BH domain), which is characterized by several  $\alpha$ -helical segments. The BH-domain does not possess enzymatic activity but it allows pro- and anti-apoptotic members to bind to and to inhibit each other (Adams and Cory, 1998; Cory and Adams, 2002). Binding affinity assays using BH3-only peptides revealed that not all pro- and anti-apoptotic Bcl2 proteins can antagonize each other, but the affinity differs within the family (Fig. 1.5). Thus, level and composition of pro- and anti-apoptotic Bcl2 proteins determine whether intracellular stress results in apoptotic cell death or not (Chonghaile and Letai, 2008).

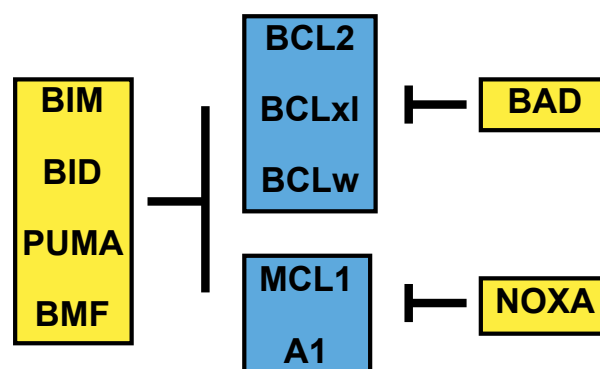


**Figure 1.5 | Binding-pattern of pro- and anti-apoptotic members of the Bcl2 protein family.** The BH3-only proteins BIM, BID, PUMA and BMF can bind and antagonize all anti-apoptotic Bcl2 proteins. In contrast, BAD can only bind BCL2, BCL<sub>xl</sub> and BCL<sub>w</sub>, and NOXA is restricted in binding to MCL1 and A1.

Anti-apoptotic members of the Bcl2 protein family possess four BH domains and a carboxy-terminal transmembrane domain (TM), which targets them with different

affinities to at least three intracellular membranes: the outer mitochondrial membrane, the endoplasmic reticulum (ER) and the nuclear envelope.

Pro-apoptotic members of the BAX/BAK like subgroup (BAX, BAK, BOK, BCL<sub>xs</sub>) possess two or three BH domains and a TM-domain while BH3-only proteins (BIK, BAD, BID, BIM, NOXA, PUMA, BMF) share only the BH3 domain (Fig. 1.6). Both subgroups of pro-apoptotic Bcl2 protein family members are essential for the induction of apoptosis (Cory and Adams, 2002; Coultas and Strasser, 2003).

**A: Anti-apoptotic Bcl2 proteins:**



**B: Pro-apoptotic Bcl2 proteins:**

**Multidomain proteins**



**BH3-only proteins**



**Figure 1.6 | Protein structure of the Bcl2 protein family.** The Bcl2 protein family consists of anti- **(A)** and pro-apoptotic members **(B)** that share at least one conserved Bcl2 homology domain (BH domain).

The anti-apoptotic members (BCL2, BCLxl, BCLw, A1, MCL1) possess four BH domains and an amino-terminal (N-terminal) transmembrane (TM) domain.

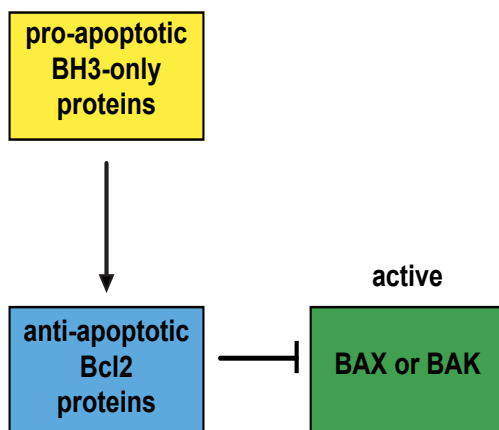
The pro-apoptotic members can be subdivided in the multidomain proteins and the BH3-only proteins. The multidomain proteins (BAX, BAK, BOK) possess 3 BH domains and an N-terminal TM-domain, while the BH3-only proteins (BID, BIM, BIK, BMF, BNIP3, HRK, NOXA, PUMA) comprise only a single BH3 domain.

### 1.3.1 Regulation of apoptosis by the Bcl2 protein family

To date, there are two proposed models that explain how the Bcl2 protein family regulates MOMP: (i) the indirect activator model and (ii) the direct activator-derepressor model. Both models result in the activation of BAX and BAK and the permeabilization of the outer mitochondrial membrane.

The indirect activator model postulates that BAX and BAK are bound in a constitutively active state to anti-apoptotic Bcl2 proteins. Competitive interactions with pro-apoptotic BH3-only proteins and anti-apoptotic Bcl2 proteins are sufficient to release active BAX and BAK and induce MOMP (Fig. 1.7).

### A: indirect activator model



### B: direct activator-derepressor model

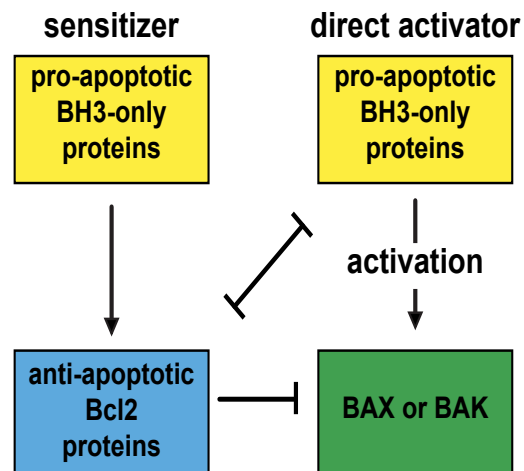


**Figure 1.7 | Regulation of MOMP by the Bcl2 protein family.** **A**, The indirect activator model postulates that BAX and BAK are bound in a constitutively active state to anti-apoptotic Bcl2 proteins. Competitive interactions with pro-apoptotic BH3-only proteins and anti-apoptotic Bcl2 proteins are sufficient to release active BAX and BAK and induce MOMP. **B**, The direct-activator-derepressor or neutralization model implies that BAX and BAK are activated after binding to a subset of BH3-only proteins, referred to as direct activators. Anti-apoptotic Bcl2-proteins prevent MOMP either by sequestering activated BAX and BAK or by inhibiting the direct activator BH3-only proteins. A second subset of BH3-only proteins cannot directly activate BAX or BAK but neutralize anti-apoptotic Bcl2 proteins. In the indirect activator model BAX and BAK are thought to be in a constitutively active state, and bound and thereby inhibited by anti-apoptotic Bcl2 proteins. In this model the competitive interaction of BH3-only proteins with anti-apoptotic Bcl2 proteins is sufficient to release of BAX and BAK and initiate MOMP.

In the direct activator-derepressor model (also called neutralization model), BAX and BAK are activated by the interaction with a subset of BH3-only proteins, such as BID and BIM, called direct activators. In this model, anti-apoptotic Bcl2 proteins either inhibit MOMP by antagonizing BAX or BAK directly or by sequestering the direct activator BH3-only proteins thus preventing them to activate BAX or BAK. A second subset of BH3-only proteins, called sensitizer, such as NOXA or BAD, cannot directly

activate BAX or BAK but antagonize anti-apoptotic Bcl2 proteins and thereby release BAX and BAK for the activation by direct activator BH3-only proteins (Fig. 1.7). Definitive proof for either model has been difficult to obtain, it is likely that certain aspects of both models are correct (Tait and Green, 2010).

## 1.4 p53-mediated apoptosis in response to DNA damage

In response to DNA damage, cells activate a highly conserved signalling network to arrest the cell cycle and initiate DNA repair. If the extent of damage is beyond repair capacity, additional pathways leading to the induction of apoptosis are activated to eliminate these potentially cancerous cells (Levine, 1997). The decision whether cell survival is sustained or the DNA damage induced apoptotic pathway (DDIA) is initiated depends on the nature of the DNA damage and the physiologic status of the damaged cell. For instance, thymocytes are highly primed to undergo DDIA. By contrast, primary fibroblasts appear to resist DDIA (Norbury and Zhivotovsky, 2004). In germ cells, mechanisms for limiting genome alterations are required for faithful propagation of the species, whereas in somatic cells, responses to DNA damage prevent the accumulation of mutations that might lead to altered cell proliferation. Not surprisingly, several genes that regulate cellular responses to DNA damage function as tumour suppressors and defects in the DDIA contribute to tumourigenesis.

Central in the DDIA is the ATM (ataxia telangiectasia mutated) family of PI3 kinases such as ATM and ATR (Wang, 1998) responding to double strand breaks and single-stranded lesions (Shiloh, 2003). ATM and ATR are responsible for the post-translational stabilization and thus accumulation of p53 (Oren, 1999). ATM directly phosphorylates p53 at serine 15 and indirectly at serine 20 residues through the induction of the CHK2 kinase (Banin et al., 1998). Phosphorylation of p53 is believed to be critical for the stabilization and activation of p53. Activated p53 translocates to the nucleus where it induces the transcription of several pro-apoptotic molecules, including BAX and the BH3-only proteins PUMA and NOXA (Miyashita and Reed, 1995; Nakano and Vousden, 2001; Oda et al., 2000) which in turn initiate MOMP and apoptosis (Fig. 1.8). Interestingly, p53 is required for DDIA in certain but not all cell types (Clarke et al., 1993; Lowe and Gold, 1993; Strasser et al., 1994).

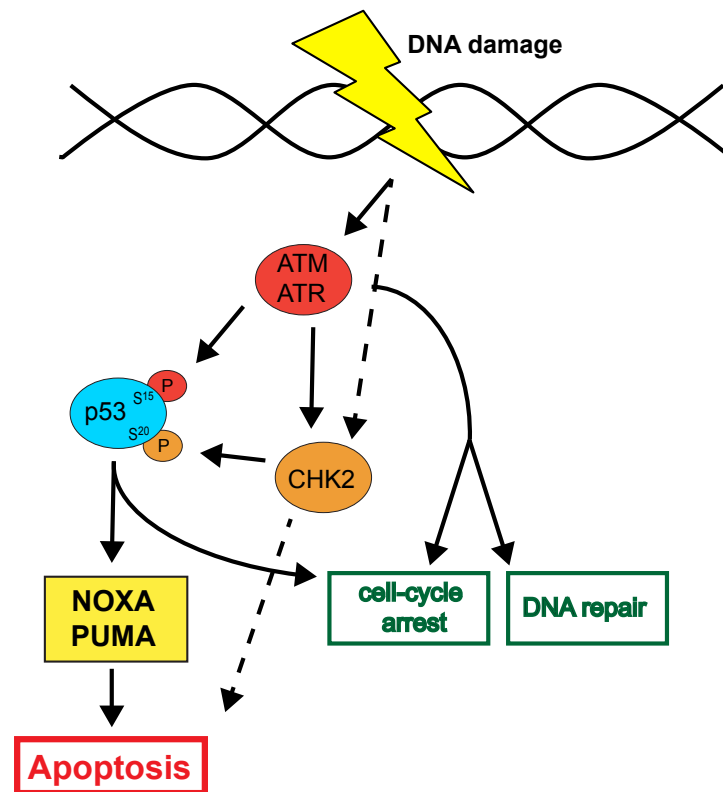


**Figure 1.8 | DNA damage-induced apoptosis.** Upon DNA damage ATM and ATR kinases get activated. ATM phosphorylates and thereby stabilizes p53 directly at serine 15 and indirectly at serine 20 by the induction of CHK2. Activated p53 induces the transcription of BAX, PUMA and NOXA, ultimately resulting in MOMP. Activated CHK2 can also induce apoptosis by less investigated p53-independent signalling pathways. Besides apoptosis, ATM/ATR also induce signalling pathways resulting in cell-cycle arrest and DNA repair.

Common anti-cancer chemotherapeutics frequently engage the DDIA and thus defects in this critical regulatory mechanism promote resistance of cancer cells to a variety of therapeutic agents. Since de novo protein synthesis is supposed to be essential in mediating DDIA, it is widely believed that deregulation of transcription represents the main factor giving rise to chemoresistance. For instance, loss of p53 function is described in over 50% of human cancers, resulting in the inability of p53-mediated transcriptional up-regulation of pro-apoptotic molecules (Hollstein et al., 1994). However, disturbed post-transcriptional regulatory mechanisms, such as degradation of components of the DDIA pathway are now beginning to be recognized as a potential mediators of chemoresistance.

## 1.5 The Ubiquitin-Proteasome System

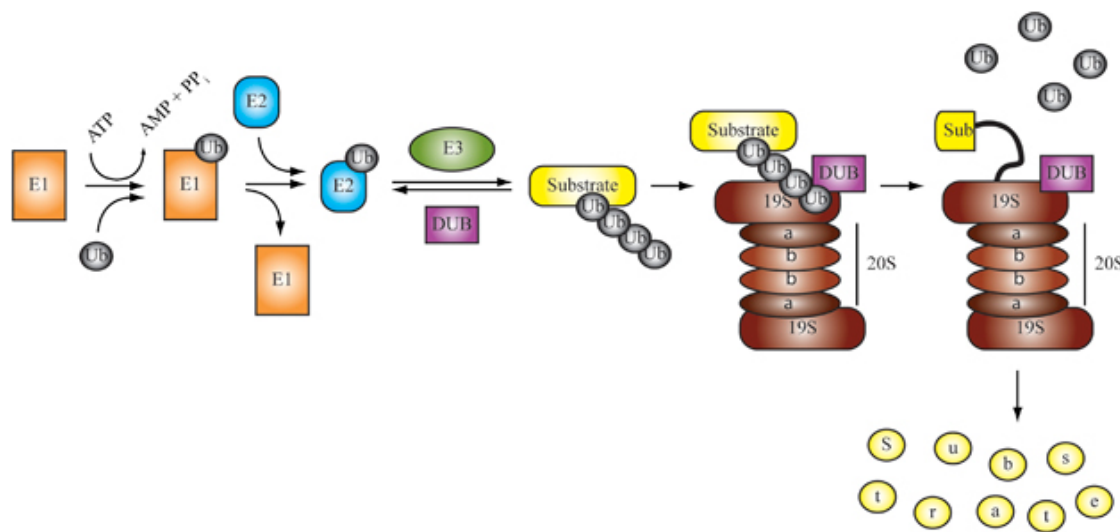
The Ubiquitin-Proteasome System (UPS) is the main driver of regulated protein degradation in all eukaryotic cells (Ciechanover et al., 1984). Defects in UPS pathway have been implicated in a number of human pathologies, most notably in cancer and neurodegenerative diseases. In addition to the regulation of critical cellular pathways, including cell growth and proliferation, protein quality control, DNA repair, transcription, and immune response the UPS plays a critical role in regulating cell death (Eldridge and O'Brien, 2010). On the one hand the UPS is responsible for the direct degradation of several proteins involved in the regulation of apoptosis, on the other hand the UPS impacts on the transcription of several pro- and anti-apoptotic proteins through the degradation of their transcription factors such as p53 (Bernassola et al., 2010).

Degradation of a protein by the UPS involves two distinct and successive steps: (i) covalent attachment of multiple ubiquitin molecules to the target protein, and (ii) degradation of the tagged protein by the 26S proteasome.

Proteins are targeted for proteasomal degradation by the covalent attachment of multiple ubiquitin molecules (Ub). The Ub conjugating system operates in a three-step mechanism, with three distinct enzymes catalyzing each step. First, a Ub gets activated in its amino-terminal glycine by the Ub-activating enzyme (E1). Next, the activated Ub is transferred by one of several dozens of Ub-conjugating enzymes (E2) to one of several hundreds of substrate specific Ub-ligases (E3s) that finally attaches the Ub to the target protein (Pickart, 2001; Wilkinson, 1999). Finally, there are nearly 100 deubiquitylating enzymes (DUBs) that counter the activity of E3 ligases in regulatory pathways, as well as functioning in ubiquitin maturation and ubiquitin cleavage and -recycling at the 26S proteasome (Fig. 1.9) (Nijman et al., 2005).

The first Ub is either transferred to a  $\epsilon$ -NH<sub>2</sub> group of a lysine residue (K) of the target protein to generate an isopeptide bond, or in a linear manner to the N-terminal residue of the substrate. Subsequent Ub addition can occur through isopeptide linkage on all of ubiquitin's seven lysine residues as well as its N-terminal primary amine, thereby generating a diverse range of chain topologies that can drive a variety of different protein fates (Breitschopf et al., 1998; Peng et al., 2003). K48-linked polyubiquitin chains serve as a specific tag for protein degradation by the 26S proteasome, while other polyubiquitin chains such as K63 chains are involved in

other signalling processes such as NF $\kappa$ B-activation and DNA repair (Chen, 2005; Sun and Chen, 2004; Voges et al., 1999).



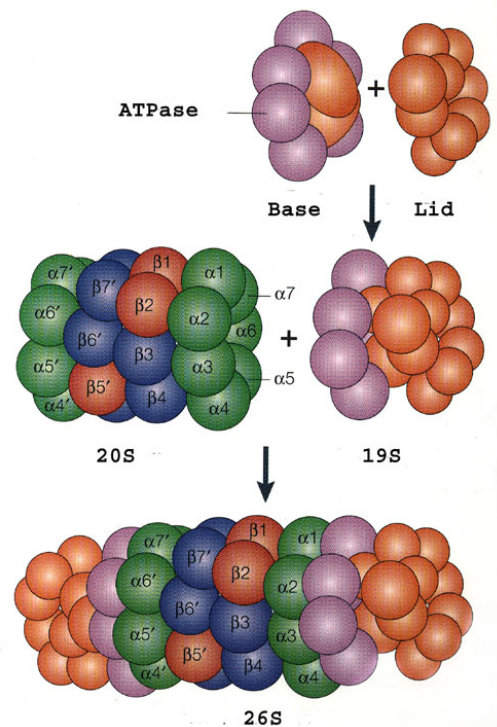
Eldridge and O'Brien, 2010

**Figure 1.9 | The Ubiquitin Proteasome System.** Ubiquitin is activated and conjugated to target proteins by a conserved series of E1 (ubiquitin-activating enzyme), E2 (ubiquitin-conjugating enzyme), and E3 (ubiquitin ligase) activities. In some cases, an isopeptidase or a deubiquitylating enzyme (DUB) may oppose the activity of the E3. Polyubiquitylated proteins are recruited (via ubiquitin receptors) to the 26S proteasome, a multisubunit, barrel-shaped cellular protease consisting of a 20S core particle bound at one or both ends by 19S cap particles. This 19S cap confers both ATP- and ubiquitin-dependency to proteolysis by the 26S proteasome, and contains isopeptidase activities that remove ubiquitin from the substrate for recycling and ATPase activities that unfold the substrate and feed it into the 20S core for degradation (Eldridge and O'Brien, 2010).

The 26S proteasome is a multisubunit protease complex, which in eukaryotic cells shows both nuclear and cytosolic localization. It is comprised of the 20S proteasome, which serves as the catalytic core, as well as two regulatory 19S subunits (cap) at either end. The regulatory 19S cap is composed of an 11-protein lid and a 10-protein base. The lid is responsible for recognition of polyubiquitylated substrates and detachment of the poly-Ub-chain. The base is essential for substrate-unfolding and entry of the substrate into the 20S core. The 20S core is responsible for proteolysis of the substrates (Voges et al., 1999). It comprises three different catalytic subunits ( $\beta$ 1,  $\beta$ 2,  $\beta$ 5), each with a different proteolytic specificity: the trypsin-like-activity ( $\beta$ 1), caspase-like-activity ( $\beta$ 2) and chymotrypsin-like-activity ( $\beta$ 5) (Fig. 1.10). In all three  $\beta$ -subunits, a threonin-residue in the catalytic centre is essential for



catalysis, with the  $\gamma$ -hydroxy-group serving as nucleophile and the  $\alpha$ -amino-group serving as proton-donor/acceptor during hydrolysis (Dick et al., 1998; Nussbaum et al., 1998).



Klötzel et al., 2001

**Figure 1.10 | Structure of the 26S proteasome.** The 26S proteasome is comprised of two 19S regulatory subunits and a 20S core unit.

The 19S complex consists of two sub-complexes: (i) the base (purple), which includes six AAA-ATPases and two non-ATPase proteins, is responsible for protein-unfolding and entry into the 20S core; and (ii) the lid (orange) consisting of 9 non-ATPase proteins, which is responsible for poly-Ub-recognition and detachment.

The 20S catalytic core complex is assembled of 28 subunits (14 different) building the outer  $\alpha$ -subunits (green) and the inner  $\beta$ -subunit (blue). The  $\beta$ -subunit includes the catalytic centres  $\beta$ 1,  $\beta$ 2,  $\beta$ 5 (red) responsible for caspase-like, trypsin-like and chymotrypsin-like activity, respectively.

### 1.5.1 Inhibition of the UPS as a therapeutic approach

Given the important role of the UPS in maintaining protein homeostasis and in regulating cellular processes such as apoptosis, the inhibition of components of the UPS has been seen as a promising target in the development of new therapeutics in the anti-cancer treatment. In 1994 inhibitors of the proteasome have first been described to induce apoptosis (Rock, Gramm et al. 1994), probably by changing the expression level of pro- and anti-apoptotic proteins, for instance pro-apoptotic members of the Bcl2 protein family. Accordingly, several pro-apoptotic members,

such as BAX, BIK, BIM and NOXA have been reported to accumulate upon proteasome inhibition. While BAX and BIK are thought to accumulate due to a block in their proteasomal degradation (Liu et al., 2008; Zhu et al., 2005), NOXA and BIM accumulation is reported to occur at the transcriptional level as a result of stabilization of their transcription factors, such as p53 (Fernandez et al., 2005; Perez-Galan et al., 2006).

The proteasome inhibitor bortezomib (PS-341, Velcade) (Adams, 2002) was the first drug that targets a component of the UPS and was first approved for clinical use in the United States (Chauhan, Hideshima et al. 2005). Bortezomib functions as a reversible inhibitor of the chymotrypsin-like activity of the 26S proteasome with a  $K_i$  of 0.6 nM. It binds the catalytic threonine in the active site of the  $\beta 5$  subunit, which also results in a reduction of the catalytic activities of the caspase-like and trypsin-like subunits. Developed by ProScript Inc in 1995, Bortezomib entered clinical trials in 1997 and was approved by the Federal Drug Administration (FDA) in 2003. Bortezomib-treatment results in clinical benefit in the treatment of haematological malignancies, such as multiple myeloma or mantle cell lymphoma. Bortezomib is currently undergoing Phase III clinical trials for follicular non-Hodgkin's lymphoma, in Phase II trials for diffuse large B cell lymphoma, and a great many other clinical trials (Yang et al., 2009). Interestingly, bortezomib-induced apoptosis preferentially occurs in malignant but not in non-malignant cells of some tumour tissues, although the detailed mechanism is still under investigation (Fernandez et al., 2005; Qin et al., 2005).

Besides the clinical benefit, substantial side-effects and resistance have been observed following bortezomib-treatment. Furthermore, the effect of bortezomib in the treatment of solid tumours has been less promising. Nevertheless, the surprising efficacy (and rapid clinical approval) of bortezomib for the treatment of multiple myeloma and mantle cell lymphoma has encouraged researchers to explore the possibility of targeting other components of the UPS in order to introduce more specific anti-cancer therapies.

## **1.6 Aim of the work**

Numerous reports show that compounds inhibiting proteasomal activity are able to selectively induce tumour cell apoptosis (Rock, Gramm et al. 1994). However the

underlying mechanisms giving rise to the selective cytotoxicity of tumour cells toward proteasome inhibitors are incompletely understood. Bortezomib, a pharmacological inhibitor of the proteasome, is already successfully used in the clinical treatment of several types of cancer. However, besides beneficial effects substantial side-effects and resistance have been reported (Yang et al., 2009). Nevertheless, the initial beneficial effects clearly highlight the promising role of the UPS as a valuable therapeutic target in the treatment of cancer.

The current work aims to understand the detailed mechanisms of bortezomib-induced apoptosis. Moreover, the knowledge of why tumour cells are more susceptible to proteasome inhibitors may contribute to understand the pathophysiology of malignant transformation and may facilitate efforts aiming to design a novel anti-cancer therapy.

## 2 Material and methods

### 2.1 Chemicals

Unless indicated otherwise, all chemicals were from Roth (Karlsruhe, Germany) or Sigma (Deisenhofen, Germany).

Trichostatin A, 5-Aza-2'-Deoxycytidine, etoposide, doxorubicin, and LDN-57444 were from Sigma (Deisenhofen, Germany) and bortezomib from Teva (Berlin, Germany).

### 2.2 DNA constructs

For construction of GFP-fusion proteins, open reading frames (ORF) encoding human NOXA-wt, NOXA-K0 or UCH-L1, were amplified by PCR and cloned into pEGFP-C3 vector (Clontech, Takara Bio Europe, Saint-Germain-en-Laye, France). GFP-UCH-L1<sup>D176N</sup> was obtained by site directed mutagenesis PCR using GFP-UCH-L1 as template and UCH-L1-mut primer.

For the construction of myc-fusion proteins ORF encoding human NOXA-wt or NOXA-K0 were amplified by PCR and cloned into pCDNA3.1+ vector (Invitrogen, Karlsruhe, Germany) already containing an amino-terminal myc-sequence.

For the construction of HA-fusion proteins ORF encoding human NOXA-wt or NOXA-K0 were amplified by PCR with primers encoding an amino-terminal HA-sequence and cloned into pCDNA3.1+ vector.

NOXA-wt and NOXA-K0 cDNA were obtained from Addgene (Cambridge, USA).

Myc-UCH-L1 cDNA was a kind gift from Prof. K.J. Lee (Ewha Womans University, Seoul, Korea).

Myc-XIAP has been described previously (Kashkar et al., 2007).

All PCR amplifications have been performed with appropriate primers containing specific restriction sequences using Phusion™ High Fidelity DNA Polymerase. After restriction with the appropriate enzyme PCR-Fragments and vectors have been

separated by agarose gel electrophoresis (Agarose from Peqlab, Erlangen, Germany) in TE buffer (10 mM Tris-Cl, pH 7.5. 1 mM EDTA) using ethidiumbromide for nucleic acid staining, cleaned up with NucleoSpin® Gel and PCR Clean-up Kit and ligated using the Rapid DNA Ligation Kit according to the instructions of the manufacturer with a molecular template:vector ratio of 3:1. Plasmid-DNA has been propagated in *E.coli XL1-blue* and prepared using NucleoSpinPlasmid (Mini) or NucleoBondPlasmid (Maxi) according to the instructions of the manufacturer. All constructs used in this work have been sequenced by GATC (Tübingen, Germany).

**Table 2.1 | Kits and enzymes used for the construction of DNA constructs**

Name	Company
Phusion™ High Fidelity DNA Polymerase	Finnzymes, Fisher Scientific GmbH, Schwerte, Germany
Rapid DNA Ligation Kit	Fermentas, Leon-Roth, Deutschland
Restriction enzymes	Fermentas, Leon-Roth, Deutschland
NucleoSpinPlasmid (Mini) NucleoBondPlasmid (Maxi)	<i>MACHEREY-NAGEL GmbH &amp; Co. KG, Düren, Germany</i>
NucleoSpin® Gel and PCR Clean-up	<i>MACHEREY-NAGEL GmbH &amp; Co. KG, Düren, Germany</i>

**Table 2.2 | DNA constructs used in this work with specific primers**

Construct in pEGFP-C3	MW (kDa)	aa (bp)	5' primer with restriction side	3' primer with restriction side
GFP-NOXA-wt	35,9	915	5' EcoR1-NOXA	3' BamH1-NOXA
GFP-NOXA-K0	35,9	915	5' EcoR1-NOXA	3' BamH1-NOXA
GFP-UCH-L1	52,7	1413	5' HindIII-UCH-L1	3' BamH1-UCH-L1
GFP-UCH-L1 <sup>D176N</sup>	52,7	1413	5' UCH-L1-mut	3' UCH-L1-mut

Construct in pCDNA3.1+	MW (kDa)	aa (bp)	5' primer with restriction side	3' primer with restriction side
HA-NOXA-wt	7,8	192	5' HindIII-HA-NOXA-wt	3' XhoI-NOXA
HA-NOXA-K0	7,8	192	5' HindIII-HA-NOXA-K0	3' XhoI-NOXA
Myc-NOXA-wt	8,2	210	5' BamH1-NOXA	3' XhoI-NOXA
Myc-NOXA-K0	8,2	210	5' BamH1-NOXA	3' XhoI-NOXA

**Table 2.3 | Primer used for the generation of DNA constructs used in this work**

<b>Primer name</b>	<b>Sequence (5'-3')</b>
5' BamH1-NOXA	CCC CCC CCC GGA TCC ATG CCT GGG AAG AAG GCG CG
3' XhoI-NOXA	CCC CCC CCC TCG AGT CAG GTT CCT GAG CAG AAG
5' EcoR1-NOXA	CCC CCC CCG AAT TCT GAT GCC TGG GAA GAA GGC GCG
3' BamH1-NOXA	CCC CCC CCG GAT CCT CAG GTT CCT GAG CAG AAG
5' HindIII-UCH-L1	GAT CAA GCT TAT GCA GCT CAA GCC GAT GGA G
3' BamH1-UCH-L1	GAT CGG ATC CTT AGG CTG CCT TGC AGA GAG C
5' HindIII-HA-NOXA-wt	GAT CAA GCT TAC ATG TAC CCA TAC GAT GTT CCA GAT TAC ATG CCT GGG AAG AAG GCG CGC
5' HindIII-HA-NOXA-K0	GAT CAA GCT TAC ATG TAC CCA TAC GAT GTT CCA GAT TAC ATG CCT GGG AGA AGA GCG CGC
5' UCH-L1-mut	GGC CAC CTC TAT GAA CTT AAT GGA CGA ATG CCT TTT C
3' UCH-L1-mut	ATC CAC GTT GTT AAA CAG AAT AAA ATG G

## 2.3 Cell culture and transfection

All cell culture media and additives were from Biochrom (Berlin, Germany). Plastic material was obtained from TPP (Trasadingen, Switzerland), Nunc (Roskilde, Denmark) or BD Biosciences (Falcon™, Franklin Lakes, USA).

The establishment and maintenance of the following cells and cell lines has been described previously: *L428*, *L591*, *L1309* (Kashkar et al., 2007), *MeWo* (Seeger et al., 2010), *SKmel23*, *SKmel28*, *MV3*, *WM164* (Zigrino et al., 2005), *Colo38* (Giacomini et al., 1986), and primary melanoma cells derived from *Pat1* (HOM1), *Pat2* (HM1), *Pat3* (MOO1) (Schmidt et al., 2011). *HEK293FT*, *HeLa*, *DLD1*, *HT29* and *LS174T* were from ATCC (CRL-11268, Rockville, MD, USA) and maintained according to the instructions of the manufacturer.

In brief, cells were expanded to an adequate amount and several aliquotes were frozen by -150°C in FCS containing 10% DMSO. Experiments were performed after resawing and expanding of cells to 4 passages. Cells were cultured at 37°C in the following media:

**Table 2.4 | Cell culture media used in this work**

<b>Name</b>	<b>Media</b>	<b>Additives</b>
<i>L428, L591, L1309, LS174T, DLD1</i>	VLE-RPMI	10% FCS 1% penicillin/streptomycine
<i>MeWo, SKmel23, MV3, WM164, SKmel28, Colo38 Pat1 (HOM1), Pat2 (HM1) Pat3 (MOO1)</i>	VLE-RPMI	10% FCS 1% penicillin/streptomycine 1% non-essential aa
<i>HEK293FT</i>	DMEM	10% FCS 1% penicillin/streptomycine 1% non-essential aa 2 mM L-glutamine 10 mM sodium pyruvate 2400 U/ml G418
<i>HeLa, HT29</i>	DMEM	10% FCS 1% penicillin/streptomycine

Primary melanoma cells and HeLa cells were transfected using Lipofectamine™ LTX (Invitrogen, Karlsruhe, Germany). *HEK293FT* cells were transfected using the standard calcium phosphate method (Wiegler et. al, 1978).

For siRNA mediated knock-down *Pat1* cells were transfected with 100 pmol/μl siRNA using Lipofectamine™ LTX (Invitrogen, Karlsruhe, Germany).

**Table 2.5 | siRNAs used in this work**

<b>Name</b>	<b>Sequence</b>	<b>Company</b>
siUCH-L1	sense: AAGUUAGUCCUAAAGUGUAtt antisense: UACACUUUAGGACUAACUuct	Ambion, Applied Biosystems
Alexa Fluor-594-labelled scr-control RNA	All star non targeting mix	Invitrogen, Karlsruhe, Germany

## 2.4 Cytotoxic treatments and cell viability

Cells ( $10^5$  per well) were incubated in 96-well plastic plates at 37°C in full media and treated with increasing concentrations of etoposide, doxorubicin, 5-Aza-2'Deoxy-

cytidine, Trichostatin A, LDN-57444 or bortezomib and incubated for the indicated time periods.

Cell viability was assessed by XTT test (XTT cell viability kit, Roche Applied Sciences, Mannheim, Germany) according to the instructions of the manufacturer. Briefly, after treatments cells were incubated with the XTT reagents at 37°C for 4 hours. The absorbance of the samples was measured with an enzyme-linked immunosorbent assay (ELISA) reader (HT III, Anthos Lab Tech Instruments, Salzburg, Austria) by wavelength 450 nm and reference wavelength 620 nm. The data are mean values of 3 different experiments in triplicate. Values of absorbance of untreated cells (after background subtraction) were set as 100 % viability.

Cell death was measured by trypan blue exclusion using an automated cell counter (Countess™, Invitrogen, Karlsruhe, Germany).

## 2.5 qPCR

Total RNA was isolated from indicated cells using the standard phenol-chloroform-method (Chomczynski and Sacchi, 1987).

cDNA was synthesised using RevertAid™ Premium First Strand cDNA Synthesis Kit (Fermentas, Leon-Roth, Deutschland) using polyT-primers according to the manufacturer's instructions. qPCR was performed with specific primers for NOXA (fw GCT CCA GCA GAG CTG GAA GT; rev CCA TCT TCC GTT TCC AAG GGC) and GAPDH as a reference (fw GGT ATC GTG GAA GGA CT; rev GGG TGT CGC TGT TGA A) using LightCycler® SYBR-Green I Mix (Roche Applied Sciences, Mannheim, Germany) with a 96well-plate Multicolor Real-Time PCR Detection System (iQ™5, BIO-RAD, Herkules, USA) and data were further evaluated using the Pfaffl-method (Pfaffl, 2001).

## 2.6 Sample preparation and immunoblotting (IB)

Whole cell extracts were prepared by incubating cell pellets in CHAPS lysis buffer on ice for 20 minutes. Samples were centrifuged, and supernatants were recovered. Poly (ADP-ribose) polymerase (PARP) cleavage was assessed after incubation of cell pellets in urea extraction buffer following denaturation at 100°C for 10 minutes.



Protein concentration was determined using BCA Assay Protein Quantification (Pierce, Bonn, Germany) according to the instructions of the manufacturer.

Equal amounts of protein were separated by sodium dodecyl sulfate–polyacrylamide gel electrophoresis (SDS-PAGE) using the Miniprotean3 PAGE and Western Blotting Apparatus (BIO-RAD laboratories, Herkules, USA).

Samples were heated in SDS sample buffer for 5 minutes at 100°C and centrifuged 2 minutes at 20,000 x g. Polyacrylamid gels (10 – 14%) were started at 120 mV and continued at 180 mV in SDS running buffer. After blotting gels on nitrocellulose membranes (Protan, Schleicher & Schuell, GE healthcare, Freiburg, Germany) for 90 minutes in blot transfer buffer, membranes were blocked for 30 minutes in blocking buffer and incubated with primary antibody, diluted in antibody dilution buffer for one hour. After washing and incubation with secondary antibody for one hour, signals were detected on film (Amersham Inc., GE healthcare, Freiburg, Germany) using enhanced chemiluminescence (ECL Western Blotting Substrate, Pierce, Bonn, Germany).

**Table 2.6 | Antibodies used for IB**

Anti-β-Actin	Mouse-IgG, monoclonal	Sigma Deisenhofen, Germany
Anti-BIM	Rabbit-IgG, monoclonal	Cell Signaling, Boston, USA
Anti-Caspase-9	Rabbit-IgG, monoclonal	Cell Signaling, Boston, USA
Anti-GFP	Mouse-IgG, monoclonal	Roche Diagnostics GmbH, Mannheim, Germany
Anti-MYC	Mouse-IgG, monoclonal	Invitrogen, Karlsruhe, Germany
Anti-NOXA	Mouse-IgG, monoclonal	Calbiochem, USA
Anti-PARP	Mouse-IgG, monoclonal	BD PharMingen, USA
Anti-PUMA	Rabbit-IgG, monoclonal	Cell Siganling, Boston, USA
Anti-Ubiquitin-K48-specific (Apu2)	Rabbit-IgG, monoclonal	Millipore, Schwalbach, Germany
Anti-UCH-L1	Rabbit-IgG, monoclonal	Cell Signaling, Boston, USA
Anti-UCH-L3	Rabbit-IgG, monoclonal	Cell Signaling, Boston, USA
Anti-XIAP	Mouse-IgG, monoclonal	BD Transduction Laboratories, USA
Anti-Rabbit IgG HRP-linked	Goat	Sigma, Deisenhofen, Germany
Anti-Mouse IgG HRP-linked	Goat	Sigma, Deisenhofen, Germany

**Table 2.7 | Buffers used for sample preparation and IB**

Antibody dilution buffer	50 mM Tris, pH 7.6 150 mM NaCl 0.1% Tween-20 5% BSA
Blocking buffer	10 mM Tris-HCl, pH 7.4-7.6 150 mM NaCl 5% milk powder 2% BSA 0.1% Tween-20
Blot transfer buffer	25 mM Tris-HCl 190 mM glycine 20% methanol
CHAPS lysis buffer	10 mM HEPES, pH 7.4 150 mM NaCl 1% CHAPS complete protease inhibitor cocktail
SDS sample buffer (5x)	25% glycerol 0.6 M Tris-HCl 144 mM SDS 0.1% bromophenol blue
SDS running buffer	190 mM glycine 20 mM Tris 0.1% SDS
S-PBS	120 mM NaCl 10 mM NaH <sub>2</sub> PO <sub>4</sub> 30 mM K <sub>2</sub> HPO <sub>4</sub> pH 7.6
Urea extraction buffer	50 mM Tris, pH 6.8 6 M urea 3% SDS 10% glycerol 0.00125% bromophenol blue 5% 2-mercaptoethanol

## 2.7 Immunoprecipitations (IP)

For the detection of ubiquitylated tagged-NOXA in *HEK293FT* cells, cells were transfected with indicated plasmids. 24 hours after transfection *HEK293FT* cells were denaturated prior Immunoprecipitation (IP). Cells were lysed in 100 µl IP-lysis buffer containing 1% SDS and boiled for 30 minutes. The lysate was diluted with 900 µl IP-lysis buffer to obtain a final SDS concentration of 0.1% and HA- or myc-tagged protein IP was performed by magnetic epitope labelling using HA- or myc-tag µMACS Epitope Tag Protein Isolation Kit (Miltenyi Biotec, Bergisch Gladbach, Germany) according to the instructions of the manufacturer. Due to restricted material transfected *Pat1-2* cells were directly lysed in IP-lysis buffer 24 hours after transfection and tag-specific IP was performed without prior denaturation. After binding columns were washed 6 x with washing buffer 1 and 1x with washing buffer 2. IPs were eluted with elution buffer and further analysed by IB.

For binding assays *HEK293FT* cells were transfected with indicated plasmids. 24 hours after transfection cells were lysed in IP-lysis buffer and GFP-tagged protein IP was performed by magnetic epitope labelling using GFP-tag µMACS Epitope Tag Protein Isolation Kit (Miltenyi Biotec, Bergisch Gladbach, Germany) according to the instructions of the manufacturer. After binding columns were washed 3x with IP-lysis buffer, eluted with elution buffer and further analysed by IB.

**Table 2.8 | Buffers used for IP**

IP-lysis buffer	150 mM NaCl 1% Triton X-100 50 mM Tris HCl, pH 8.0
Washing buffer 1	150 mM NaCl 1% NP-40 0.5% sodium deoxycholate 0.1% SDS, 50 mM Tris-HCl, pH 8.0
Washing buffer 2	20 mM Tris-HCl, pH 7.5
Elution buffer	50 mM Tris-HCl 50 mM DTT 1% SDS 0.005% bromophenol blue 10% glycerol, pH 6.8

## 2.8 In vitro deubiquitylation and binding assays

*HEK293FT* cells were transfected with HA-NOXA or myc-NOXA and treated for 24 hours with 100 nM Bortezomib 8 hours post-transfection. Cells were washed twice with PBS and mechanically pulped in deubiquitylation assay-buffer (50 mM HEPES/NaOH, pH 7.8, 0.5 mM EDTA, 1 mM DTT, 0.1 mg/ml ovalbumin). Equal amounts were incubated with recombinant UCH-L1-GST or UCH-L3-HIS (ENZO lifescience, Lörrach, Germany) at 25°C. The lysate was diluted 1:10 with IP-lysis buffer to reduce the DTT concentration to 0.1 mM prior IP.

## 2.9 Fluorescence microscopy

Cells grown on coverslips were transfected with indicated plasmids. 24 hours after transfection cells were washed twice with cold PBS. Cells were then fixed with 3% paraformaldehyde in PBS for 20 minutes and blocked with 3% bovine serum albumin (BSA) in PBS (blocking buffer) for 30 minutes. Cells were permeabilised with 0.1% saponin during blocking, and incubated with the appropriate primary antibody in blocking buffer over night at 4°C. Cells were washed twice for 5 minutes with blocking buffer and incubated with secondary antibody for 1 hour at room temperature. Cells were washed twice with blocking buffer for 5 minutes and once with PBS for 5 minutes. Dapi (Molecular Probes, Invitrogen, Karlsruhe, Germany) was added into the first washing step (1:5000) for nuclei staining.

Cells were mounted on glass slides and examined using an Olympus IX81 fluorescence microscope (Objective: 60x PLAPO oil, NA 1.4) or a Leica DMIRE2 confocal microscope. If appropriate, images were processed using CellP deconvolution software (Olympus SIS).

**Table 2.9 | Antibodies used for fluorescence microscopy**

Anti-NOXA	Mouse-IgG, monoclonal	Calbiochem, USA
Alexa Fluor 568 anti-mouse	Goat	Molecular Probes, Invitrogen, Karlsruhe, Germany

## 2.10 Flow cytometry (FACS)

For the analyses of NOXA protein stability *Pat1-2* cells were transfected with GFP-NOXA and pDsRed-Express-N1 vector (Clontech, Takara Bio Europe, Saint-Germain-en-Laye, France). Cells were fixed with 3% Paraformaldehyde in PBS and analysed by flow cytometry (BD FACSCalibur™, BD Biosciences, Heidelberg, Germany) and further evaluated with the FlowJo software (Ashland, USA). Relative GFP-NOXA or dsRed expression of transfected cells was assed using FITC-median or PE-median, respectively. Values represent fold induction of NOXA-expression to control sample while each sample was normalized to fold induction of dsRed expression to account possible differences in transfection efficiency.

For the detection of endogenous NOXA cells *Pat2 cells* were transfected with GFP-UCH-L1, GFP-UCH-L1<sup>D176N</sup> or GFP-control vector. 24 hours after transfection cells were washed twice with cold PBS. Cells were then fixed with 3% paraformaldehyde/PBS for 20 minutes and blocked with 3% bovine serum albumin (BSA) in PBS (blocking buffer) for 30 minutes. Cells were permeabilised with 0.1% saponin during blocking, and incubated with the appropriate primary anti-NOXA antibody in blocking buffer over night. Cells were washed twice with blocking buffer and incubated with secondary Alexa Fluor 568 goat anti-mouse antibody for one hour. Cells were washed twice with PBS. NOXA expression was assed using PE-Median in GFP-positive cells and further evaluated with the FlowJo software. Values represent fold induction of NOXA-expression relative to GFP-control samples.

**Table 2.10 | Antibodies used for flow cytometry**

Anti-NOXA	Mouse-IgG, monoclonal	Calbiochem, USA
Alexa Fluor 568 anti-mouse	Goat	Molecular Probes, Invitrogen, Karlsruhe, Germany

## 2.11 Tissue immunohistochemistry (IHC)

Paraffin embedded tissues, 6 mm sections, were deparaffinised through three changes of xylene, incubating 10 minutes in each change. Slides were hydrated to water by dipping them 20–30 times in each of two changes of 100% ethanol, two

changes of 95% ethanol, one of 80% ethanol, one of 70% ethanol, and two changes of distilled water. Slides were placed in a 95°C water bath, covered with 10 mM Citrate buffer (pH 6) for 20 minutes. Thereafter slides were cooled for 30 minutes, rinsed in distilled water twice and once in TBS for 5 minutes. Tissue specimens were stained with the specific antibodies overnight at 4°C in humidified atmosphere. Slides were washed three times for 15 minutes in TBS and incubated with HRP-labelled anti-rabbit or anti-mouse polymer (Dako Envision®, Dako, Hamburg, Germany) for 1 hour at room temperature. Slides were washed three times for 15 minutes in TBS and bound antibodies were detected with AEC substrate (Dako Envision®, Hamburg, Germany). Nuclei were stained with haematoxylin (Thermo Scientific, Fisher Scientific GmbH, Schwerte, Germany). Specimens of human stomach were used as positive control for both antibodies staining (kindly provided from the local Department of Pathology), negative controls were performed by omitting primary specific antibodies.

**Table 2.11 | Antibodies used for tissue IHC**

Anti-NOXA (36833)	Rabbit-IgG, polyclonal	Abcam, Cambridge, UK
Anti-UCH-L1 (1673P)	Mouse-IgG, monoclonal	Acris, Herford Germany

### 3 Results

#### 3.1 Proteasome inhibition induces mitochondrial apoptosis in a cohort of tumour entities

Previous data demonstrated that proteasome inhibition has a selective anti-tumour activity and significant efficacy against a variety of malignancies (Almond and Cohen, 2002; Fennell et al., 2008; Hoeller and Dikic, 2009; Orłowski and Kuhn, 2008). Bortezomib, a pharmacologic inhibitor of the Ubiquitin Proteasome System (UPS), is being used successfully in the treatment of malignant diseases where it improves clinical outcomes. These beneficial effects clearly highlight the role of the UPS as a target for anti-cancer therapy. Therefore, understanding the molecular mechanism of proteasome inhibition in promoting tumour cell death may advance our knowledge about the pathways governing cellular homeostasis. Furthermore, this knowledge may additionally facilitate efforts aiming at the design and introduction of new cancer therapeutics.

Our viability analysis (XTT assay) of primary tumour cells derived from three melanoma patients (Seeger et al., 2010) after bortezomib-treatment showed that tumour isolates from different individuals display a highly diverse susceptibility to proteasome inhibition (Fig. 3.1A). In contrast to tumour cells derived from patient 1 (*Pat1*), *Pat2* tumour cells were highly susceptible to bortezomib. Bortezomib-mediated cell death was caused by mitochondrial apoptosis as monitored by immunoblot (IB)- analyses of caspase 9 (casp9) activation/processing and PARP cleavage (Fig. 3.2A).

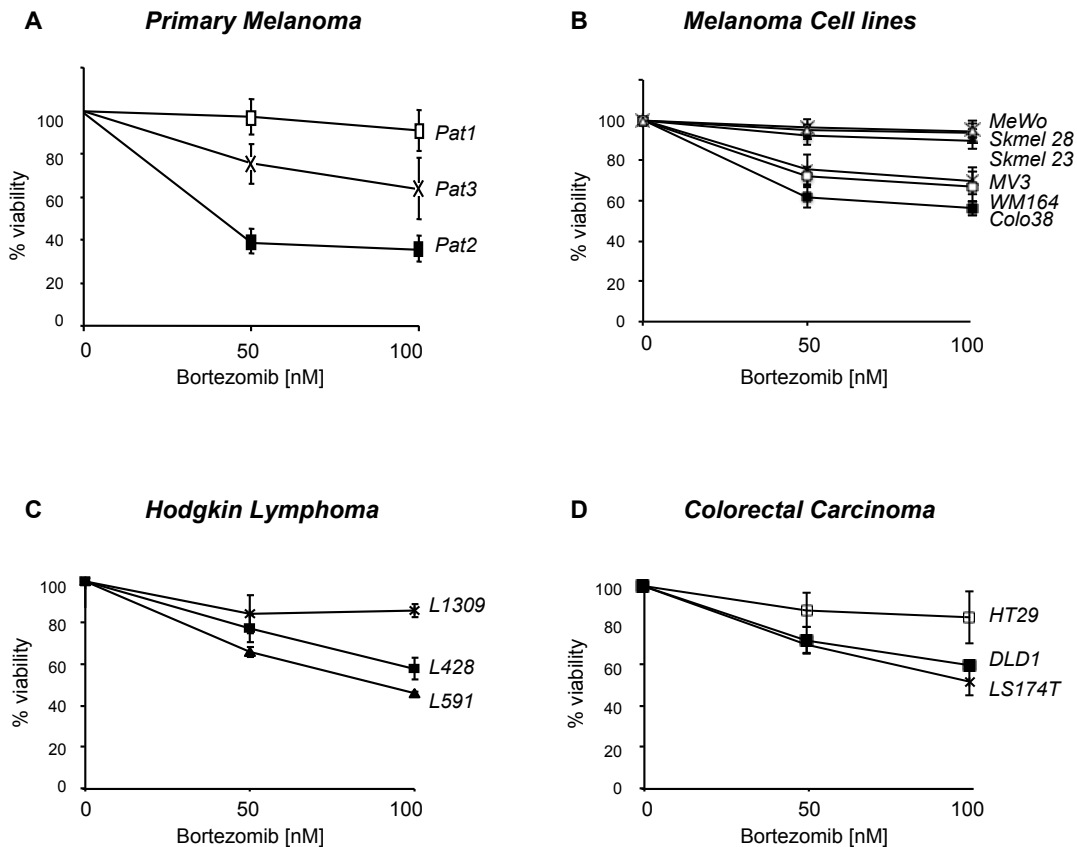


**Figure 3.1 | Cytotoxic effect of proteasome inhibition in different tumour cells.** Cell viability assay (XTT) 24 hours after treatment with increasing concentrations of bortezomib in cells derived from melanoma patients (*Pat1-3*) (A), melanoma cell lines (*MeWo*, *Skmel28*, *Skmel23*, *MV3*, *WM164*, *Colo38*) (B), Hodgkin Lymphoma (*L428*, *L591*) and control B-cell lines (*L1309*) (C) and colorectal carcinoma cell lines (*DLD1*, *LS174T*, *HT29*) (D).

Similar results in cell viability analyses and analyses of the mitochondrial apoptotic pathway were obtained when established tumour cell lines derived from melanoma (Fig 3.1B, Fig. 3.2B), Hodgkin Lymphoma (HL) (Fig. 3.1C, Fig. 3.2C) or colorectal carcinoma (CRC) patients (Fig. 3.1D, Fig. 3.2D) were exposed to bortezomib. These analyses consistently identified a cohort of tumour cells proved to be highly susceptible to proteasome inhibition.



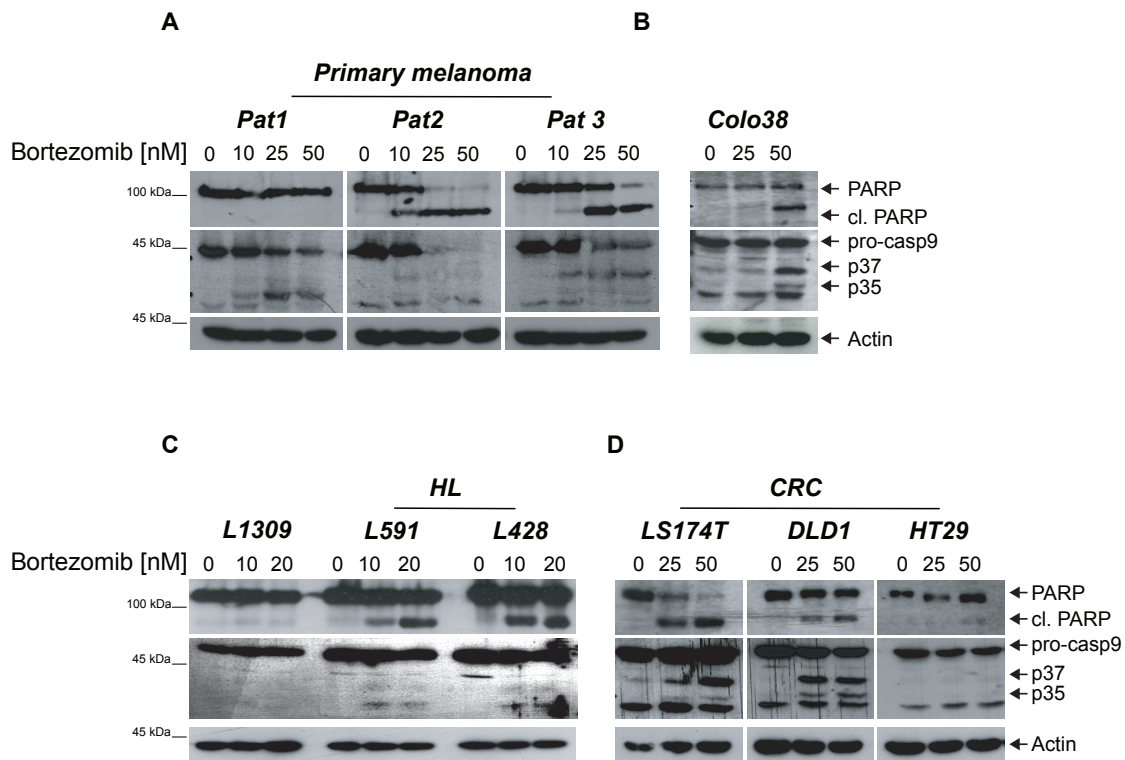


**Figure 3.2 | Proteasome inhibition engages the mitochondrial apoptotic pathway in bortezomib-sensitive tumours.** Tumour cells derived from melanoma patients (*Pat1-3*) (**A**), a melanoma cell line (*Colo38*) (**B**), Hodgkin Lymphoma (HL) cell lines (*L591*, *L428*) and a control B-cell line (*L1309*) (**C**), and colorectal carcinoma (CRC) cell lines (*LS174T*, *DLD1*, *HT29*) (**D**) were treated with increasing concentrations of bortezomib for 24 hours. IB-analyses of PARP processing were performed on nuclear extracts. IB-analyses of caspase-9 (casp9) activation/processing resulting in the p37 and p35 fragments were performed on whole cell lysates. Actin served as a loading control.

The mitochondrial apoptotic pathway is tightly controlled by the Bcl2 protein family comprising anti-apoptotic and pro-apoptotic members that are controlled by a third class of pro-apoptotic members called BH3-only proteins. Accordingly, therapeutic targeting of the crosstalk between BH3-only and Bcl2 proteins represents a promising treatment strategy for cancer (Kelly and Strasser, 2011). Indeed, several previous reports indicated that proteasome inhibition induces the mitochondrial apoptotic pathway predominantly by altering the expression level of Bcl2 protein family members (Fennell et al., 2008; Voorhees and Orlowski, 2006). To investigate their potential involvement primary cells from melanoma patients (*Pat1-3*) were treated with increasing concentrations of bortezomib for 24 hours. The following IB-analysis of the expression levels of several BH3-only-proteins identified NOXA to be specifically up-regulated after proteasome inhibition. In contrast, the expression level

of other BH3-only proteins such as PUMA and BIM remained unchanged (Fig. 3.3A). Similar results were obtained in HL B-cells (Fig. 3.3B).

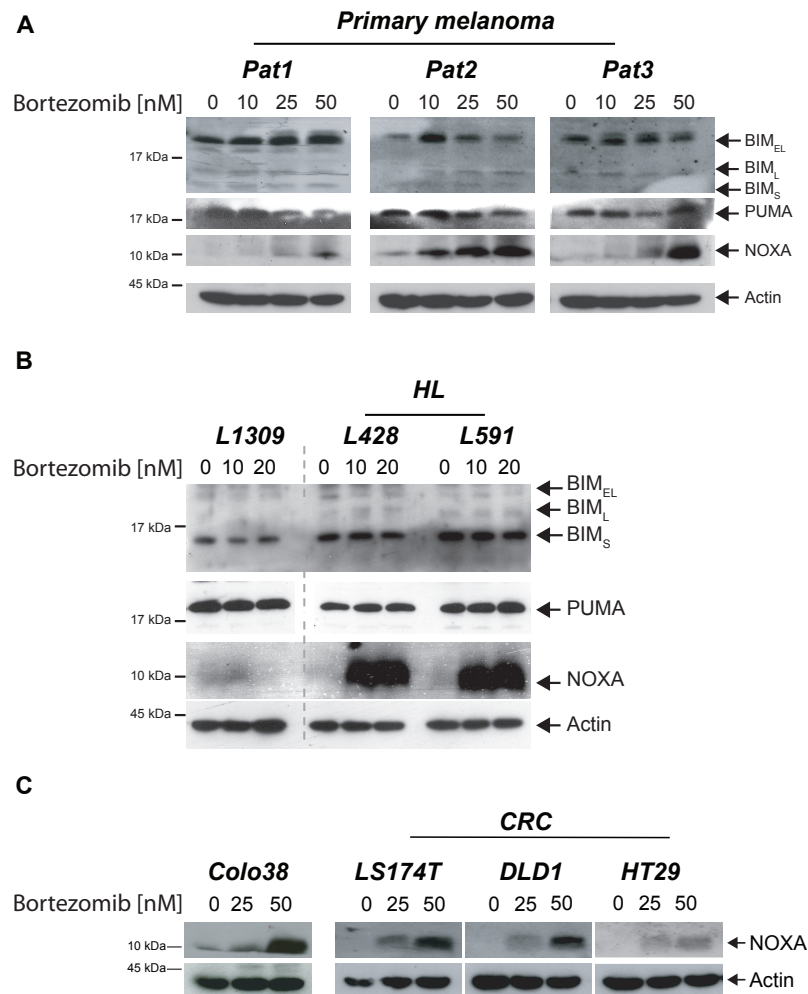


**Figure 3.3 | Proteasome inhibition results in the accumulation of the pro-apoptotic BH3-only protein NOXA.** IB-analysis of indicated BH3-only proteins in whole cell lysates from tumour cells derived from melanoma patients (*Pat1-3*) (A), Hodgkin Lymphoma (HL) cell lines (*L591*, *L428*) and a control B-cell line (*L1309*) (B), a melanoma cell line (*Colo38*) and colorectal carcinoma (CRC) cell lines (*LS174T*, *DLD1*, *HT29*) (C). Actin served as a loading control.

Remarkably, the susceptibility to bortezomib-induced apoptosis was tightly associated with the magnitude of NOXA accumulation in all tested bortezomib-sensitive tumour cells including primary cells from melanoma patients, melanoma cell lines, HL B-cell lines and CRC cell lines (Fig. 3.3 B and C).

### **3.2 NOXA accumulates at the post-transcriptional level after proteasome inhibition**

Besides the regulation of direct substrates of the UPS, proteasome inhibition has been shown to regulate the transcription of several proteins by stabilizing the relevant transcription factors including p53 or NF $\kappa$ B. To examine whether NOXA accumulation is due to its transcriptional up-regulation, NOXA-mRNA levels were analysed by qPCR after proteasome inhibition. As shown in Fig. 3.4 there was no significant up-regulation of NOXA mRNA upon proteasome inhibition, although NOXA protein was significantly accumulated in bortezomib-sensitive tumour cells derived from melanoma patients (A), melanoma cell lines (B), HL B-cell lines (C) and CRC cell lines (D). In contrast, NOXA mRNA was strongly up-regulated upon DNA-damage induced either by the DNA-intercalating agent doxorubicin, or the topoisomerase inhibitor etoposide, even though no accumulation of NOXA-protein was detectable.

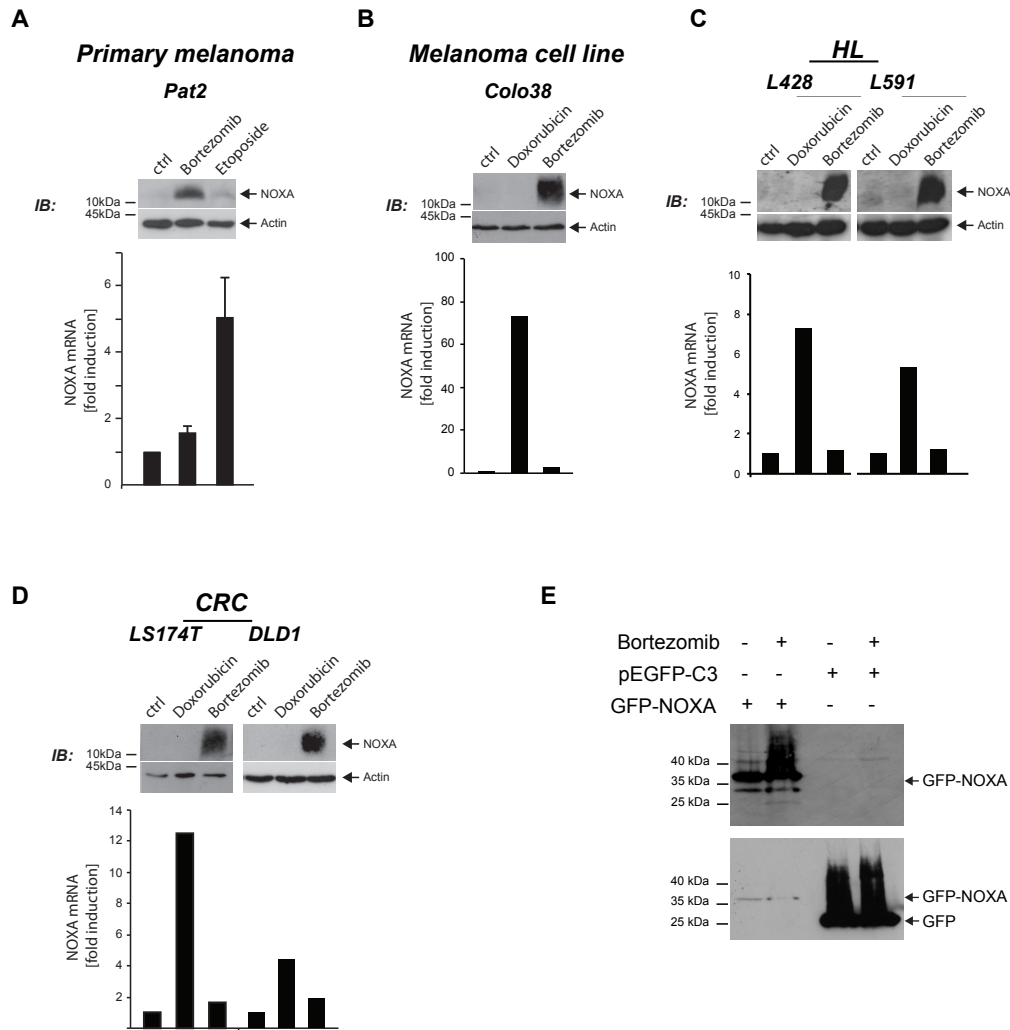


**Figure 3.4 | NOXA accumulation after proteasome inhibition is post-transcriptional.** Representative IB-analysis and according relative qPCR-analysis (normalised to GAPDH mRNA) of three independent experiments in triplicate.

NOXA expression was analysed in tumour cells derived from a Melanoma patient (*Pat2*) (**A**), a melanoma cell line (*Colo38*) (**B**), HL B-cell lines (*L428*, *L591*) (**C**) and CRC cell lines (*LS174T*, *DLD1*) (**D**) after treatment with bortezomib (**A**, **B**, **D** 25 nM; **C** 10 nM), etoposide (**A** 50  $\mu$ M) or doxorubicin (**B**, **C**, **D** 0,5  $\mu$ M) for 24 hours. HeLa cells were transfected with pEGFP-C3 or GFP-NOXA and treated 24 hours after transfection with 40 nM bortezomib for 4 hours, as indicated. IB-analyses of GFP-NOXA and GFP expression were performed with whole cell lysates. Upper Blot presents long exposure, bottom blot presents short exposure (**E**).

The non-transcriptional nature of NOXA accumulation after proteasome inhibition was confirmed using HeLa cells transiently transfected with plasmid constructs encoding GFP-NOXA under the control of the cytomegalovirus (CMV) promoter. As shown in IB-analysis, bortezomib-treatment of transiently transfected HeLa cells resulted in the accumulation of ectopically expressed GFP-NOXA but not GFP alone

(Fig. 3.4E). These data demonstrate that proteasome inhibition induces NOXA protein accumulation irrespective of the transcriptional origin.

Taken together, NOXA protein expression is controlled by a post-transcriptional regulatory mechanism, which appears to be deregulated in bortezomib-sensitive tumour cells.

### **3.3 NOXA protein is less stable in bortezomib-sensitive tumour cells**

In order to examine NOXA protein turnover, GFP-NOXA (1, 2, 3, or 4  $\mu$ g DNA constructs) was ectopically expressed in bortezomib-resistant *Pat1* and bortezomib-sensitive *Pat2* tumour cells. Transfection-efficiency among the different patient cells was highly variable and the expression levels of GFP-NOXA were normalized to the expression levels of co-transfected dsRed (also under the control of the CMV promoter) as an internal control. In contrast to dsRed, GFP-NOXA was barely detectable in *Pat2* tumour cells in IB-analyses even though increasing amounts of DNA were transfected. In contrast, *Pat1* tumour cells exhibited a high GFP-NOXA expression even though little amounts of DNA were transfected (Fig. 3.5A). In order to illustrate the statistical significance of these findings, expression levels of NOXA-GFP were quantified by flow cytometry (FACS). The expression levels of GFP-NOXA (FITC-median of GFP-positive cells) were normalized to the expression levels of dsRed (PerCP-median of PerCP-positive cells) from the same samples and are presented as fold induction to the control sample (1  $\mu$ g GFP-NOXA). Fig 3.5B shows GFP-NOXA expression in *Pat1* versus *Pat2* cells. A linear increase of GFP-NOXA expression upon increasing amounts of transfected DNA in *Pat1* cells was observed, whereas GFP-NOXA was only weakly expressed in *Pat2* cells.

NOXA protein stability was further examined using cycloheximide (CHX) treatment to block protein synthesis 24 hours post-transfection. As described above, GFP-NOXA expression was quantified by FACS-analysis using dsRed as an internal control. Values are presented as fold induction of GFP-NOXA expression compared to the control sample (t=0h). Congruently, GFP-NOXA was found to be markedly unstable in *Pat2* tumour cells (Fig. 3.5C).

These data demonstrate the reduced stability of NOXA protein in bortezomib-sensitive tumour cells.

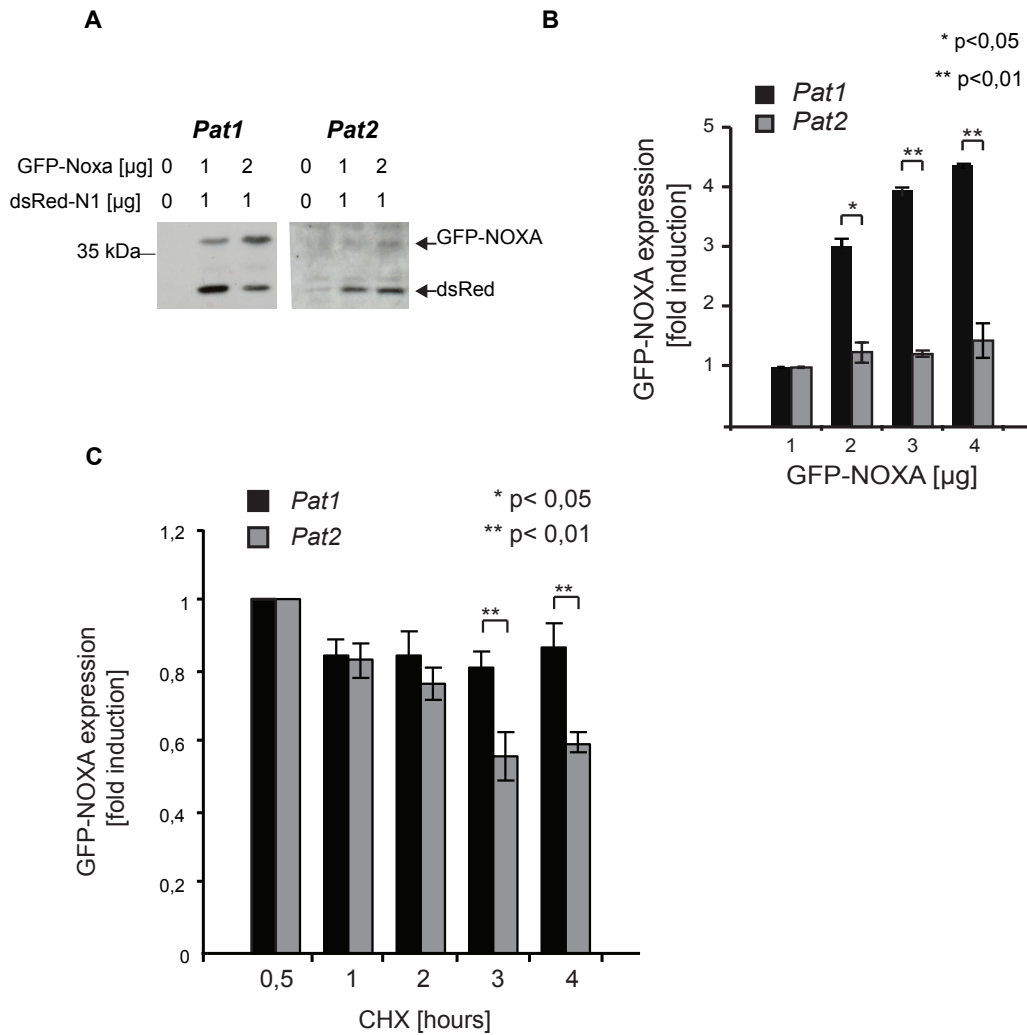


**Figure 3.5 | NOXA protein is less stable in bortezomib-sensitive tumours.** Primary cells from melanoma *Pat1-2* were transfected with increasing amounts of GFP-NOXA DNA and 1  $\mu$ g dsRed. GFP-NOXA expression was analysed by IB (**A**) and FACS (**B**). Cells were transfected with 2  $\mu$ g (*Pat1*) or 4  $\mu$ g (*Pat2*) of GFP-NOXA DNA and 1  $\mu$ g dsRed and treated with 25  $\mu$ g/ml Cycloheximide (CHX) and GFP-NOXA expression was analysed by FACS (**C**). GFP-NOXA expression was normalized to co-transfected dsRed and then normalized to the  $\mu$ g=1 or t=0 (**B,C**, respectively) controls. Data are presented as mean  $\pm$  SEM of 3 independent experiments, with statistical significance determined by Student's *t*-test.

### 3.4 NOXA is increasingly ubiquitinated in bortezomib-sensitive tumour cells

The UPS is responsible for the degradation of cellular proteins in eukaryotic organisms and represents a fundamental cellular quality control pathway to modulate cell fate. Substrates of the UPS are tagged for degradation by the 26S proteasome

with a polyubiquitin chain, which is specifically linked at Lysine<sup>48</sup> (K48) of each ubiquitin molecule. If NOXA is a direct substrate of the UPS, it will be ubiquitylated with a K48-linked ubiquitin chain prior to its degradation. To investigate this issue, HA-tagged NOXA (HA-NOXA) (Fig. 3.6A) or myc-tagged NOXA (myc-NOXA) (Fig. 3.6B) was overexpressed in *HEK293 FT* cells and K48-linked ubiquitylation of NOXA was investigated in tag-specific immunoprecipitates.

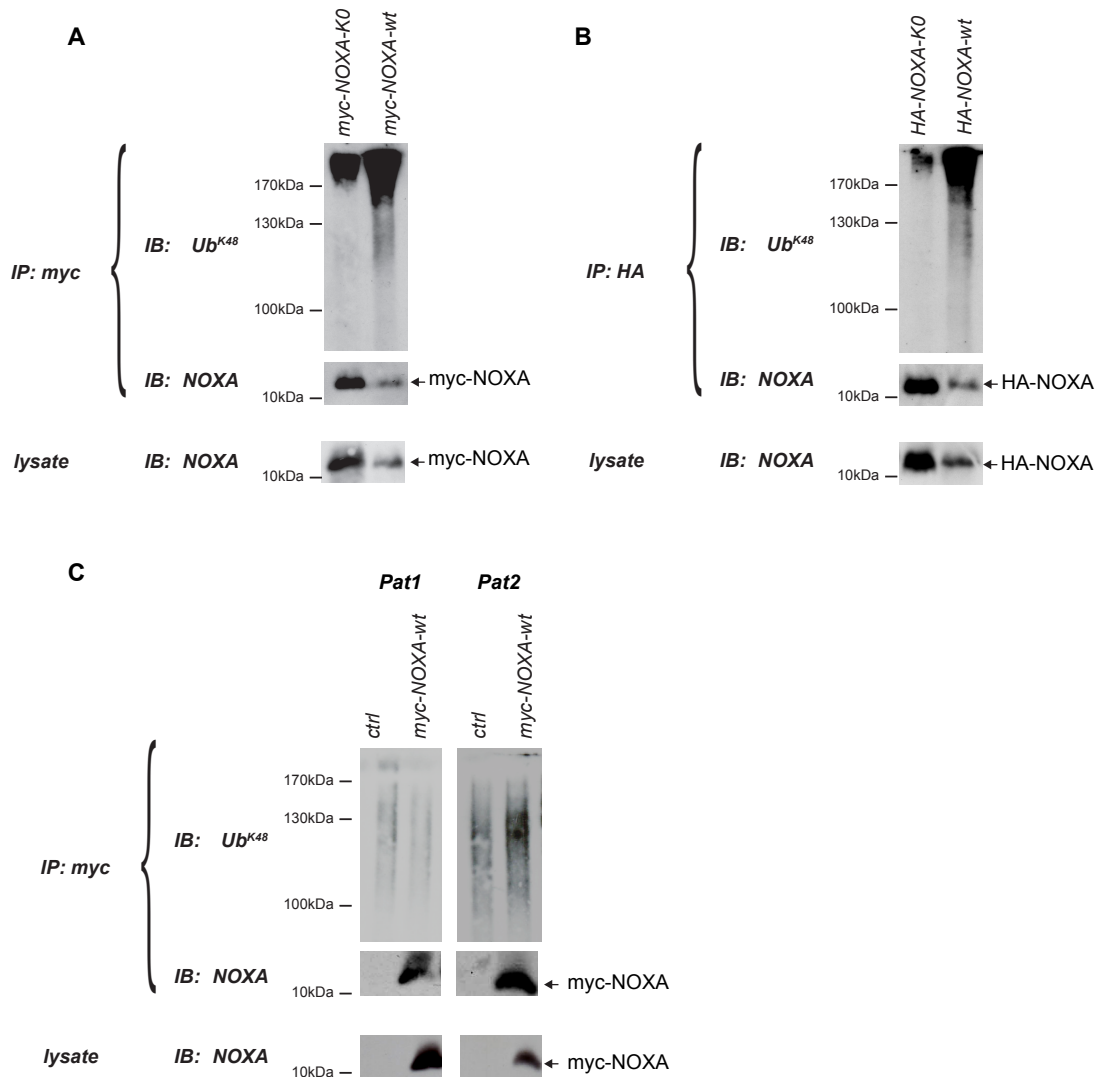


**Figure 3.6 | NOXA ubiquitylation is accelerated in bortezomib-sensitive tumour cells.** *HEK293FT* cells were transfected with myc-NOXA-wt and myc-NOXA-KO (A) or HA-NOXA-wt and HA-NOXA-KO (B). 24 hours after transfection proteins were denatured by boiling lysates in 1% SDS. IB-analyses of K48-linked polyubiquitin (Ub<sup>K48</sup>) and NOXA were performed in myc- (A) and HA-tag (B) immunoprecipitates (IP) or whole cell lysates. *Pat1-2* cells were transfected with myc-NOXA or left untransfected (ctrl). IB-analyses of K48-linked polyubiquitin (Ub<sup>K48</sup>) and NOXA were performed in myc-tag IPs or whole cell lysates (C).

To exclude a detection of K48-linked polyubiquitin of potential binding partners of NOXA, lysates were denatured by boiling in 1% SDS prior to immunoprecipitation (IP). Subsequent IB-analysis detected K48-polyubiquitylation of wild-type NOXA (NOXA-wt). In contrast, no polyubiquitin chains were detected on NOXA-K0, a construct that cannot be ubiquitylated because it lacks all lysine residues.

Confirming these in vitro analyses, NOXA ubiquitylation in tumour cells derived from melanoma patients revealed a significant increase in ubiquitylation of ectopically overexpressed myc-NOXA in *Pat2* compared to *Pat1* tumour cells (Fig. 3.6C).

Taken together, these data provide strong evidence for the elevated ubiquitylation and proteasomal degradation of NOXA in bortezomib-sensitive *Pat2* tumour cells.

### **3.5 The deubiquitylating enzyme (DUB) UCH-L1 is absent in bortezomib-sensitive tumour cells**

The turnover of UPS-substrate is regulated by continuous ubiquitylation and deubiquitylation involving E3-ubiquitin-ligases and deubiquitylating enzymes (DUBs), respectively. The presence of more than 500 E3-ubiquitin-ligases and approximately 100 DUBs in human cells illustrates the intrinsic specificity of components of the UPS for particular cellular substrates. Conceivably, selective manipulation of this machinery could affect the stability of specific UPS-substrates. In order to monitor the possible alterations of UPS-components, which may impact on NOXA turnover, PIQOR™ Ubiquitin-PS Microarrays (Miltenyi Biotec) were performed in primary melanoma samples (*Pat1-3 versus* non-malignant primary melanocytes), HL B-cell lines (HL B-cell lines *L428* and *L591 versus* the non-malignant control B-cell line *L1309*) and melanoma cell lines (bortezomib-sensitive *Colo38 versus* the bortezomib-resistant *SKmel23*). The PIQOR™ Ubiquitin-PS Microarray is a dual colour array that allows the analyses of mRNA expression of more than 1300 genes presumed to be involved in UPS regulation. Ratios represent normalized Cy5/Cy3 ratios of four replicates per gene. Genes that are more than 1.7 up- or down-regulated (presented as ratios  $>1.7$  or  $<0.58$ , respectively) represent putative candidate genes. In the present analysis a number of deregulated genes were identified in each individual tumour sample. Since accumulation of NOXA upon proteasome inhibition was a common feature among the bortezomib-sensitive tumour cells tested, the E3-ubiquitin-ligases and DUBs being similarly up- or down-regulated



in the tumour samples were first assumed to be possible candidates responsible for the enhanced NOXA ubiquitylation and turnover. After neglecting genes amplified in less than 4 of the performed 6 arrays, 31 DUBs (Tab. 5.1A) and 56 RING-domain-containing proteins as potential E3-ubiquitin-ligases (Tab. 5.1B) and remained in the analyses. Given that NOXA ubiquitylation and turnover was enhanced in bortezomib-sensitive tumour cells, the responsible E3-ubiquitin-ligase should be expressed higher the more susceptible the cells are towards bortezomib-treatment (e.g. *Pat1* < *Pat2*) and correspondingly the responsible DUB should be expressed less (e.g. *Pat1* > *Pat2*). Indeed, a strong correlation between the three tumour sample groups was observed in the regulation of the Ubiquitin-Carboxy-terminal-hydrolase-L1 (UCH-L1). Strikingly, UCH-L1 was the only DUB found to be highly down-regulated in all tested bortezomib-sensitive tumour samples including primary melanoma *Pat2* tumour cells, melanoma cell line *Colo38* and HL B-cell lines *L428* or *L591* (Table 5.1B). To illustrate these results, a gene expression profile of DUBs was generated for the performed microarrays of melanoma patients and HL B-cell lines (Fig. 3.7A). Further protein expression analyses by IB confirmed the loss of expression of UCH-L1 in bortezomib-sensitive tumour samples (Fig. 3.7B).

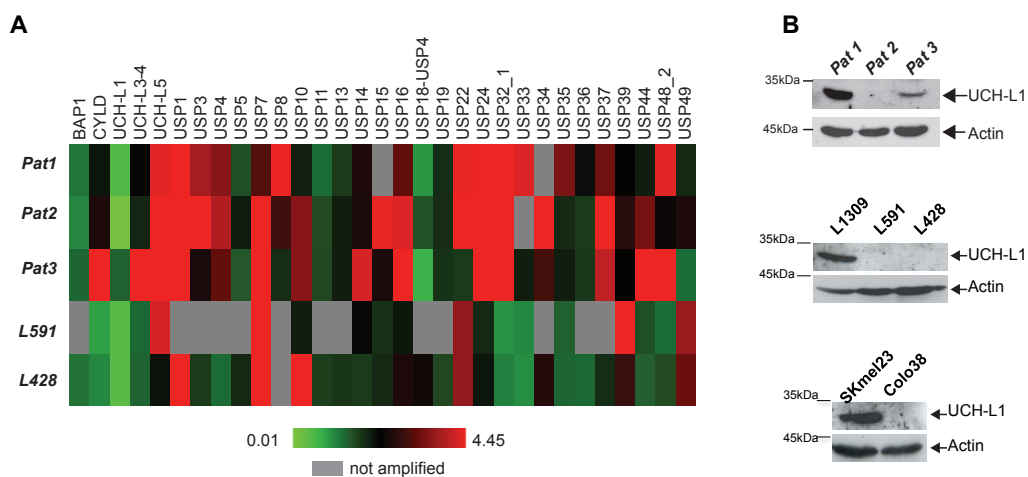


**Figure 3.7 | Gene expression profile of selected DUBs.** Dual colour PIQUOR-UPS-microarray (Miltenyi Biotech) was performed in primary cells from melanoma *Pat1-3* using non-malignant primary melanocytes as a reference and in *L428* and *L591* HL B-cell lines using the non malignant *L1309* B-cell line as a reference. Green colour indicates down-regulated genes, red colour indicates up-regulated genes compared to the reference. Grey colour indicates genes that were not amplified (**A**). IB-analyses of UCH-L1 expression in primary cells from melanoma *Pat1-3*, HL B-cell lines (*L428*, *L591*) with the corresponding non-malignant control B-cell line (*L1309*) and melanoma cell lines (*SKmel23*, *Colo38*). Actin served as a loading control (**B**).

In summary, all of the tumour cells tested, showed that accumulation of NOXA upon proteasome inhibition was linked to the simultaneous lack of UCH-L1 expression.

### 3.6 The DUB UCH-L1, binds, deubiquitylates and stabilizes NOXA *in vitro*

UCH-L1 (also called PARK5; PGP 9.5) possesses K48-dependent ubiquitin hydrolase activity and has been involved in the onset of human diseases including cancer and neurological disorders. However, the substrates of UCH-L1 are unknown and its precise function and the relevant cellular regulatory mechanisms are still unclear. To investigate whether UCH-L1 is a DUB of NOXA and thereby responsible for stabilizing NOXA protein, myc-NOXA was overexpressed in *HEK293FT* cells either together with GFP or GFP-UCH-L1. Strikingly, the expression levels of ectopically expressed myc-NOXA were significantly elevated by co-expression of GFP-UCH-L1 but not GFP alone. A similar pattern of NOXA protein expression was obtained when cells expressing myc-NOXA and GFP were additionally treated with bortezomib, highlighting the continuous degradation of myc-NOXA in the absence of UCH-L1 (Fig. 3.8).

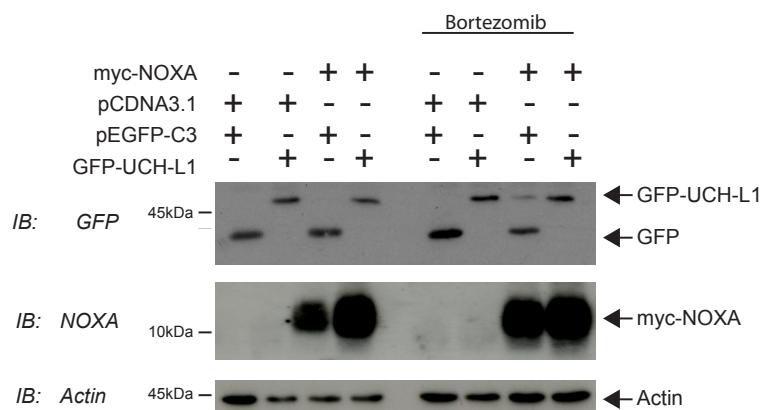


**Figure 3.8 | UCH-L1 stabilizes NOXA.** *HEK293FT* cells were transfected with pCDNA3.1 or myc-NOXA-wt and GFP-UCH-L1 or GFP, as indicated and treated with 50 nM bortezomib (10 hours after transfection) for 4 hours, as indicated. IB-analyses of indicated proteins were performed in whole cell lysates.

To investigate if NOXA and UCH-L1 directly interact, co-IP-analyses with ectopically overexpressed myc-NOXA with GFP-UCH-L1 or GFP alone were performed in

*HEK293 FT* cells. GFP-specific IP analyses revealed that myc-NOXA co-precipitated with GFP-UCH-L1 but not GFP alone (Fig. 3.9A) providing the first evidence that UCH-L1 directly interacted with NOXA.

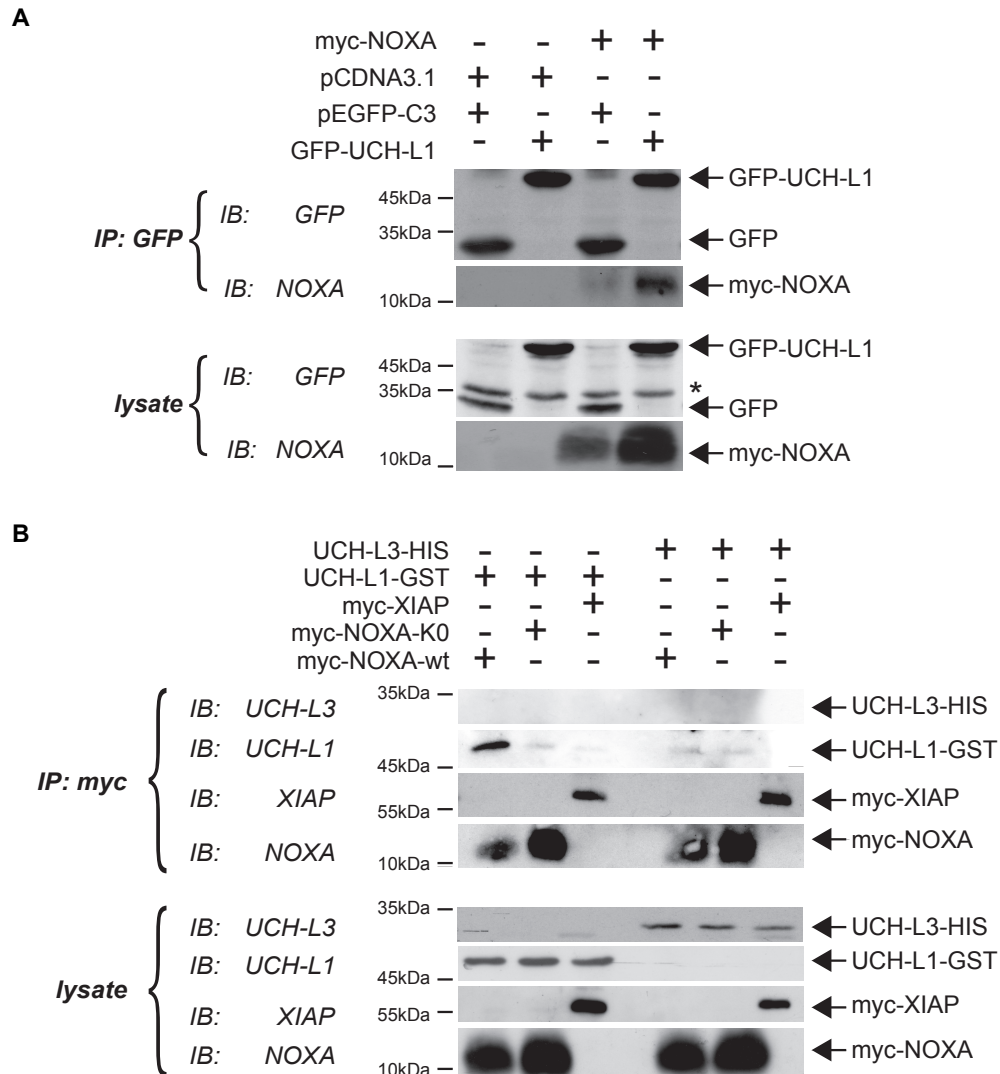


**Figure 3.9 | UCH-L1 and NOXA are direct interaction partners.** *HEK293 FT* cells were co-transfected with indicated expression plasmids. 24 hours after transfection IB-analyses of the indicated proteins were performed in GFP-IPs or whole cell lysates (**A**). *HEK293 FT* cells were transfected with myc-NOXA-wt, myc-NOXA-K0 or myc-XIAP and treated with 100 nM bortezomib for 4 hours. Lysates were incubated with either recombinant UCH-L1-GST or UCH-L3-His. IB-analyses of the indicated proteins were performed in myc-tag-IPs or whole cell lysates (**B**). \*unspecific band resulting from the GFP-antibody.

Additionally, cell-free binding assays were performed in cell lysates of *HEK293FT* cells overexpressing myc-NOXA-wt, myc-NOXA-K0 (as a non-ubiquitylated control) or myc-XIAP (as an unspecific ubiquitylated control). 8 hours after transfection cells

where treated with 50 nM bortezomib for 24 hours to accumulate the ubiquitylated proteins. Whole cell lysates were further incubated with either recombinant GST-UCH-L1 or HIS-UCH-L3, another member of the UCH-family that shares 51% of amino acid sequence identity with UCH-L1. Unlike UCH-L3, UCH-L1 was capable of binding NOXA but not XIAP (which has been shown to be K48-ubiquitylated), demonstrating the specific interaction of UCH-L1 with NOXA. This interaction was likely dependent on NOXA ubiquitylation since almost no NOXA-K0 was co-precipitated with UCH-L1 (Fig. 3.9B).

The potency of UCH-L1 in hydrolyzing the polyubiquitin chains of NOXA was further investigated with an in vitro deubiquitylation assay. *HEK293FT* cells were transfected with myc-NOXA or HA-NOXA and treated with 50 nM bortezomib (8 hours post transfection) for 24 hours. Lysates were incubated with recombinant GST-UCH-L1 and IB-analyses of K48-polyubiquitin were performed in either HA- or myc-tag specific immunoprecipitates. As expected, recombinant UCH-L1 protein was able to potently deubiquitylate NOXA in a time dependent manner (Fig. 3.10).

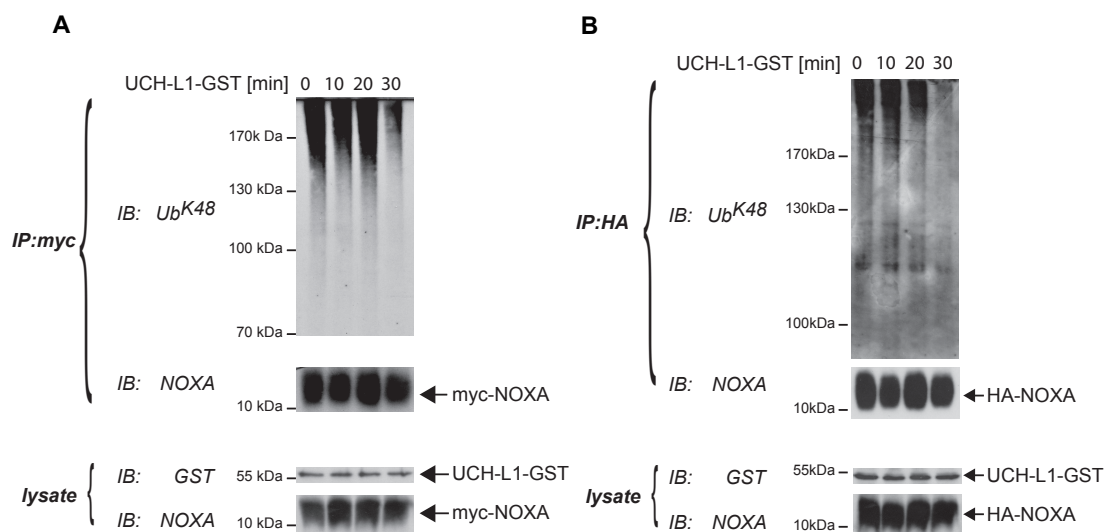


**Figure 3.10 | UCH-L1 deubiquitylates NOXA in vitro.** *HEK293 FT* cells were transfected with HA- or myc-NOXA-wt. Lysates were incubated with recombinant UCH-L1-GST for indicated time periods. 24 hours after transfection IB-analyses of K48-linked polyubiquitin (Ub<sup>K48</sup>) and NOXA were performed in myc- or HA-tag-IPs (**A,B** respectively) or whole cell lysates.

To confirm the data obtained from overexpressed tagged-NOXA, the ability of UCH-L1 to stabilize endogenous NOXA was determined by fluorescence microscopy and FACS-analyses. Bortezomib-sensitive *Pat2* tumour cells lacking endogenous UCH-L1 expression were transfected with GFP-UCH-L1 and endogenous NOXA was

immunostained. Fig. 3.11A shows the accumulation of endogenous NOXA (red) in microscopic analyses only in cells co-expressing GFP-UCH-L1 (green). To assess the statistical significance FACS-analyses were performed in cells overexpressing GFP, wild-type GFP-UCH-L1 (GFP-UCH-L1-wt) and mutant GFP-UCH-L1 (GFP-UCH-L1<sup>D176N</sup> possessing only 2.5 % enzymatic activity of UCH-L1-wt). Endogenous NOXA was immunostained (red) and its intensity was measured by PerCP-mean in GFP-positive cells. Expression levels of endogenous NOXA in GFP-UCH-L1-wt or GFP-UCH-L1<sup>D176N</sup> are presented as fold induction to the expression level in GFP-expressing cells. A significant accumulation of endogenous NOXA was observed only when GFP-UCH-L1-wt but not when the mutant UCH-L1<sup>D176N</sup> was expressed, indicating that the enzymatic activity of UCH-L1 is required for the accumulation of endogenous NOXA (Fig. 3.11B).

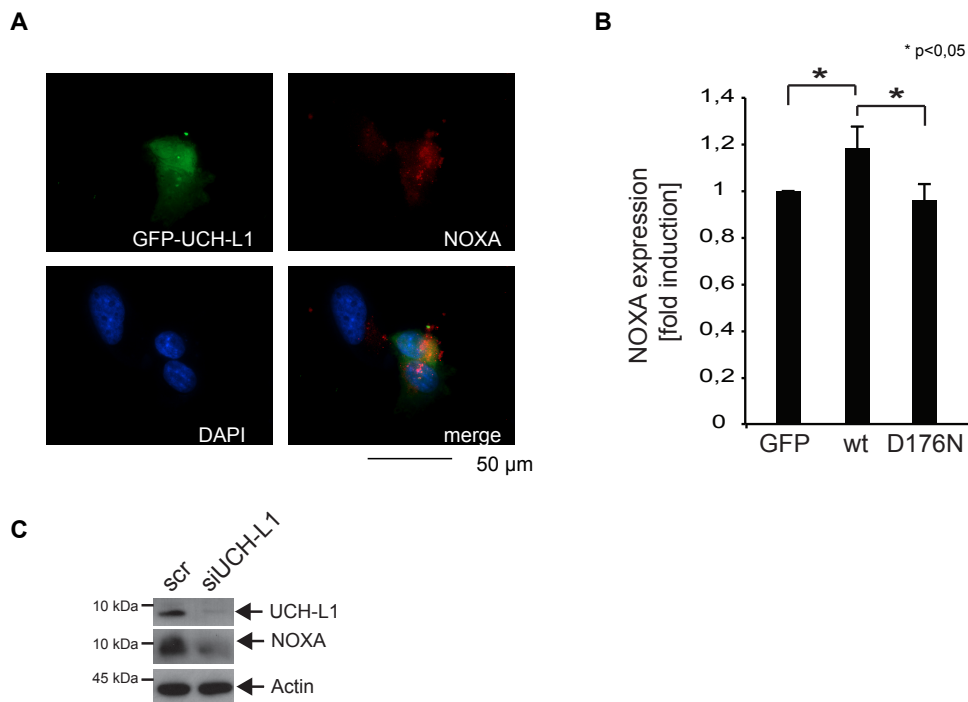


**Figure 3.11 | UCH-L1 stabilizes endogenous NOXA.** Immunofluorescence analysis of primary cells of melanoma *Pat2* transfected with GFP-UCH-L1 (green) for 24 hours and stained for endogenous NOXA (red) and dapi (blue) (**A**) and FACS-analyses of primary cells from melanoma *Pat2* transfected with GFP, GFP-UCH-L1-wt (wt) or GFP-UCH-L1<sup>D176N</sup> (D176N) for 24 hours and stained for endogenous NOXA. Expression levels of endogenous NOXA in GFP-UCH-L1-wt or GFP-UCH-L1<sup>D176N</sup> expressing cells are presented as fold induction to the expression level in GFP-expressing cells. Data are presented as mean  $\pm$  SEM of 3 independent experiments, with statistical significance determined by Students *t*-test (**B**). IB-blot analyses of NOXA and UCH-L1 expression in primary cells from melanoma *Pat1* transfected with scr-siRNA or siUCH-L1 for 48 hours. Actin served as a loading control (**C**).

Consistent with the analyses using overexpressed UCH-L1, specific knock-down of UCH-L1 by specific siRNA significantly reduced the expression level of endogenous NOXA in UCH-L1 positive *Pat1* tumour cells (Fig. 3.11C).

These data identify UCH-L1 as a specific DUB of NOXA that stabilizes NOXA protein through its specific deubiquitylation.

### **3.7 UCH-L1-expression correlates with increased NOXA-expression in tumour tissue sections of melanoma and CRC patients**

If UCH-L1 is responsible for stabilizing NOXA, then tumour samples expressing UCH-L1 might also exhibit increased expression of NOXA compared with UCH-L1 negative tumours. In order to address this point, immunohistochemical (IHC)-analyses of UCH-L1 and NOXA in a cohort of melanoma (81 cases) and CRC (26 cases) patients were performed in collaboration with the Departments of Dermatology (Prof. Dr. C. Mauch), Internal Medicine (PD Dr. Ulrich Hacker) and Pathology (Dr. U. Drebber) of the University of Cologne. Figure 3.12A shows a representative positive and negative example of IHC staining of NOXA and UCH-L1 in melanoma patients. Fig. 3.12B illustrates the results of the IHC stainings of all patient tissue samples tested. In tumour tissues the expression of UCH-L1 was tightly associated with elevated NOXA expression (96% of melanoma and 100% of CRC patients) (Tab. 5.2, 5.3). Interestingly, increased NOXA-expression was also observed in tumour samples lacking UCH-L1 expression indicating the involvement of UCH-L1-independent regulatory mechanisms controlling NOXA expression such as its transcriptional regulation.

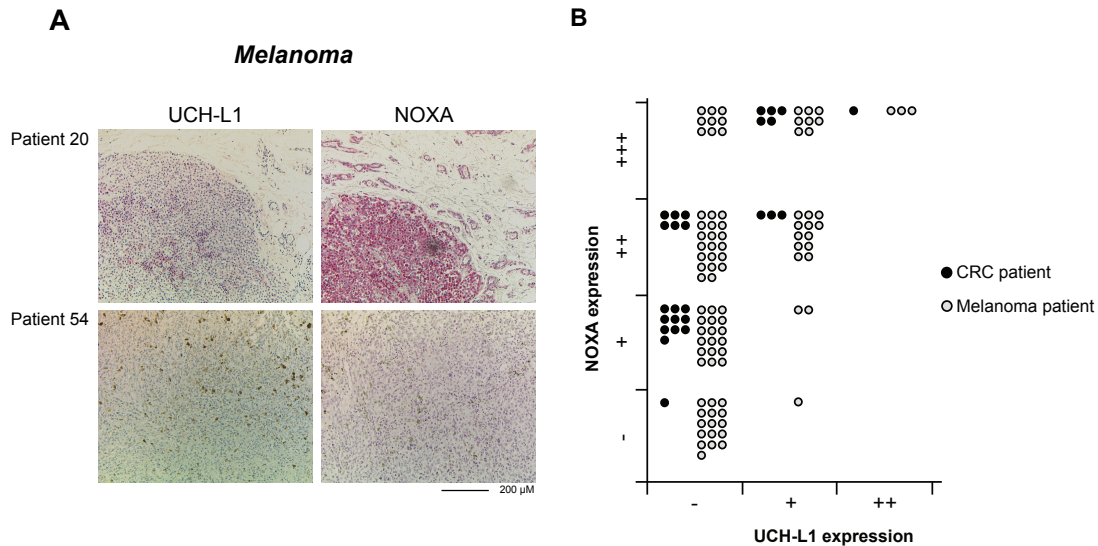


**Figure 3.12 | UCH-L1 expression is correlated with increased NOXA expression in melanoma and CRC patients.** Representative immunohistochemical staining (IHC) of UCH-L1 and NOXA in tumour sections derived from melanoma patient number 20 (UCH-L1++; NOXA+++), and patient number 54 (UCH-L1-; NOXA-) (A). NOXA and UCH-L1-expression in IHC in 81 melanoma patients (black circles) and 26 CRC patients (grey circles). Intensities of specific staining were arbitrarily set as the following: -, no expression; +, low expression; ++, moderate expression; +++, strong expression (B). Microscopic analyses of IHC-stainings of tumour sections from melanoma and CRC patients used to generate Fig 3.14B were performed by Dr. P. Zigrino and Dr. U. Drebber, respectively. IHC-stainings were carried out by Dr. P Zigrino.

Furthermore, these data demonstrate that UCH-L1 expression is missing in the majority of tumour samples tested (70%). Importantly, UCH-L1 has previously been shown to be epigenetically silenced in diverse tumour entities. Accordingly, pharmacological unmasking approaches such as demethylating agents and histone deacetylase inhibitors (HDACi) have been shown to induce UCH-L1 expression and promote cytotoxic actions. To investigate if UCH-L1 expression could be restored by preventing epigenetic silencing, *Pat2* tumour cells were treated with increasing concentration of the demethylating agent 5-aza-2(')-deoxycytidine or the HDACi Trichostatin A. The following IB-analyses demonstrate a significant up-regulation of UCH-L1 which was followed by NOXA accumulation (Fig. 3.13).

These results provide strong evidence for a prevalent epigenetic silencing of UCH-L1 leading to the destabilization of NOXA.

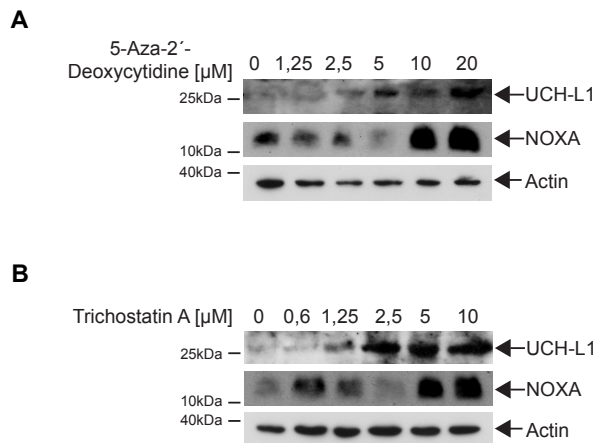


**Figure 3.13 | UCH-L1 depletion is caused by epigenetic silencing.** Primary cells from melanoma *Pat2* were treated with the indicated concentrations of 5-Aza-2'-Deoxycytidine for 4 days (**A**) or Trichostatin A for 24 hours (**B**). IB-analyses of UCH-L1 and NOXA expression was performed in whole cell lysates. Actin served as a loading control.

### 3.8 UCH-L1 depletion is associated with chemoresistance in tumour cells

NOXA has initially been described as a critical factor in mediating genotoxic stress-induced apoptosis. Thus, UCH-L1 expression might interfere with the cellular response to genotoxic stress. To investigate this hypothesis primary cells from melanoma patients (*Pat1-3*), melanoma cell lines (*Colo38*, *SKmel23*, *SKmel28*, *MV3*, *WM164*, *MeWo*) and HL B-cell lines (*L428*, *L591*) with the non-malignant control B-cell line (*L1309*) were analysed for UCH-L1-expression by IB (Fig. 3.14A) and their susceptibility to bortezomib- (Fig. 3.14B) or doxorubicin- (Fig. 3.14C) treatment was analysed in a cell viability assay. Strikingly, increased susceptibility to proteasome inhibition and the loss of UCH-L1 expression were accompanied by simultaneous chemoresistance to the DNA damaging agent doxorubicin.



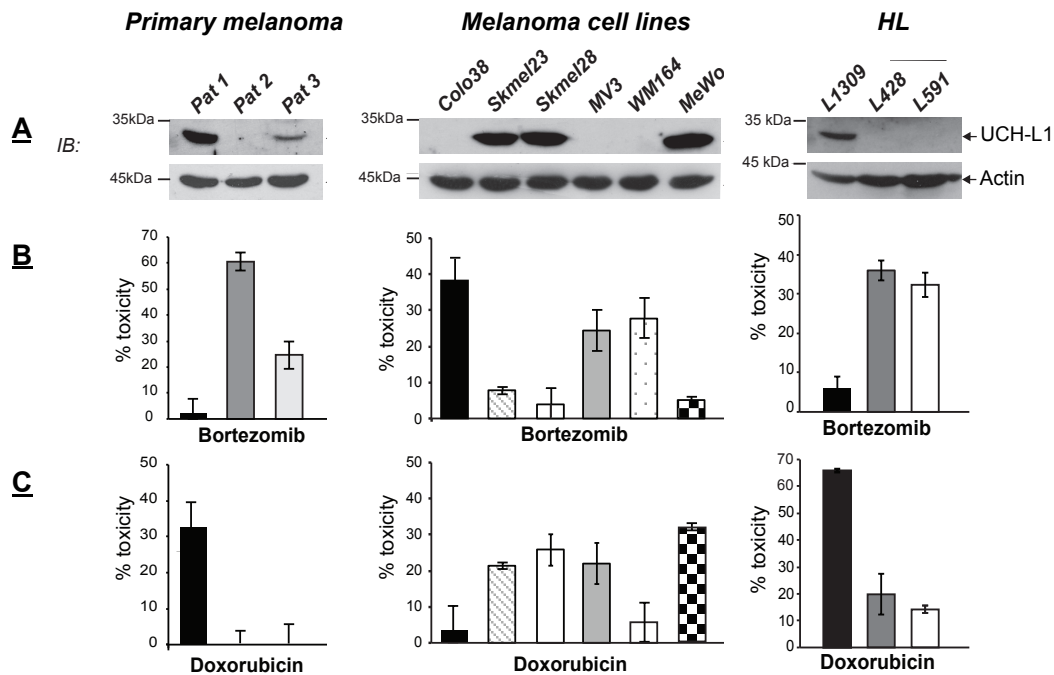


**Figure 3.14 | UCH-L1 depletion is associated with chemoresistance.** IB-analyses of UCH-L1 expression in the indicated cells. Actin served as a loading control (A). Primary cells from melanoma patients (*Pat1-3*), melanoma- (*Mel*) cell lines (*Colo38*, *Skmel23*, *Skmel28*, *MV3*, *WM164*, *MeWo*), HL B-cell lines (*L428*, *L591*) and a control B-cell line (*L1309*) were treated with bortezomib (*Pat1-3*, *Mel* 50 nM, *HL* 10 nM) (B) or doxorubicin (0,5  $\mu$ M) (C). Toxicity was measured by XTT assay (*Pat1-3*, *Mel*) or counting of trypan blue positive cells (*HL*). Data are presented as mean  $\pm$  SEM of 3 independent experiments.

To further assess the role of UCH-L1-depletion in conferring chemoresistance, UCH-L1 was depleted by specific siRNA in UCH-L1 positive *Pat1* cells and treated with doxorubicin. The following cell viability assay revealed that down-regulation of UCH-L1 in UCH-L1-expressing *Pat1* cells increased the resistance to the DNA damaging agent doxorubicin (Fig. 15A) as a result of inefficient NOXA accumulation, shown by IB-analysis. The impact of UCH-L1 activity on DNA damage-induced NOXA accumulation was further investigated using LDN-57444, a potent inhibitor of UCH-L1 enzymatic activity. Co-treatment of *Pat1* cells with LDN-57444 significantly reduced the accumulation of NOXA in response to DNA damage induced by doxorubicin, additionally supporting our findings that UCH-L1 is a key regulator of NOXA stability. (Fig. 15B)

Taken together, these data identify UCH-L1 as an important regulator of the DNA damage-induced apoptosis by stabilizing the DNA damage-induced NOXA protein.

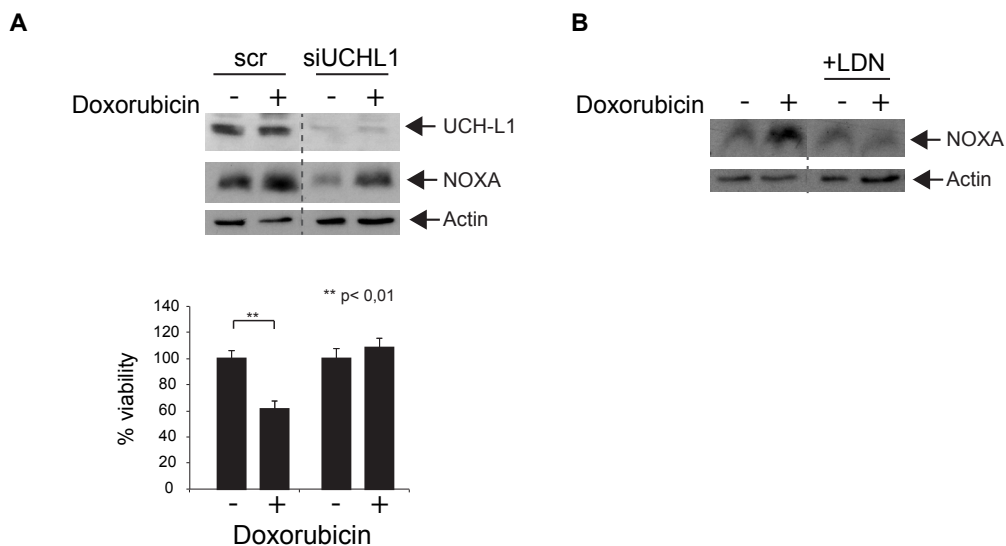


**Fig. 3.15 | Decreased UCH-L1 activity results in increased chemoresistance accompanied by decreased NOXA accumulation.** Primary cells from melanoma *Pat1* were transfected with scr-siRNA or siUCH-L1. IB-blot analyses of UCH-L1 and NOXA expression and cell viability analyses were performed after treatment with doxorubicin (0.5  $\mu$ M, 8 hours for IB-analysis; 2  $\mu$ M, 24 hours for viability analysis) 24 hours after transfection. Data of cell viability analysis are presented as mean  $\pm$  SEM of 1 representative experiment in 6 replicates, with statistical significance determined by Student's *t*-test. **(A)**. IB-analyses of NOXA and UCH-L1 expression in *Pat1* cells treated with doxorubicin and LDN-57444 for 8 hours. Actin served as a loading control **(B)**.

## 4 Discussion

### 4.1 NOXA accumulation as a key event in proteasome inhibition-induced apoptosis

In 2000, Weinberg and Hanahan defined six hallmarks of cancer describing biological capabilities acquired during the multistep development of human tumours. They include sustaining proliferative signalling, evading growth suppressors, enabling replicative immortality, inducing angiogenesis, activating invasion and metastasis and resisting cell death. Ten years later they updated this list to also include reprogramming of energy metabolism and evading immune destruction (Hanahan and Weinberg, 2000, 2011).

Conventional chemotherapy used to treat cancer usually engages the mitochondrial apoptotic pathway. Not surprisingly, its deregulation results in treatment resistance. In line with several publications the present work shows that the proteasome inhibitor bortezomib can promote direct cytotoxicity only in a cohort of tumour samples including primary tumour cells derived from melanoma patients, melanoma cell lines, HL cell lines and CRC cell lines by inducing the mitochondrial apoptotic pathway (Fernandez et al., 2005; Herrmann et al., 1998; Lopes et al., 1997; Qin et al., 2005) (Fig. 3.1-2). Analyses of BH3-only proteins, as central regulators of mitochondrial outer membrane permeabilization (MOMP), identified NOXA as the key mediator of proteasome inhibition-induced apoptosis (Fig 3.3). Congruent with the present results, the majority of research aiming to unravel the molecular mechanism of apoptosis-induction upon proteasome inhibition recognized NOXA as an essential factor and induction of NOXA has been reported upon proteasome inhibition in tumour *versus* healthy tissues (Gomez-Bougie et al., 2007; Qin et al., 2005). Conversely, when NOXA was down-regulated by siRNA, a significant reduction in the susceptibility to bortezomib was observed in initially sensitive tumour cells (Fernandez et al., 2005; Gomez-Bougie et al., 2007; Qin et al., 2005).

However, the underlying molecular mechanisms giving rise to the selective accumulation of NOXA in the above mentioned cohort of tumour samples are largely unknown.

In 1990 Hijikata et al. isolated the first NOXA cDNA clone from an adult T-cell leukemia (ATL) library (Hijikata et al., 1990; Ploner et al., 2009). The transcript was up-regulated by phorbol 12-myristate 13-acetate (PMA) and was therefore called ATL-derived PMA-responsive gene (APR). Later on it was given the Human Genome Organisation (HUGO) designation PMA-induced protein 1 (PMAIP1) (Ploner et al., 2009). A differential display approach using mRNA from  $\gamma$ -irradiated wild type (wt) and IRF-1/p53 double-deficient MEFs rediscovered APR/PMAIP1 as a 103 amino-acid protein, which the authors termed NOXA (Latin for damage). Further sequence analyses identified a Bcl2 homology (BH) domain 3 and NOXA was characterized as a novel BH3-only protein family (Oda et al., 2000).

Recent biochemical analyses employing cell-free systems described NOXA as a “sensitizer” BH3-only protein with weak pro-apoptotic activity capable of initiating cell death only in conjunction with other BH3-only members (Chen et al., 2005). In contrast, the present data suggest that accumulation of NOXA alone might be sufficient to initiate the mitochondrial apoptotic pathway resulting in apoptotic cell death (Fig. 3.2). These data are in agreement with the initial report demonstrating that NOXA is capable of directly initiating MOMP and cell death (Hallaert et al., 2007; Mackus et al., 2005; Zaher et al., 2009). Since NOXA has the most restricted potential to neutralize certain anti-apoptotic members of the Bcl2 protein family such as MCL1 and A1, the differential expression levels of NOXA binding partners could potentially impact on the susceptibility to NOXA action (Chen et al., 2005). Accordingly, cell free analyses of isolated mitochondria overexpressing MCL1 have been shown to be particularly sensitive or “primed” to NOXA-induced MOMP (Certo et al., 2006).

A model for the NOXA dependent induction of MOMP upon proteasome inhibition has been proposed in Multiple Myeloma. In this model MCL-1 protein sequesters the “direct activator” BH3-only protein BIM. Under bortezomib-treatment, induction of the “sensitizer” BH3-only protein NOXA allows the displacement of the “direct activator” BIM, which is now able to activate BAX/BAK-dependent MOMP (Fig. 4.1) (Gomez-Bougie et al., 2007).

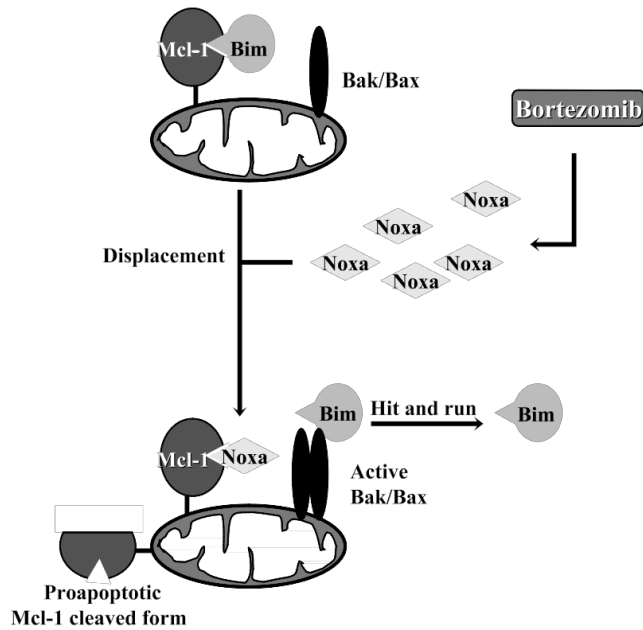


**Figure 4.1 | Model of the interplay between anti-apoptotic and pro-apoptotic molecules of the Bcl-2 family under bortezomib-treatment.** In myeloma cells, Mcl-1 protein sequesters the “direct activator” BH3-only protein BIM. Under bortezomib-treatment, induction of the “sensitizer” BH3-only NOXA allows the displacement of the “direct activator” BIM, which is now able to activate BAX/BAK-dependent MOMP.

Regardless of its pro-apoptotic properties, the critical role of NOXA in fine-tuning BAX/BAK-dependent MOMP and cell death is widely accepted. Particularly, NOXA-dependent cell death appears to be highly relevant for apoptosis induction in malignant or highly proliferating *versus* primary or differentiated cells, implicating NOXA as a tumour suppressor or valuable therapeutic target (Fernandez et al., 2005; Qin et al., 2005). However, in the present analysis NOXA expression levels did not correlate with overall or disease-free survival in human melanoma and colon carcinoma patients (Tab. 5.2-3). This is in line with a previous report showing that deregulation of NOXA expression is not associated with disease development in acute lymphoblastic leukaemia (Ploner et al., 2009).

Albeit a possible involvement of NOXA in carcinogenesis remains to be shown, its importance as a drug target is becoming increasingly evident. Accordingly NOXA is essential in p53-induced apoptosis triggered by classical anticancer agents such as etoposide or  $\gamma$ -irradiation but also for tumour cell death triggered by the cyclin-dependent kinase inhibitor R-roscovitine, histone deacetylases inhibitors (HDACi), and in particular, by proteasome inhibition (Dransfeld et al., 2007; Hallaert et al., 2007; Oda et al., 2000; Qin et al., 2005). By conclusively showing the impact of the regulation of NOXA expression on the chemosusceptibility of tumour cells the present findings clearly support the idea that NOXA represents an important anti-cancer target.

## 4.2 Post-transcriptional regulation of NOXA by the UPS

Although the impact of NOXA on chemosusceptibility in cancer is indisputable, most previous work suggested that chemotherapy including proteasome inhibitors targets NOXA's transcriptional regulation (Fernandez et al., 2005; Perez-Galan et al., 2006; Qin et al., 2005). Accordingly, NOXA accumulation upon proteasome inhibition is supposed to be due to the stabilization of its transcription factors, the best described of which is p53. Interestingly, initial publications show that cell death induced by proteasome inhibition occurs independently of p53 (Herrmann et al., 1998; Lopes et al., 1997) and more recent publications confirm NOXA accumulation upon proteasome inhibition to be independent of p53 (Nikiforov et al., 2007; Qin et al., 2005).

NOXA transcription is also regulated by HIF1- $\alpha$  (Kim et al., 2004a), E2F-1 (Hershko and Ginsberg, 2004) and c-myc (Nikiforov et al., 2007). Importantly Nikiforov et al., 2007 demonstrated that NOXA mRNA accumulation upon proteasome inhibition is independent of p53, HIF1- $\alpha$  and E2F, but relies on the activity of c-myc. Nevertheless complete reliance of NOXA protein accumulation for c-myc has not been shown and additional regulatory mechanisms resulting in NOXA accumulation upon proteasome inhibition could not be excluded.

The present analysis showed that in a cohort of tumour samples NOXA accumulation was not a result of transcriptional up-regulation. Further analyses conclusively demonstrated enhanced NOXA-ubiquitylation and degradation by the ubiquitin-proteasome system (UPS) in this tumour cohort highlighting an as yet unrecognized alteration of NOXA regulation in cancer (Fig. 3.5-6). In line, a recent publication confirmed that NOXA can be ubiquitylated (Baou et al., 2010). However any further characterization of its biologic or pathobiological significance and the underlying molecular mechanism are still lacking.

## 4.3 Increased NOXA degradation as a result of lacking UCH-L1 expression, the specific DUB of NOXA

Analysis of components of the UPS identified the deubiquitylating enzyme UCH-L1 as a possible candidate responsible for the variation in NOXA stability (Fig. 3.8-3.12).

The present data clearly identified UCH-L1 as the specific deubiquitylating enzyme (DUB) of NOXA. UCH-L1 directly interacts and stabilizes NOXA by removing the K48 linked polyubiquitin chains that mark NOXA for proteasomal degradation (Fig. 3.8-3.11).

UCH-L1 was initially reported to play a role in the development and progression of Parkinson's disease by stabilization of  $\alpha$ -synuclein levels. Of note, UCH-L1 has meanwhile been described to possess an ubiquitin ligase activity. The identification of the ligase activity is based on the initial accumulation of polyubiquitylated  $\alpha$ -synuclein upon transient overexpression of UCH-L1, followed by a rapid decrease in high-molecular  $\alpha$ -synuclein. Detailed analyses indicated that K63 might be the primary ubiquityl acceptor residue of UCH-L1, in contrast to the E2/E3 ligases involved in proteasomal degradation, which ubiquitylate K48 (Liu et al., 2002).

However, there is no further evidence of a ligase activity of UCH-L1, and since it is only observed at high enzyme concentrations in vitro the relevance of these findings is debatable. In contrast the deubiquitylating activity and thus involvement in the UPS pathway of UCH-L1 has been widely accepted.

Our analyses of melanoma and colon carcinoma patient samples revealed a strong correlation of NOXA and UCH-L1 expression (Fig. 3.12). Whenever UCH-L1 was expressed, a high level of NOXA expression was detected supporting the proposed model of UCH-L1-mediated stabilization of NOXA in vivo. However, high levels of NOXA expression were also found in patients where UCH-L1 was not detectable, implicating additional regulatory mechanisms involved in NOXA expression, such as transcriptional regulation. NOXA transcription is reportedly regulated by p53. Certainly, p53 amplification is not a common feature of tumour cells, in fact, p53 is inactive in up to 50% of human cancers (Hollstein et al., 1994). The transcription factor c-myc, shown to induce NOXA transcription (Nikiforov et al., 2007), might be a promising candidate for enhanced NOXA expression since it is highly active in the vast majority of tumour samples (Nesbit et al., 1999). However final confirmation of this awaits further analyses.

It is also noted that UCH-L1 expression is lacking in 69% of melanoma patients and in 64% of colorectal carcinoma patients. Congruently, UCH-L1 has previously been shown to be epigenetically silenced in various tumour entities such as hepatocellular carcinoma (Yu et al., 2008), pancreatic cancer (Sato et al., 2003), gastric cancer (Yamashita et al., 2006), breast cancer (Xiang et al., 2012) and colon carcinoma

(Fukutomi et al., 2007). Accordingly, pharmacological unmasking approaches such as demethylating agents and HDACi have been shown to induce UCH-L1 expression and promote cytotoxic actions. However, the mechanism of UCH-L1-promoted cytotoxic effects was not addressed.

In this work it was demonstrated that re-expression of UCH-L1 in UCH-L1 negative *Pat2* cells through treatment with HDACi was followed by an accumulation of NOXA (Fig. 3.13). In line with this HDACi are already described to induce NOXA expression, and strikingly, siRNA mediated knock-down of NOXA reduced HDACi-mediated cell death (Inoue et al., 2007). Conversely, siRNA mediated knock-down of the NOXA antagonist MCL1 potentiated HDACi-mediated apoptosis (Inoue et al., 2008). Finally, mice lacking the MCL1 specific E3-ubiquitin ligase MULE (resulting in enhanced MCL1-stability) are protected from HDACi-mediated apoptosis (Jing et al., 2011). In conclusion, the ratio of NOXA and MCL1 expression determines the susceptibility toward HDACi-mediated apoptosis while NOXA accumulation seems to be an essential event.

The present data provide the first evidence that the reactivation of epigenetically silenced UCH-L1 is responsible for the accumulation of NOXA and thereby plays an essential role in HDACi-mediated cell death.

#### **4.4 UCH-L1 as a modulator of apoptosis**

Several publications indicate a contribution of UCH-L1 in germ cell apoptosis and spermatogenesis (Fraile et al., 1996; Kon et al., 1999; Kwon et al., 2003; Martin et al., 1995). Mice lacking UCH-L1 expression (*gad* (gracile axonal dystrophy) mice) exhibit defects in spermatogenesis, which are thought to be associated with impaired germ cell apoptosis (Kim et al., 2004b). Moreover, apoptosis induced by neuronal injury is suppressed by up to 70% in *gad* mice (Harada et al., 2004). Remarkably, a comparable insufficiency in apoptosis upon neuronal injury is observed in NOXA knock-out mice (Kiryu-Seo et al., 2005). On the other hand, transgenic mice overexpressing EF1 $\alpha$  promoter-driven UCH-L1 in the testis are sterile due to a block in spermatogenesis at an early stage (pachytene) of meiosis. This turned out to be the result of accelerated apoptosis suggesting UCH-L1 as a DUB with pro-apoptotic functions (Wang et al., 2006).



In line with these observations, recent publications also point at a role of UCH-L1 in tumour cell apoptosis. UCH-L1 is reported to play an essential role in tumour cell invasion in melanoma patients through up-regulation of Akt-signalling (Kim et al., 2009). Furthermore, it has been shown that overexpression of UCH-L1 induces apoptosis in breast cancer and gastric cancer (Kim et al., 2011; Wang et al., 2008). Apoptosis induction in breast cancer cells upon overexpression of UCH-L1 is thought to be due to the stabilization of p53 and associated induction of G0/G1 cell cycle arrest and apoptosis (Xiang et al., 2012). However, no evidence for deubiquitylation and post-translational stabilization of any of these factors has been demonstrated and the mechanistic insight as to how UCH-L1 interferes with the apoptotic pathway is still lacking. In the present work NOXA was clearly demonstrated as a target of UCH-L1 that mediates UCH-L1-potentiated apoptosis.

#### **4.5 UCH-L1 as an important component of the DNA damage response by stabilization of NOXA**

NOXA has been initially described as a critical factor mediating genotoxic stress-induced apoptosis. Upon DNA damage NOXA is transcriptionally up-regulated, resulting in the activation of the mitochondrial apoptotic pathway (Oda et al., 2000). Here it is demonstrated, that besides the transcriptional up-regulation of NOXA, tumour cells rely on functional UCH-L1 in order to stabilize NOXA protein and sufficiently induce apoptosis in response to genotoxic stress (Fig. 3.14). Accordingly, cells lacking UCH-L1 expression failed to accumulate NOXA protein after treatment with DNA damaging agents, even though NOXA was transcriptionally activated (Fig. 3.4). Furthermore, down-regulation of UCH-L1 expression or the inhibition of its deubiquitylating activity in DNA damage-susceptible tumour cells attenuated the cytotoxic activity of DNA damaging agents (Fig. 3.15) resulting from a reduction in DNA damage-induced NOXA accumulation.

In addition to biochemical and cell biological analyses carried out in human tissue cultures, the impact of UCH-L1 on apoptosis was further demonstrated in *Caenorhabditis elegans* (*C.elegans*) in cooperation with the group of Prof. Thorsten Hoppe (University of Cologne). DNA damage induced by ionizing radiation (IR) initiates several cellular responses in *C.elegans*, including germ cell apoptosis. On

the other hand, dysfunction of DNA damage responsive genes has been shown to enhance the embryonic lethality of IR and genomic instability (Gartner et al., 2000). Strikingly, RNAi mediated knock-down of the *C.elegans* UCH-L1 homologues *ubh-2* or *ubh-3* resulted in reduced apoptosis and embryonal hypersensitivity in response to IR (Michael Schell, Leena Ackermann, respectively).

These data confirm our analyses and highlight the conserved role of UCH-L1 in the DNA damage-induced apoptotic pathway.

## 4.6 Conclusion

In conclusion, the present data showed for the first time, that UCH-L1 is an important component of the DNA damage response and impacts on the susceptibility of cancer cells toward chemotherapy by stabilizing NOXA. DNA damage-inducing chemotherapy usually results in the transcriptional up-regulation of NOXA. NOXA protein is immediately marked for proteasomal degradation with K48-polyubiquitin chains by an as yet unknown ubiquitin ligase.

In UCH-L1 positive cells, UCH-L1 deubiquitylates and stabilizes NOXA resulting in NOXA-triggered cell death.

In contrast, in cells lacking UCH-L1, NOXA is markedly unstable as a result of continuous degradation by the UPS. Accordingly, DNA damage-inducing chemotherapy does not result in a sufficient accumulation of NOXA protein and thus does not induce cell death (Fig. 4.1).

Notably, NOXA executes its pro-apoptotic action through specific binding to its anti-apoptotic counterpart, MCL1. Two independent recent reports identified the specific DUB and ubiquitin ligase of MCL1 to substantially impact on MCL1 protein turnover and apoptosis in response to cytostatic treatments of cancer (Inuzuka et al., 2011; Wertz et al., 2011). In line with these observations, increasing and maintaining NOXA protein levels by promoting UCH-L1 expression may hold promise in the treatment of chemoresistant cancer.

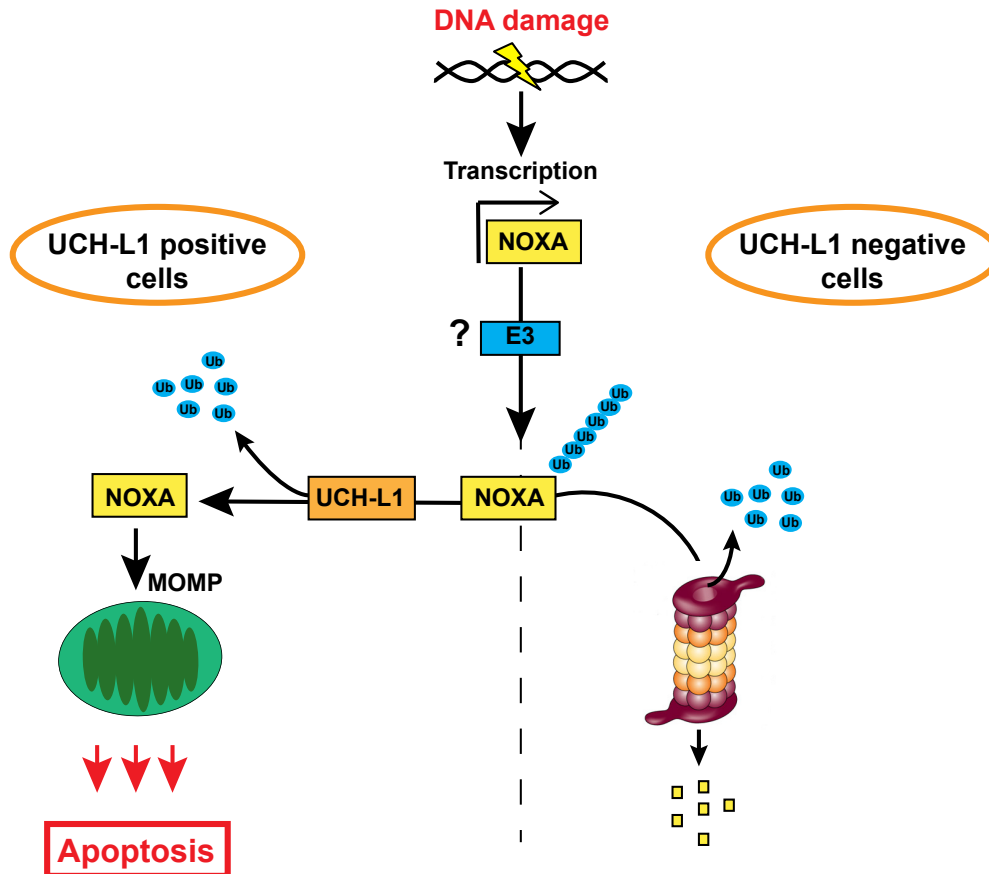


**Figure 4.1 | Conclusion.** DNA damage induced by chemotherapy results in the transcriptional up-regulation of NOXA. By an as yet unknown mechanism NOXA gets polyubiquitylated. In UCH-L1 positive cells, UCH-L1 deubiquitylates NOXA and liberated NOXA is able to induce mitochondrial outer membrane permeabilization (MOMP) and thus apoptotic cell death (left). In UCH-L1 negative cells, ubiquitylated NOXA is continuously degraded by the proteasome and thus is not able to induce mitochondrial apoptosis (**right**).

## 5 References

- Adams, J.M., and Cory, S. (1998). The Bcl-2 protein family: arbiters of cell survival. *Science* **281**, 1322-1326.
- Almond, J.B., and Cohen, G.M. (2002). The proteasome: a novel target for cancer chemotherapy. *Leukemia : official journal of the Leukemia Society of America, Leukemia Research Fund, UK* **16**, 433-443.
- Alnemri, E.S., Livingston, D.J., Nicholson, D.W., Salvesen, G., Thornberry, N.A., Wong, W.W., and Yuan, J. (1996). Human ICE/CED-3 protease nomenclature. *Cell* **87**, 171.
- Ashkenazi, A. (2002). Targeting death and decoy receptors of the tumour-necrosis factor superfamily. *Nature reviews Cancer* **2**, 420-430.
- Ashkenazi, A., and Dixit, V.M. (1998). Death receptors: signaling and modulation. *Science* **281**, 1305-1308.
- Banin, S., Moyal, L., Shieh, S., Taya, Y., Anderson, C.W., Chessa, L., Smorodinsky, N.I., Prives, C., Reiss, Y., Shiloh, Y., *et al.* (1998). Enhanced phosphorylation of p53 by ATM in response to DNA damage. *Science* **281**, 1674-1677.
- Baou, M., Kohlhaas, S.L., Butterworth, M., Vogler, M., Dinsdale, D., Walewska, R., Majid, A., Eldering, E., Dyer, M.J., and Cohen, G.M. (2010). Role of NOXA and its ubiquitination in proteasome inhibitor-induced apoptosis in chronic lymphocytic leukemia cells. *Haematologica* **95**, 1510-1518.
- Barr, P.J., and Tomei, L.D. (1994). Apoptosis and its role in human disease. *Biotechnology (N Y)* **12**, 487-493.
- Bernassola, F., Ciechanover, A., and Melino, G. (2010). The ubiquitin proteasome system and its involvement in cell death pathways. *Cell death and differentiation* **17**, 1-3.
- Boatright, K.M., Renatus, M., Scott, F.L., Sperandio, S., Shin, H., Pedersen, I.M., Ricci, J.E., Edris, W.A., Sutherlin, D.P., Green, D.R., *et al.* (2003). A unified model for apical caspase activation. *Molecular cell* **11**, 529-541.
- Breitschopf, K., Bengal, E., Ziv, T., Admon, A., and Ciechanover, A. (1998). A novel site for ubiquitination: the N-terminal residue, and not internal lysines of MyoD, is essential for conjugation and degradation of the protein. *The EMBO journal* **17**, 5964-5973.
- Certo, M., Del Gaizo Moore, V., Nishino, M., Wei, G., Korsmeyer, S., Armstrong, S.A., and Letai, A. (2006). Mitochondria primed by death signals determine cellular addiction to antiapoptotic BCL-2 family members. *Cancer cell* **9**, 351-365.
- Chen, L., Willis, S.N., Wei, A., Smith, B.J., Fletcher, J.I., Hinds, M.G., Colman, P.M., Day, C.L., Adams, J.M., and Huang, D.C. (2005). Differential targeting of prosurvival Bcl-2 proteins by their BH3-only ligands allows complementary apoptotic function. *Molecular cell* **17**, 393-403.
- Chen, Z.J. (2005). Ubiquitin signalling in the NF-kappaB pathway. *Nature cell biology* **7**, 758-765.
- Chomczynski, P., and Sacchi, N. (1987). Single-step method of RNA isolation by acid guanidinium thiocyanate-phenol-chloroform extraction. *Analytical biochemistry* **162**, 156-159.
- Chonghaile, T.N., and Letai, A. (2008). Mimicking the BH3 domain to kill cancer cells. *Oncogene* **27 Suppl 1**, S149-157.

- Ciechanover, A., Finley, D., and Varshavsky, A. (1984). The ubiquitin-mediated proteolytic pathway and mechanisms of energy-dependent intracellular protein degradation. *Journal of cellular biochemistry* 24, 27-53.
- Clarke, A.R., Purdie, C.A., Harrison, D.J., Morris, R.G., Bird, C.C., Hooper, M.L., and Wyllie, A.H. (1993). Thymocyte apoptosis induced by p53-dependent and independent pathways. *Nature* 362, 849-852.
- Cory, S., and Adams, J.M. (2002). The Bcl2 family: regulators of the cellular life-or-death switch. *Nature reviews Cancer* 2, 647-656.
- Coultas, L., and Strasser, A. (2003). The role of the Bcl-2 protein family in cancer. *Seminars in cancer biology* 13, 115-123.
- Denault, J.B., and Salvesen, G.S. (2002). Caspases: keys in the ignition of cell death. *Chemical reviews* 102, 4489-4500.
- Dick, T.P., Nussbaum, A.K., Deeg, M., Heinemeyer, W., Groll, M., Schirle, M., Keilholz, W., Stevanovic, S., Wolf, D.H., Huber, R., *et al.* (1998). Contribution of proteasomal beta-subunits to the cleavage of peptide substrates analyzed with yeast mutants. *The Journal of biological chemistry* 273, 25637-25646.
- Dransfeld, C.L., Schaich, M., Ho, A.D., Thiede, C., Ehninger, G., and Mahlknecht, U. (2007). Class I HDAC SNP analysis in healthy donors compared to AML patients. *Leukemia : official journal of the Leukemia Society of America, Leukemia Research Fund, UK* 21, 1587-1590.
- Eldridge, A.G., and O'Brien, T. (2010). Therapeutic strategies within the ubiquitin proteasome system. *Cell death and differentiation* 17, 4-13.
- Ellis, H.M., and Horvitz, H.R. (1986). Genetic control of programmed cell death in the nematode *C. elegans*. *Cell* 44, 817-829.
- Enari, M., Sakahira, H., Yokoyama, H., Okawa, K., Iwamatsu, A., and Nagata, S. (1998). A caspase-activated DNase that degrades DNA during apoptosis, and its inhibitor ICAD. *Nature* 391, 43-50.
- Fadok, V.A., and Henson, P.M. (1998). Apoptosis: getting rid of the bodies. *Current biology : CB* 8, R693-695.
- Fennell, D.A., Chacko, A., and Mutti, L. (2008). BCL-2 family regulation by the 20S proteasome inhibitor bortezomib. *Oncogene* 27, 1189-1197.
- Fernandez, Y., Verhaegen, M., Miller, T.P., Rush, J.L., Steiner, P., Pipari, A.W., Jr., Lowe, S.W., and Soengas, M.S. (2005). Differential regulation of noxa in normal melanocytes and melanoma cells by proteasome inhibition: therapeutic implications. *Cancer research* 65, 6294-6304.
- Fraile, B., Martin, R., De Miguel, M.P., Arenas, M.I., Bethencourt, F.R., Peinado, F., Paniagua, R., and Santamaria, L. (1996). Light and electron microscopic immunohistochemical localization of protein gene product 9.5 and ubiquitin immunoreactivities in the human epididymis and vas deferens. *Biology of reproduction* 55, 291-297.
- Fukutomi, S., Seki, N., Koda, K., and Miyazaki, M. (2007). Identification of methylation-silenced genes in colorectal cancer cell lines: genomic screening using oligonucleotide arrays. *Scandinavian journal of gastroenterology* 42, 1486-1494.
- Gartner, A., Milstein, S., Ahmed, S., Hodgkin, J., and Hengartner, M.O. (2000). A conserved checkpoint pathway mediates DNA damage--induced apoptosis and cell cycle arrest in *C. elegans*. *Molecular cell* 5, 435-443.
- Giacomini, P., Aguzzi, A., and Ferrone, S. (1986). Differential susceptibility to modulation by recombinant immune interferon of HLA-DR and -DQ antigens synthesized by melanoma COLO 38 cells. *Hybridoma* 5, 277-288.
- Gomez-Bougie, P., Wuilleme-Toumi, S., Menoret, E., Trichet, V., Robillard, N., Philippe, M., Bataille, R., and Amiot, M. (2007). Noxa up-regulation and Mcl-1

- cleavage are associated to apoptosis induction by bortezomib in multiple myeloma. *Cancer research* 67, 5418-5424.
- Goodlett, C.R., and Horn, K.H. (2001). Mechanisms of alcohol-induced damage to the developing nervous system. *Alcohol research & health : the journal of the National Institute on Alcohol Abuse and Alcoholism* 25, 175-184.
- Green, D.R. (2000). Apoptotic pathways: paper wraps stone blunts scissors. *Cell* 102, 1-4.
- Hallaert, D.Y., Spijker, R., Jak, M., Derks, I.A., Alves, N.L., Wensveen, F.M., de Boer, J.P., de Jong, D., Green, S.R., van Oers, M.H., *et al.* (2007). Crosstalk among Bcl-2 family members in B-CLL: seliciclib acts via the Mcl-1/Noxa axis and gradual exhaustion of Bcl-2 protection. *Cell death and differentiation* 14, 1958-1967.
- Hanahan, D., and Weinberg, R.A. (2000). The hallmarks of cancer. *Cell* 100, 57-70.
- Hanahan, D., and Weinberg, R.A. (2011). Hallmarks of cancer: the next generation. *Cell* 144, 646-674.
- Harada, T., Harada, C., Wang, Y.L., Osaka, H., Amanai, K., Tanaka, K., Takizawa, S., Setsuie, R., Sakurai, M., Sato, Y., *et al.* (2004). Role of ubiquitin carboxy terminal hydrolase-L1 in neural cell apoptosis induced by ischemic retinal injury in vivo. *The American journal of pathology* 164, 59-64.
- Herrmann, J.L., Briones, F., Jr., Brisbay, S., Logothetis, C.J., and McDonnell, T.J. (1998). Prostate carcinoma cell death resulting from inhibition of proteasome activity is independent of functional Bcl-2 and p53. *Oncogene* 17, 2889-2899.
- Hershko, T., and Ginsberg, D. (2004). Up-regulation of Bcl-2 homology 3 (BH3)-only proteins by E2F1 mediates apoptosis. *The Journal of biological chemistry* 279, 8627-8634.
- Hijikata, M., Kato, N., Sato, T., Kagami, Y., and Shimotohno, K. (1990). Molecular cloning and characterization of a cDNA for a novel phorbol-12-myristate-13-acetate-responsive gene that is highly expressed in an adult T-cell leukemia cell line. *Journal of virology* 64, 4632-4639.
- Hoeller, D., and Dikic, I. (2009). Targeting the ubiquitin system in cancer therapy. *Nature* 458, 438-444.
- Hollstein, M., Rice, K., Greenblatt, M.S., Soussi, T., Fuchs, R., Sorlie, T., Hovig, E., Smith-Sorensen, B., Montesano, R., and Harris, C.C. (1994). Database of p53 gene somatic mutations in human tumors and cell lines. *Nucleic acids research* 22, 3551-3555.
- Horvitz, H.R. (2003a). Nobel lecture. Worms, life and death. *Bioscience reports* 23, 239-303.
- Horvitz, H.R. (2003b). Worms, life, and death (Nobel lecture). *Chembiochem : a European journal of chemical biology* 4, 697-711.
- Hsu, Y.T., Wolter, K.G., and Youle, R.J. (1997). Cytosol-to-membrane redistribution of Bax and Bcl-X(L) during apoptosis. *Proceedings of the National Academy of Sciences of the United States of America* 94, 3668-3672.
- Inoue, S., Riley, J., Gant, T.W., Dyer, M.J., and Cohen, G.M. (2007). Apoptosis induced by histone deacetylase inhibitors in leukemic cells is mediated by Bim and Noxa. *Leukemia : official journal of the Leukemia Society of America, Leukemia Research Fund, UK* 21, 1773-1782.
- Inoue, S., Walewska, R., Dyer, M.J., and Cohen, G.M. (2008). Downregulation of Mcl-1 potentiates HDACi-mediated apoptosis in leukemic cells. *Leukemia : official journal of the Leukemia Society of America, Leukemia Research Fund, UK* 22, 819-825.

- Inuzuka, H., Shaik, S., Onoyama, I., Gao, D., Tseng, A., Maser, R.S., Zhai, B., Wan, L., Gutierrez, A., Lau, A.W., *et al.* (2011). SCF(FBW7) regulates cellular apoptosis by targeting MCL1 for ubiquitylation and destruction. *Nature* 471, 104-109.
- Jing, H., Kase, J., Dorr, J.R., Milanovic, M., Lenze, D., Grau, M., Beuster, G., Ji, S., Reimann, M., Lenz, P., *et al.* (2011). Opposing roles of NF-kappaB in anti-cancer treatment outcome unveiled by cross-species investigations. *Genes Dev* 25, 2137-2146.
- Kashkar, H., Deggerich, A., Seeger, J.M., Yazdanpanah, B., Wiegmann, K., Haubert, D., Pongratz, C., and Kronke, M. (2007). NF-kappaB-independent down-regulation of XIAP by bortezomib sensitizes HL B cells against cytotoxic drugs. *Blood* 109, 3982-3988.
- Kelly, P.N., and Strasser, A. (2011). The role of Bcl-2 and its pro-survival relatives in tumourigenesis and cancer therapy. *Cell death and differentiation* 18, 1414-1424.
- Kerr, J.F., Winterford, C.M., and Harmon, B.V. (1994). Apoptosis. Its significance in cancer and cancer therapy. *Cancer* 73, 2013-2026.
- Kerr, J.F., Wyllie, A.H., and Currie, A.R. (1972). Apoptosis: a basic biological phenomenon with wide-ranging implications in tissue kinetics. *British journal of cancer* 26, 239-257.
- Kim, D.A., Jeon, Y.K., and Nam, M.J. (2011). Galangin induces apoptosis in gastric cancer cells via regulation of ubiquitin carboxy-terminal hydrolase isozyme L1 and glutathione S-transferase P. *Food and chemical toxicology : an international journal published for the British Industrial Biological Research Association* 50, 684-688.
- Kim, H.J., Kim, Y.M., Lim, S., Nam, Y.K., Jeong, J., Kim, H.J., and Lee, K.J. (2009). Ubiquitin C-terminal hydrolase-L1 is a key regulator of tumor cell invasion and metastasis. *Oncogene* 28, 117-127.
- Kim, J.Y., Ahn, H.J., Ryu, J.H., Suk, K., and Park, J.H. (2004a). BH3-only protein Noxa is a mediator of hypoxic cell death induced by hypoxia-inducible factor 1alpha. *The Journal of experimental medicine* 199, 113-124.
- Kim, S.W., Wang, W., Nielsen, J., Praetorius, J., Kwon, T.H., Knepper, M.A., Frokiaer, J., and Nielsen, S. (2004b). Increased expression and apical targeting of renal ENaC subunits in puromycin aminonucleoside-induced nephrotic syndrome in rats. *American journal of physiology Renal physiology* 286, F922-935.
- Kiryu-Seo, S., Hirayama, T., Kato, R., and Kiyama, H. (2005). Noxa is a critical mediator of p53-dependent motor neuron death after nerve injury in adult mouse. *The Journal of neuroscience : the official journal of the Society for Neuroscience* 25, 1442-1447.
- Kluck, R.M., Bossy-Wetzell, E., Green, D.R., and Newmeyer, D.D. (1997). The release of cytochrome c from mitochondria: a primary site for Bcl-2 regulation of apoptosis. *Science* 275, 1132-1136.
- Kon, Y., Endoh, D., and Iwanaga, T. (1999). Expression of protein gene product 9.5, a neuronal ubiquitin C-terminal hydrolase, and its developing change in sertoli cells of mouse testis. *Molecular reproduction and development* 54, 333-341.
- Kumar, S., and Lavin, M.F. (1996). The ICE family of cysteine proteases as effectors of cell death. *Cell death and differentiation* 3, 255-267.
- Kwon, J., Kikuchi, T., Setsuie, R., Ishii, Y., Kyuwa, S., and Yoshikawa, Y. (2003). Characterization of the testis in congenitally ubiquitin carboxy-terminal hydrolase-1 (Uch-L1) defective (gad) mice. *Experimental animals / Japanese Association for Laboratory Animal Science* 52, 1-9.
- Levine, A.J. (1997). p53, the cellular gatekeeper for growth and division. *Cell* 88, 323-331.

- Liu, F.T., Agrawal, S.G., Gribben, J.G., Ye, H., Du, M.Q., Newland, A.C., and Jia, L. (2008). Bortezomib blocks Bax degradation in malignant B cells during treatment with TRAIL. *Blood* 111, 2797-2805.
- Liu, Y., Fallon, L., Lashuel, H.A., Liu, Z., and Lansbury, P.T., Jr. (2002). The UCH-L1 gene encodes two opposing enzymatic activities that affect alpha-synuclein degradation and Parkinson's disease susceptibility. *Cell* 111, 209-218.
- Lopes, U.G., Erhardt, P., Yao, R., and Cooper, G.M. (1997). p53-dependent induction of apoptosis by proteasome inhibitors. *The Journal of biological chemistry* 272, 12893-12896.
- Lord, S.J., Rajotte, R.V., Korbutt, G.S., and Bleackley, R.C. (2003). Granzyme B: a natural born killer. *Immunological reviews* 193, 31-38.
- Lowe, G., and Gold, G.H. (1993). Nonlinear amplification by calcium-dependent chloride channels in olfactory receptor cells. *Nature* 366, 283-286.
- Luo, X., Budihardjo, I., Zou, H., Slaughter, C., and Wang, X. (1998). Bid, a Bcl2 interacting protein, mediates cytochrome c release from mitochondria in response to activation of cell surface death receptors. *Cell* 94, 481-490.
- Mackus, W.J., Kater, A.P., Grummels, A., Evers, L.M., Hooijbrink, B., Kramer, M.H., Castro, J.E., Kipps, T.J., van Lier, R.A., van Oers, M.H., *et al.* (2005). Chronic lymphocytic leukemia cells display p53-dependent drug-induced Puma upregulation. *Leukemia : official journal of the Leukemia Society of America, Leukemia Research Fund, UK* 19, 427-434.
- Martin, R., Santamaria, L., Fraile, B., Paniagua, R., and Polak, J.M. (1995). Ultrastructural localization of PGP 9.5 and ubiquitin immunoreactivities in rat ductus epididymidis epithelium. *The Histochemical journal* 27, 431-439.
- Masson, M., Rolli, V., Dantzer, F., Trucco, C., Schreiber, V., Fribourg, S., Molinete, M., Ruf, A., Miranda, E.A., Niedergang, C., *et al.* (1995). Poly(ADP-ribose) polymerase: structure-function relationship. *Biochimie* 77, 456-461.
- McDonnell, T.J., and Korsmeyer, S.J. (1991). Progression from lymphoid hyperplasia to high-grade malignant lymphoma in mice transgenic for the t(14; 18). *Nature* 349, 254-256.
- Miyashita, T., and Reed, J.C. (1995). Tumor suppressor p53 is a direct transcriptional activator of the human bax gene. *Cell* 80, 293-299.
- Nakano, K., and Vousden, K.H. (2001). PUMA, a novel proapoptotic gene, is induced by p53. *Molecular cell* 7, 683-694.
- Nesbit, C.E., Tersak, J.M., and Prochownik, E.V. (1999). MYC oncogenes and human neoplastic disease. *Oncogene* 18, 3004-3016.
- Newmeyer, D.D., and Ferguson-Miller, S. (2003). Mitochondria: releasing power for life and unleashing the machineries of death. *Cell* 112, 481-490.
- Nicholson, D.W. (1999). Caspase structure, proteolytic substrates, and function during apoptotic cell death. *Cell death and differentiation* 6, 1028-1042.
- Nicholson, D.W., and Thornberry, N.A. (1997). Caspases: killer proteases. *Trends in biochemical sciences* 22, 299-306.
- Nijman, S.M., Luna-Vargas, M.P., Velds, A., Brummelkamp, T.R., Dirac, A.M., Sixma, T.K., and Bernards, R. (2005). A genomic and functional inventory of deubiquitinating enzymes. *Cell* 123, 773-786.
- Nikiforov, M.A., Riblett, M., Tang, W.H., Gratchouck, V., Zhuang, D., Fernandez, Y., Verhaegen, M., Varambally, S., Chinnaiyan, A.M., Jakubowiak, A.J., *et al.* (2007). Tumor cell-selective regulation of NOXA by c-MYC in response to proteasome inhibition. *Proceedings of the National Academy of Sciences of the United States of America* 104, 19488-19493.



- Nussbaum, A.K., Dick, T.P., Keilholz, W., Schirle, M., Stevanovic, S., Dietz, K., Heinemeyer, W., Groll, M., Wolf, D.H., Huber, R., *et al.* (1998). Cleavage motifs of the yeast 20S proteasome beta subunits deduced from digests of enolase 1. *Proceedings of the National Academy of Sciences of the United States of America* *95*, 12504-12509.
- Oda, E., Ohki, R., Murasawa, H., Nemoto, J., Shibue, T., Yamashita, T., Tokino, T., Taniguchi, T., and Tanaka, N. (2000). Noxa, a BH3-only member of the Bcl-2 family and candidate mediator of p53-induced apoptosis. *Science* *288*, 1053-1058.
- Oren, M. (1999). Regulation of the p53 tumor suppressor protein. *The Journal of biological chemistry* *274*, 36031-36034.
- Orlowski, R.Z., and Kuhn, D.J. (2008). Proteasome inhibitors in cancer therapy: lessons from the first decade. *Clinical cancer research : an official journal of the American Association for Cancer Research* *14*, 1649-1657.
- Peng, J., Schwartz, D., Elias, J.E., Thoreen, C.C., Cheng, D., Marsischky, G., Roelofs, J., Finley, D., and Gygi, S.P. (2003). A proteomics approach to understanding protein ubiquitination. *Nature biotechnology* *21*, 921-926.
- Perez-Galan, P., Roue, G., Villamor, N., Montserrat, E., Campo, E., and Colomer, D. (2006). The proteasome inhibitor bortezomib induces apoptosis in mantle-cell lymphoma through generation of ROS and Noxa activation independent of p53 status. *Blood* *107*, 257-264.
- Pfaffl, M.W. (2001). A new mathematical model for relative quantification in real-time RT-PCR. *Nucleic acids research* *29*, e45.
- Pickart, C.M. (2001). Mechanisms underlying ubiquitination. *Annual review of biochemistry* *70*, 503-533.
- Ploner, C., Rainer, J., Lobenwein, S., Geley, S., and Kofler, R. (2009). Repression of the BH3-only molecule PMAIP1/Noxa impairs glucocorticoid sensitivity of acute lymphoblastic leukemia cells. *Apoptosis : an international journal on programmed cell death* *14*, 821-828.
- Qin, J.Z., Ziffra, J., Stennett, L., Bodner, B., Bonish, B.K., Chaturvedi, V., Bennett, F., Pollock, P.M., Trent, J.M., Hendrix, M.J., *et al.* (2005). Proteasome inhibitors trigger NOXA-mediated apoptosis in melanoma and myeloma cells. *Cancer research* *65*, 6282-6293.
- Sakahira, H., Enari, M., and Nagata, S. (1998). Cleavage of CAD inhibitor in CAD activation and DNA degradation during apoptosis. *Nature* *391*, 96-99.
- Sanghavi, D.M., Thelen, M., Thornberry, N.A., Casciola-Rosen, L., and Rosen, A. (1998). Caspase-mediated proteolysis during apoptosis: insights from apoptotic neutrophils. *FEBS letters* *422*, 179-184.
- Sato, N., Fukushima, N., Maitra, A., Matsubayashi, H., Yeo, C.J., Cameron, J.L., Hruban, R.H., and Goggins, M. (2003). Discovery of novel targets for aberrant methylation in pancreatic carcinoma using high-throughput microarrays. *Cancer research* *63*, 3735-3742.
- Schmidt, P., Kopecky, C., Hombach, A., Zigrino, P., Mauch, C., and Abken, H. (2011). Eradication of melanomas by targeted elimination of a minor subset of tumor cells. *Proceedings of the National Academy of Sciences of the United States of America* *108*, 2474-2479.
- Seeger, J.M., Schmidt, P., Brinkmann, K., Hombach, A.A., Coutelle, O., Zigrino, P., Wagner-Stippich, D., Mauch, C., Abken, H., Kronke, M., *et al.* (2010). The proteasome inhibitor bortezomib sensitizes melanoma cells toward adoptive CTL attack. *Cancer research* *70*, 1825-1834.
- Shiloh, Y. (2003). ATM and related protein kinases: safeguarding genome integrity. *Nature reviews Cancer* *3*, 155-168.

- Strasser, A., Harris, A.W., Bath, M.L., and Cory, S. (1990). Novel primitive lymphoid tumours induced in transgenic mice by cooperation between *myc* and *bcl-2*. *Nature* **348**, 331-333.
- Strasser, A., Harris, A.W., Jacks, T., and Cory, S. (1994). DNA damage can induce apoptosis in proliferating lymphoid cells via p53-independent mechanisms inhibitable by Bcl-2. *Cell* **79**, 329-339.
- Strasser, A., O'Connor, L., and Dixit, V.M. (2000). Apoptosis signaling. *Annual review of biochemistry* **69**, 217-245.
- Strasser, A., Whittingham, S., Vaux, D.L., Bath, M.L., Adams, J.M., Cory, S., and Harris, A.W. (1991). Enforced BCL2 expression in B-lymphoid cells prolongs antibody responses and elicits autoimmune disease. *Proceedings of the National Academy of Sciences of the United States of America* **88**, 8661-8665.
- Sun, L., and Chen, Z.J. (2004). The novel functions of ubiquitination in signaling. *Current opinion in cell biology* **16**, 119-126.
- Tait, S.W., and Green, D.R. (2010). Mitochondria and cell death: outer membrane permeabilization and beyond. *Nature reviews Molecular cell biology* **11**, 621-632.
- Thomson, D.J. (1995). The seasons, global temperature, and precession. *Science* **268**, 59-68.
- Vander Heiden, M.G., Chandel, N.S., Williamson, E.K., Schumacker, P.T., and Thompson, C.B. (1997). Bcl-xL regulates the membrane potential and volume homeostasis of mitochondria. *Cell* **91**, 627-637.
- Vaux, D.L., Cory, S., and Adams, J.M. (1988). Bcl-2 gene promotes haemopoietic cell survival and cooperates with c-myc to immortalize pre-B cells. *Nature* **335**, 440-442.
- Voges, D., Zwickl, P., and Baumeister, W. (1999). The 26S proteasome: a molecular machine designed for controlled proteolysis. *Annual review of biochemistry* **68**, 1015-1068.
- Voorhees, P.M., and Orłowski, R.Z. (2006). The proteasome and proteasome inhibitors in cancer therapy. *Annu Rev Pharmacol Toxicol* **46**, 189-213.
- Walker, N.P., Talanian, R.V., Brady, K.D., Dang, L.C., Bump, N.J., Ferenz, C.R., Franklin, S., Ghayur, T., Hackett, M.C., Hammill, L.D., *et al.* (1994). Crystal structure of the cysteine protease interleukin-1 beta-converting enzyme: a (p20/p10)<sub>2</sub> homodimer. *Cell* **78**, 343-352.
- Wang, J.Y. (1998). Cellular responses to DNA damage. *Current opinion in cell biology* **10**, 240-247.
- Wang, W.J., Li, Q.Q., Xu, J.D., Cao, X.X., Li, H.X., Tang, F., Chen, Q., Yang, J.M., Xu, Z.D., and Liu, X.P. (2008). Over-expression of ubiquitin carboxy terminal hydrolase-L1 induces apoptosis in breast cancer cells. *International journal of oncology* **33**, 1037-1045.
- Wang, Y.L., Liu, W., Sun, Y.J., Kwon, J., Setsuie, R., Osaka, H., Noda, M., Aoki, S., Yoshikawa, Y., and Wada, K. (2006). Overexpression of ubiquitin carboxyl-terminal hydrolase L1 arrests spermatogenesis in transgenic mice. *Molecular reproduction and development* **73**, 40-49.
- Watanabe-Fukunaga, R., Brannan, C.I., Copeland, N.G., Jenkins, N.A., and Nagata, S. (1992). Lymphoproliferation disorder in mice explained by defects in Fas antigen that mediates apoptosis. *Nature* **356**, 314-317.
- Wei, M.C., Lindsten, T., Mootha, V.K., Weiler, S., Gross, A., Ashiya, M., Thompson, C.B., and Korsmeyer, S.J. (2000). tBID, a membrane-targeted death ligand, oligomerizes BAK to release cytochrome c. *Genes Dev* **14**, 2060-2071.
- Weinberg, R.A. (1996). How cancer arises. *Sci Am* **275**, 62-70.

- Wertz, I.E., Kusam, S., Lam, C., Okamoto, T., Sandoval, W., Anderson, D.J., Helgason, E., Ernst, J.A., Eby, M., Liu, J., *et al.* (2011). Sensitivity to antitubulin chemotherapeutics is regulated by MCL1 and FBW7. *Nature* **471**, 110-114.
- Widlak, P., Lanuszewska, J., Cary, R.B., and Garrard, W.T. (2003). Subunit structures and stoichiometries of human DNA fragmentation factor proteins before and after induction of apoptosis. *The Journal of biological chemistry* **278**, 26915-26922.
- Wilkinson, K.D. (1999). Ubiquitin-dependent signaling: the role of ubiquitination in the response of cells to their environment. *The Journal of nutrition* **129**, 1933-1936.
- Wilson, K.P., Black, J.A., Thomson, J.A., Kim, E.E., Griffith, J.P., Navia, M.A., Murcko, M.A., Chambers, S.P., Aldape, R.A., Raybuck, S.A., *et al.* (1994). Structure and mechanism of interleukin-1 beta converting enzyme. *Nature* **370**, 270-275.
- Wyllie, A.H., Kerr, J.F., and Currie, A.R. (1980). Cell death: the significance of apoptosis. *International review of cytology* **68**, 251-306.
- Xiang, T., Li, L., Yin, X., Yuan, C., Tan, C., Su, X., Xiong, L., Putti, T.C., Oberst, M., Kelly, K., *et al.* (2012). The ubiquitin peptidase UCHL1 induces G0/G1 cell cycle arrest and apoptosis through stabilizing p53 and is frequently silenced in breast cancer. *PloS one* **7**, e29783.
- Yamashita, K., Park, H.L., Kim, M.S., Osada, M., Tokumaru, Y., Inoue, H., Mori, M., and Sidransky, D. (2006). PGP9.5 methylation in diffuse-type gastric cancer. *Cancer research* **66**, 3921-3927.
- Yang, H., Zonder, J.A., and Dou, Q.P. (2009). Clinical development of novel proteasome inhibitors for cancer treatment. *Expert opinion on investigational drugs* **18**, 957-971.
- Yang, J., Liu, X., Bhalla, K., Kim, C.N., Ibrado, A.M., Cai, J., Peng, T.I., Jones, D.P., and Wang, X. (1997). Prevention of apoptosis by Bcl-2: release of cytochrome c from mitochondria blocked. *Science* **275**, 1129-1132.
- Yin, X.M., Wang, K., Gross, A., Zhao, Y., Zinkel, S., Klocke, B., Roth, K.A., and Korsmeyer, S.J. (1999). Bid-deficient mice are resistant to Fas-induced hepatocellular apoptosis. *Nature* **400**, 886-891.
- Yu, J., Tao, Q., Cheung, K.F., Jin, H., Poon, F.F., Wang, X., Li, H., Cheng, Y.Y., Rocken, C., Ebert, M.P., *et al.* (2008). Epigenetic identification of ubiquitin carboxyl-terminal hydrolase L1 as a functional tumor suppressor and biomarker for hepatocellular carcinoma and other digestive tumors. *Hepatology* **48**, 508-518.
- Zaher, M., Akrouf, I., Mirshahi, M., Kolb, J.P., and Billard, C. (2009). Noxa upregulation is associated with apoptosis of chronic lymphocytic leukemia cells induced by hyperforin but not flavopiridol. *Leukemia : official journal of the Leukemia Society of America, Leukemia Research Fund, UK* **23**, 594-596.
- Zhu, H., Zhang, L., Dong, F., Guo, W., Wu, S., Teraishi, F., Davis, J.J., Chiao, P.J., and Fang, B. (2005). Bik/NBK accumulation correlates with apoptosis-induction by bortezomib (PS-341, Velcade) and other proteasome inhibitors. *Oncogene* **24**, 4993-4999.
- Zigrino, P., Mauch, C., Fox, J.W., and Nischt, R. (2005). Adam-9 expression and regulation in human skin melanoma and melanoma cell lines. *International journal of cancer Journal international du cancer* **116**, 853-859.

## 6 Appendix

### 6.1 Microarray

**Table 5.1 | Gene based list of mRNA expression.** Dual colour PIQUOR-UPS-microarray (Miltényi) was performed in *Pat1-3* cells using non-malignant melanocytes as a reference, bortezomib sensitive *Colo38* melanoma cells using bortezomib resistant *SKmel23* melanoma cells as a reference and *L428/L591* Hodgkin Lymphoma cells using non-malignant *L1309* B-cells as a reference. List represents a selection of DUBs (**A**) and RING-domain containing proteins (**B**) which were amplified in at least 4 of 6 assays. Ratios represent normalized Cy5/Cy3 ratios of 4 replicates per gene. Genes that are >1.7 up- or down- regulated (ratio>1.7 and ratio<0.58, respectively) represent putative candidate genes which are significantly dysregulated in comparison to the control. n.a.-not amplified.

A									
Name	UniProt/trEMBL	RefSeq	Pat1	Pat2	Pat3	Colo38	L428	L591	
BAP1	Q92560 Q6LEM0 Q7Z5E8 Q9NQC7 Q94934 Q7L3N6 Q96EH0 Q9NZX9	NM_004656	0,5	0.50	0.57	n.a.	0.58	n.a.	
CYLD		NM_015247	2,14	1,1	0,97	n.a.	0.49	0.40	
UCHL1	P09936 Q71UM0	NM_004181	0.65	0.06	0.23	0.23	0.20	0.22	
UCHL34	P15374 Q5TBK8 Q6IBE9 Q9Y5K5 Q9UQN2 Q9P0I3 Q9H1W5 Q5LJA6 Q5LJA7 Q8TBS4 Q96BJ9	NM_006002	3.47	0.89	1.05	1,42	0.64	0.62	
UCHL5		NM_015984	1.54	1.49	1.43	n.a.	0.99	1.41	
USP1	O94782 Q9UFR0 Q9UNJ3	NM_003368	4.85	3.67	2.78	n.a.	1.57	n.a.	
USP3	Q9Y6I4Q9Y2R8	NM_006537	1.09	1.51	1.33	n.a.	0.80	n.a.	
USP4	Q13107 O43452 O43453	NM_003363	1.22	1.35	1.28	n.a.	0.61	n.a.	
USP5	P45974 Q96J22	NM_003481	0.69	0.94	0.72	n.a.	0.88	n.a.	
USP7	Q93009 P40818 Q7Z3U2 Q86VA0	NM_003470	1.62	1.65	1.19	n.a.	1.46	1.89	
USP8	Q8IWI7	NM_005154	0.85	1.16	1.45	n.a.	n.a.	n.a.	
USP10	Q14694 Q9NSL7 Q9BWG7	NM_005153	1.28	1.28	0.92	1.30	1.65	0.93	
USP11	P51784 Q9BWE1 Q8IUG6	NM_004651	0.75	0.74	0.61	n.a.	0.79	n.a.	
USP13	Q92995	NM_003940	0.93	0.93	0.80	n.a.	0.82	n.a.	
USP14	P54578	NM_005151	1.41	1.09	1.10	n.a.	0.80	1.02	
USP15	Q9Y4E8 Q9HCA6 Q9UNP0 Q9Y5B5	NM_006313	1.09	1.44	n.a.	n.a.	0.88	0.84	
USP16	Q9Y5T5 Q8NEL3	NM_001001992 NM_001032410 NM_006447	2.31	1.42	1.22	1,37	1.10	0.96	
USP18									
USP4	Q9UMW8 Q9NY71 Q70BM7	NM_017414	0.32	0.71	0.44	n.a.	1.07	n.a.	
USP19	O94966	NM_006677	0.83	0.86	0.85	n.a.	0.75	n.a.	
USP22	Q9UPT9 Q9UPU5 Q9NXD1 Q6ZSY2	-	0.80	1.67	1.44	n.a.	1.30	1.30	
USP24	Q8N2Y4	-	1.88	1.63	1.68	n.a.	0.97	0.88	
USP32_1	Q9BX85 Q8NFA0 Q9Y591 Q9UPQ5 Q9H9F0 Q8TEY7 Q8TEY6 Q96AV6	NM_032582	2.12	1.53	2.96	n.a.	0.53	0.46	
USP33	Q8N3T9 Q9UGA1 Q3B777 Q6P6C9 Q70CQ2 Q7L8P6	NM_015017	0.93	n.a.	1.42	n.a.	0.47	0.49	
USP34		NM_014709	1.17	1.57	n.a.	n.a.	1.11	n.a.	
USP35	Q9P2H5	-	0.93	0.87	1.26	n.a.	0.63	0.65	
USP36	Q9P275 Q8NDM8 Q9NVC8	NM_025090	0.81	0.80	1.01	n.a.	0.62	n.a.	
USP37	Q9HCH8 Q86T82 Q9H381 Q96RK9 Q9BV89 Q53GS9 Q6NX47 Q9P050 Q9Y310	NM_020935	1.37	1.55	1.24	n.a.	0.85	n.a.	
USP39		NM_006590	1.04	1.12	1.04	n.a.	1.15	1.74	
USP44	Q9H0E7 Q96F64 Q9H5N3 Q9H5T7 Q8N3F6 Q9NUJ6 Q9NXR0 Q96IQ3 Q86UV5 Q2M3I4 Q	NM_032147	1.63	1.25	0.93	n.a.	0.66	0.72	
USP48_2		NM_032236	1.47	1.06	1.43	n.a.	0.74	0.61	
USP49	Q96CK4 Q70CQ1	NM_018561	0.61	1.10	0.88	n.a.	1.23	1.31	

B

Name	UniProt/trEMBL	RefSeq	Pat1	Pat2	Pat3	Colo38	L428	L591
RNF138	Q9UKI6 Q9H8K2 Q8WVVD3 Q9UF87	NM_016271 NM_198128 NM_007294 NM_007297 NM_007298 NM_007299 NM_007300 NR_027676	9.01	1.86	n.a.	n.a.	1.23	1.51
BRCA1	P38398		0.72	0.94	0.83	0.63	0.82	0.64
BARD1	Q99728 Q43574	NM_000465	1.86	1.74	1.03	0.64	0.95	0.63
RNF8	O76064	NM_003958 NM_183078	0.88	0.89	0.90	0.53	0.50	0.49
ITCH	O43584 Q96J02 Q96F66 Q9BY75 Q9H451 Q9H4U5 Q5TELO	NM_031483	0.63	1.24	1.74	0.56	0.37	0.50
HECW1	O15036 Q9HCC7 Q76N89 O43165 Q9H2W4 Q7Z5F Q7Z5F2 Q7Z5N3 Q8N5A7 Q8WUU9 Q96PU5 Q9BW58 Q	NM_015052	0.49	0.58	0.57	0.47	0.17	0.42
NEDD4LA	P46934	NM_015277	0.09	0.35	1.05	0.73	0.39	0.36
NEDD4	O00308 Q96CZ2 Q9BWN6	NM_006154 NM_198400 NM_007014 NM_199424	0.54	0.90	0.99	0.49	0.30	0.42
WWP2_1	P22681	NM_005188	0.96	0.81	0.71	0.47	0.53	0.57
CBL	Q14848 O75615 Q9BUZ4 Q2PJN8	NM_004295	0.86	0.78	1.54	1.07	0.59	0.50
TRAF4	O00463	NM_004619 NM_145759	1.08	1.31	n.a.	n.a.	0.70	0.84
TRAF5	Q9Y4K3 Q8NEH5	NM_004620 NM_145803	0.94	0.86	0.85	n.a.	0.82	n.a.
TRAF6	Q03518 Q16149	NM_000593	0.83	0.61	1.32	0.95	0.94	0.79
TAP1	P28062 Q29824 Q96J48	NM_004159 NM_148919	0.02	0.39	0.13	1.23	0.51	0.55
PSMB8	P28065 Q16523	NM_002800 NM_148954 NM_001007278 NM_005798 NM_052811 NM_213590	0.04	0.51	0.12	1.37	0.42	0.33
PSMB9								
RFP2	O60858 Q9C021 Q9BQ47 Q93040 O00677 Q13263 Q7Z632 Q96IM1	NM_005762	0.81	0.85	0.86	0.66	0.32	0.36
TRIM28	P28328 Q9BW41 Q567S6	NM_000318	1.05	1.04	n.a.	n.a.	0.78	0.87
PXMP3	O75150 Q9HC82 Q8N615 Q6AHZ6 Q6N005 Q7L3T6 Q96T18 Q9BSV9 P14373 Q6LA73 Q6NXR9 Q9BZY6 Q9UJL3 Q5ST26	NM_014771	2.86	0.89	0.71	1.17	0.81	0.74
RNF40	Q9Y4Y1 Q9H5H9 Q9UFG0 Q9H8M8 Q9UFX6 Q9NV58	NM_030950	0.48	0.44	0.50	0.59	0.35	0.45
RFP	P78355 Q93066 Q05086 Q9UEP4 Q9UEP5 Q9UEP6 Q9UEP7 Q9UEP8 Q9UEP9	NM_000462 NM_130838 NM_130839	0.90	1.49	1.48	0.71	0.59	0.67
RNF19	Q13064	NM_005664	0.51	0.50	0.56	0.39	0.28	0.35
UBE3A	Q9NPD8	NM_014176	2.74	1.70	1.50	1.26	1.71	2.44
MKR3	P51966 Q9HAV1 P70653 P68036 104444	NM_003347 NM_198157	0.93	1.42	1.02	1.22	0.56	0.85
UBE2L3	Q9H5F1 Q96EP0 Q86VI2 Q8TEI0 Q96GB4 Q96NF1 Q9NWD2	NM_017999	0.75	0.75	0.73	n.a.	n.a.	1.11
RNF31	Q8NBD1 Q86T96 Q0JSU3 Q495A	NM_178532	0.82	0.71	0.74	0.47	0.31	0.40
RNF180	Q8NA67 Q8IYW5 Q96NS4	NM_152617	1.21	1.33	1.41	n.a.	0.61	1.02
RNF168		NM_001002244 NM_001002248	1.13	1.41	1.96	0.85	1.31	2.21
ANAPC11	Q9NYG5 Q9P0R2 Q9BW64 Q502X9	NM_005180	2.07	2.12	2.26	0.95	1.24	1.14
PCGF4	P35226 Q96F37 Q16030	NM_014455	2.21	1.18	1.45	n.a.	0.64	0.52
ZNF364	Q9Y4L5 Q7Z2J2 Q5T2V9	NM_006568	0.60	0.62	0.60	n.a.	0.32	0.53
ZNF364	Q99675 Q96BX2							
CGRRF1	Q9NRT4 Q96EP1 Q96SL3 Q9NT32 Q9NVD5	NM_018223	1.04	0.85	n.a.	n.a.	0.43	0.55
CHFR	Q9UNE7 Q969U2 O60526 Q9HBT1	NM_005861	0.84	0.60	0.59	0.87	1.11	1.79
STUB1	Q9H6L7 Q8NHY2 Q6H103	NM_022457	0.94	1.54	0.86	0.70	0.65	0.65
RFWD2	Q99496 Q5TEN1 Q5TEN2	NM_007212	1.19	1.10	1.20	0.50	0.41	0.60
RNF2	Q9Y225 Q9UMH1	NM_007219	0.59	0.81	0.59	n.a.	0.59	n.a.
RNF24	Q9Y508 Q6N0B0	NM_018683	0.62	1.63	1.98	0.91	1.40	1.48
ZNF313	Q9H0M8 Q5I022 Q8IW18 Q6PFW4 Q5XPI4							
RNF123	Q9H9T2 Q71RH0 Q9H5L8	NM_022064	0.84	0.62	0.55	n.a.	0.58	n.a.
FANCL	Q9NW38	NM_018062	1.54	1.33	1.73	n.a.	1.59	n.a.
PJA1	Q9HAC1 Q8NG27 Q8NG28	NM_022368	0.74	0.72	0.71	n.a.	1.36	2.16
RNF186	Q9NXI6 Q53GE0	NM_019062	0.11	0.21	0.20	n.a.	0.65	0.54
RNF167	Q9H6Y7 Q8NDC1 Q9Y3V1 Q6XYE0	NM_015528	0.29	0.50	0.50	0.90	n.a.	1.04
ZNRF2	Q8NHG8 Q8NEX1	NM_147128	1.36	1.03	1.80	1.07	1.03	0.97
MKR2	Q9NRY1 Q9H000 Q9BUY2 Q8N391 Q96BD4	NM_014160	1.92	1.18	1.48	1.37	1.12	0.95
RNF181	Q9P0P0	NM_016494	0.95	1.31	1.20	n.a.	1.01	0.82
MARCH2	Q9P0N8 Q8N5A3 Q96B78	NM_001005415 NM_001005416 NM_016496	0.59	0.63	0.65	0.49	0.82	0.99
RNF5	Q99942 Q9UMQ2	NM_006913	1.25	0.82	0.78	1.62	0.76	0.64
RNF10	Q9ULW4 Q92550 Q8N5U6 Q9NPP8	NM_014868	0.61	0.69	0.63	n.a.	0.83	0.89
MARCH6	O60337 O14670 Q86X77 O75162 Q86Y13 Q6P3R9 Q6PH82 Q86Y14	NM_005885	1.15	1.72	2.16	1.34	0.70	0.95
DZIP3	Q86Y15 Q86Y16 Q8IW10 Q96RS9	NM_014648	1.00	0.58	0.60	n.a.	0.95	1.75
MYLIP	Q9UHE7 Q8WY64 Q9BU73 Q9NRL9	NM_013262	0.93	1.61	2.18	0.90	2.89	n.a.
MKR1_1	Q9UEZ7 Q9UHC7 Q9H0G0 Q6GSF1	NM_013446	1.21	0.67	0.95	0.41	1.15	0.93
SIAH2	O43255 Q43270	NM_005067	0.81	0.88	0.92	n.a.	1.25	0.98
TRIM22	Q15521 Q8IYM9	NM_006074	0.22	0.42	0.30	n.a.	0.25	0.22
RNF139	O75485 Q7LDL3 Q8WU17	NM_007218	1.82	1.59	1.82	n.a.	1.70	1.54

## 6.1 Patient data

**Table 5.2 | NOXA and UCH-L1 expression in melanoma patients.** Samples were selected from the archives of the University Hospital of Cologne with local research ethics committee approval. Melanomas were grouped into one of the four major subtypes according to histopathology and positivity to routinely analysed melanoma markers, HMB45 and S100. The 81 samples comprise these major subtypes, 22 superficial spreading malignant melanomas (SSM), 15 nodular melanomas (NMM), 1 lentigo maligna melanomas (LMM), 2 acral lentiginous melanomas (ALM), but also 40 cutaneous and 1 brain melanoma metastasis.

Intensities of specific staining in tumour cells were arbitrarily set as the following: -, no expression; +, low expression; ++, moderate expression; +++, strong expression.

Patient ID	Sex		Age (Y)	pathology	localization	TD	Noxa	UCHL1
	M(1)	W(0)						
1	1		74	met	trunk	-	+++	-
2	1		31	met	rectal tag	-	++	-
3	1		82	met	extremity	-	+++	+
4	1		73	met	extremity	-	++	-
5	1		27	met	extremity	-	++	-
6	0		78	met	trunk	-	+	-
7	1		62	met	extremity	-	++	-
8	0		61	met	extremity	-	++	-
9	1		70	met	trunk	-	+	-
10	0		79	met	face	-	-	-
11	0		78	met	face	-	-	-
12	1		79	met	face	-	++	+
13	1		73	met	trunk	-	+++	-
14	1		78	met	n.i.	-	+	+
15	0		64	met	n.i.	-	++	+
16	0		44	met	n.i.	-	+	-
17	0		57	met	n.i.	-	++	+
18	1		42	met	n.i.	-	++	+
19	1		83	met	trunk	-	++	-
20	1		52	met	inguinal	-	+++	++
21	0		82	met	n.i.	-	-	-
22	1		54	met	n.i.	-	-	-
23	0		77	met	n.i.	-	++	-
24	1		83	met	n.i.	-	+	-
25	1		56	met	n.i.	-	-	-
26	0		44	met	n.i.	-	-	-
27	1		72	met	n.i.	-	+	-
28	0		78	met	n.i.	-	+	-
29	1		60	met	n.i.	-	++	-
30	1		73	met	n.i.	-	+	+
31	1		43	met	n.i.	-	++	+
32	1		12	met	n.i.	-	++	-
33	0		79	met	face	-	+	-

34	1	73	met	n.i.	-	++	+
35	1	62	met	trunk	-	+++	-
36	0	64	met	n.i.	-	+++	-
37	0	77	met	n.i.	-	++	-
38	1	44	met	extremity	-	++	-
39	0	37	met	brain	-	+++	++
40	1	70	met	trunk	-	+++	+
41	1	70	met	extremity	-	++	-
42	0	81	LMM	foot	0,78	+++	-
43	0	69	SSM	trunk	4,05	++	+
44	1	58	NMM	extremity	2,41	+++	-
45	1	34	SSM	trunk	4,80	+	-
46	1	59	SSM	trunk	0,96	++	-
47	1	72	SSM	extremity	1,94	++	-
48	0	40	NMM	extremity	2,80	+++	-
49	1	39	NMM	trunk	5,10	+++	-
50	0	81	NMM	extremity	3,40	+	-
51	1	77	SSM	extremity	13,91	++	+
52	1	76	SSM	trunk	1,33	++	-
53	1	50	SSM	trunk	1,51	++	-
54	1	36	SSM	trunk	0,52	+	-
55	1	40	NMM	extremity	0,44	-	-
56	0	82	NMM	extremity	2,34	+++	-
57	1	79	NMM	nuchal	6,67	++	+
58	0	71	NMM	foot	4,92	+++	-
59	1	72	NMM	extremity	4,70	+++	-
60	0	78	NMM	extremity	19,50	+++	+
61	1	49	NMM	foot	9,53	+++	+
62	1	54	SSM	trunk	3,74	+++	+
63	1	46	SSM	trunk	3,20	-	-
64	0	55	SSM	extremity	0,65	+++	-
65	1	72	SSM	extremity	1,28	++	-
66	1	81	SSM	extremity	1,45	-	+
67	1	69	SSM	trunk	3,13	+	-
68	0	80	SSM	face	6,15	+++	-
69	1	75	SSM	trunk	1,04	+	-
70	0	58	NMM	vulva	14,00	++	+
71	1	76	NMM	trunk	3,60	++	-
72	1	41	NMM	trunk	8,36	+++	+
73	1	79	SSM	extremity	5,45	+++	+
74	0	82	SSM,	rectal tag	1,33	++	-
75	1	56	SSM	trunk	4,25	+++	++
76	1	62	SSM	extremity	2,84	+	+
77	0	79	ALM	extremity	4,22	+	-
78	0	75	SSM	trunk	3,80	++	-
79	1	68	SSM	trunk	3,05	++	+

80	0	88	ALM	toe	2,89	+	-
81	1	79	NMM	n.i.	n.i.	+	-

N. i. not indicated

Met cutaneous metastasis

LMM Lentigo Maligna Melanoma

ALM Acral Lentiginous Melanoma

SSM Superficial Spreading Melanoma

NMM Nodular Malignant Melanoma

**Table 5.3 | NOXA and UCH-L1 expression in colorectal carcinoma patients.**

Intensities of specific staining in tumour cells were arbitrarily set as the following: -, no expression; +, low expression; ++, moderate expression; +++, strong expression.

Patient ID	Sex		UICC Stage	T	N	M	Grade	NOXA	UCH-L1
	M(1) W (0)	Age (Y)							
8	0	65	2	3	1	0	2	++	-
10	1	65						++	-
15	1	78	2	3	0	0	2	+	-
16	1	77	3	3	2	0	3	+	-
17	1	74	2	3	0	0	2	+++	+
19	0	72	2	3	0	0	2	+	-
20	1	65	4	3	0	1	2	++	-
21	1	64	4	3	1	1	2	+	-
26	0	72	3	3	2	0	2	+++	+
28	1	62	3	4	2	0	3	++	-
33	0	74	3	3	2	0	2	++	+
34	1	64	4	3	2	1	2	+++	+
35	1	76	2	3	0	0	2	++	-
36	1	67	1	2	0	0	2	+	-
37	0	82	2	3	0	0	2	++	-
38	0	59	2	3	0	0	2	+	-
46	0	65	2	4	0	0	3	+	-
48	0	83	4	4	0	1	3	++	-
55	1	73	3	3	1	0	2	+++	+
74	1	67	2	3	0	0	2	+++	+
76	1	68	2	3	0		2	++	+
79	1	70	3	3	1	0	2	++	-
80	1	68	2	3	0	0	2	+++	++
88	1	76	4	4	1	1	3	++	+
91	0	62	2	3	0	0	2	-	-

T1-4: size and/or extension of the primary tumor

N: degree of spread to regional lymph nodes

N0: tumor cells absent from regional lymph nodes

N1: regional lymph node metastasis present; (at some sites: tumor spread to closest or small number of regional lymph nodes)

N2: tumor spread to an extent between N1 and N2

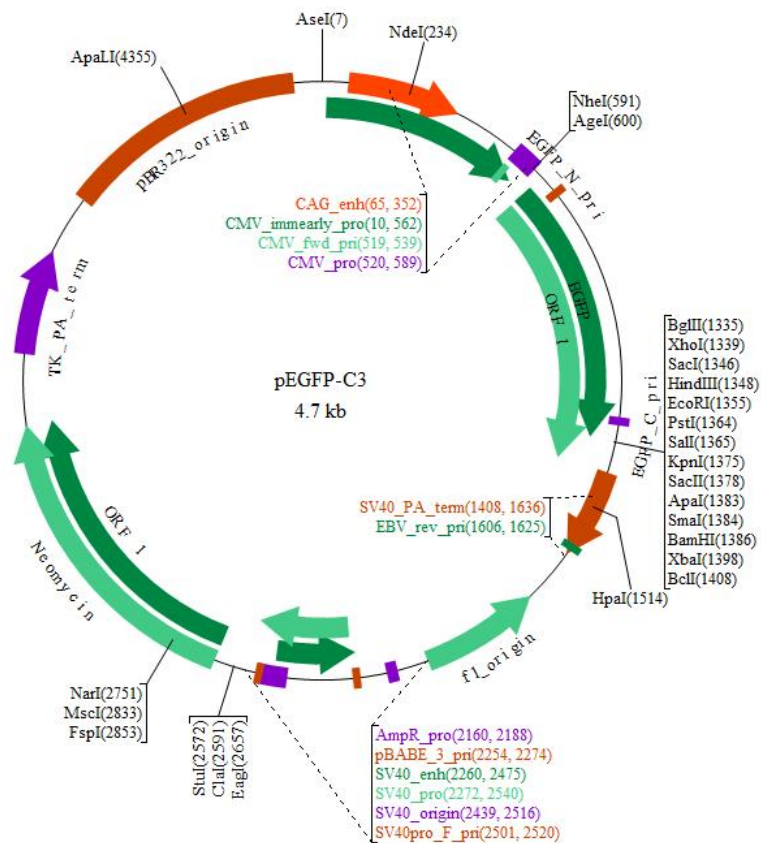
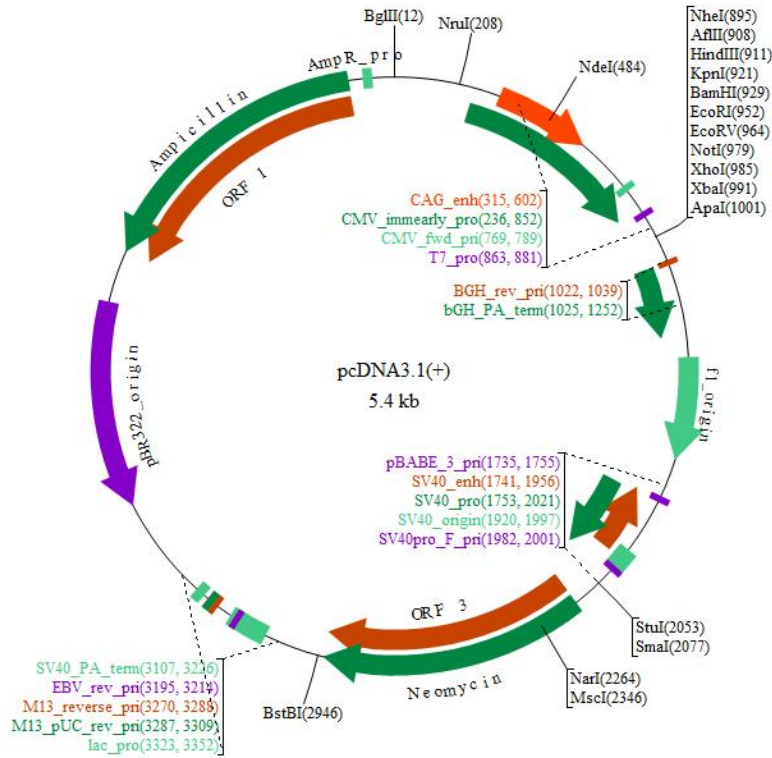
M: presence of metastasis

M0: no distant metastasis

M1: metastasis to distant organs (beyond regional lymph nodes)



## 6.2 Vector maps



## 6.3 Danksagung

Ich möchte mich bei Prof. Dr. Thomas Langer und Prof. Dr. Thorsten Hoppe für die Betreuung meiner Doktorarbeit von Seiten der Mathematisch-Naturwissenschaftlichen Fakultät bedanken.

Für die interne Betreuung meiner Arbeit und die hervorragende fachliche und persönliche Unterstützung möchte ich mich bei PD Dr. Hamid Kashkar bedanken. Prof. Dr. Martin Krönke möchte ich danken, dass ich meine Doktorarbeit in seinem Institut anfertigen durfte.

Außerdem möchte ich mich bei meinen Arbeitskollegen für das freundliche Arbeitsklima und die schönen Ablenkungen bedanken. Vor allem möchte Daniela Klubertz für die hervorragende technische Unterstützung danken. Bei Dr. Carola Pongratz, Dr. Benyamin Yazdanpanah und Dr. Dr. Oliver Coutelle möchte ich mich für sowohl fachliche als auch persönliche Unterstützung und Motivation bedanken.

Dank gilt außerdem unseren Kooperationspartnern Prof. Dr. Thorsten Hoppe, Michael Schell und Leena Ackermann für die gute Zusammenarbeit.

Meinen Freunden möchte dafür danken, dass sie immer für mich da sind und mich immer wieder motiviert und unterstützt haben.

Insbesondere danke ich meiner Familie, die mich durch ihre kompromisslose Unterstützung immer wieder bestätigt und mir dieses Studium ermöglicht haben.

## 6.4 Erklärung

Ich versichere, dass ich die von mir vorgelegte Dissertation selbständig angefertigt, die benutzten Quellen und Hilfsmittel vollständig angegeben und die Stellen der Arbeit – einschließlich Tabellen, Karten und Abbildungen –, die anderen Werken im Wortlaut oder dem Sinn nach entnommen sind, in jedem Einzelfall als Entlehnung kenntlich gemacht habe; dass diese Dissertation noch keiner anderen Fakultät oder Universität zur Prüfung vorgelegen hat; dass sie noch nicht veröffentlicht worden ist sowie, dass ich eine solche Veröffentlichung vor Abschluss des Promotionsverfahrens nicht vornehmen werde. Die Bestimmungen dieser Promotionsordnung sind mir bekannt. Die von mir vorgelegte Dissertation ist von PD Dr. Hamid Kashkar, Prof. Dr. Thorsten Hoppe und Prof. Dr. Thomas Langer betreut worden.

## 6.5 Lebenslauf

### Persönliche Daten

Name: Kerstin Brinkmann

Anschrift: Venloer Str. 448  
50825 Köln  
Telefon: 0179 7005956  
E-Mail: kerstin.brinkmann@uk-koeln.de

Geburtsdatum und -ort: 20.07.1982 in Kirchheimbolanden, Deutschland

Staatsangehörigkeit: Deutsch

Familienstand: ledig

### Schulische Ausbildung

1993-2002 Nordpfalzgymnasium in Kirchheimbolanden,  
Abschluss Abitur (2,0)

### Studium

Oktober 2002-Mai 2008 Universität zu Köln  
Diplomstudiengang Biologie  
Hauptfächer: Genetik, Biochemie, Pharmakologie  
Diplomabschluss,  
Diplomarbeitsthema: Die Reaktivierung der Apoptose im  
Hodgkin-Lymphom durch die Inhibition des Proteasoms,  
angefertigt am Institut für medizinische Mikrobiologie,  
Immunologie und Hygiene der Universitätsklinik Köln

Seit Juni 2008 Wissenschaftliche Angestellte der AG Kashkar im  
Institut für medizinische Mikrobiologie, Immunologie und  
Hygiene der Universitätsklinik Köln

### Praktika

Januar 1999 Schulpraktikum in der Kreisverwaltung  
Kirchheimbolanden (Presseabteilung) im Januar 1999

August 2002 Praktikum beim Fotograf „Foto Stefan“ in  
Kirchheimbolanden im August 2000 (3 Wochen)

März 2005 – Juni 2005      Forschungspraktikum im Institut für Biochemie I der Uniklinik zu Köln

April 2006 – Juli 2006      Ökologisches Praktikum an der Iguana Station, Utila, Honduras

### **Nebentätigkeiten**

Mai 2003 – April 2004      Studentische Aushilfskraft beim Westdeutschen Rundfunk in Köln

Oktober 2004 – Juni 2007      Tätigkeit als Interviewerin bei Marktforschungsunternehmen „Sport und Markt“ in Köln

Oktober 2005 – Dezember 2005      Studentische Hilfskraft im Institut für Biochemie I der Uniklinik zu Köln

### **Sprachkenntnisse**

Englisch, fließend  
Französisch, Schulkenntnisse  
Spanisch, Grundkenntnisse

### **EDV Kenntnisse**

MS Office, Adobe Photoshop, Adobe Illustrator, Vector NTI

### **Referenzen**

PD Dr. Hamid Kashkar, hamid.kashkar@uk-koeln.de